RNA binding proteins in Idiopathic Pulmonary Fibrosis

INAUGURALDISSERTATION

zur Erlangung des Grades eines

Doktors der Medizin

des Fachbereichs Medizin

der Justus-Liebig-Universität Gießen

vorgelegt von

Lisa Arnold

aus Gießen

Gießen 2023

RNA binding proteins in Idiopathic Pulmonary Fibrosis

INAUGURALDISSERTATION

zur Erlangung des Grades eines

Doktors der Medizin

des Fachbereichs Medizin

der Justus-Liebig-Universität Gießen

vorgelegt von

Lisa Arnold

aus Gießen

Gießen 2023

Aus dem Fachbereich Medizin der Justus-Liebig-Universität Gießen

Zentrum für interstitielle und seltene Lungenerkrankungen

1. Gutacher: Prof. Dr. med. A. Günther
2. Gutachterin: Prof. Dr. Ana Pardo-Saganta

Tag der Disputation: 20.06.2023

Dedicated to
my family

I Table of contents

II Figures

III Tables

IV Abbreviations

m	mili (10^-3)
µ	micro (10^-6)
n	nano (10^-9)

A

A. dest.	Destilled water
AD	Amiodarone
AEC	Alveolar epithelial cell
AIP	Acute interstitial pneumonia
Alpha-SMA	Alpha smooth muscle actin
ALS	Amyotrophic lateral sclerosis
APS	Ammonium persulfate
ATP	Adenosinetriphoshpate
ATS	American thoracic society

B

BAL	Bronchoalveolar lavage
BCA	Bicinchoninic acid
BSA	Bovine Serum Albumin

C

°C	Degree Celsius
CCT	Chaperonin containing tailless complex
CHOP	C/EBP homologous protein 10
CLIP-seq	UV-cross-linking-immunoprecipitation-sequencing
CO2	Carbon dioxide
COP	Cryptogenic organizing pneumonia
COPD	Chronic obstructive pulmonary disease
CRP	C-reactive protein
CTD-ILD	Connective tissue disease-associated ILD

CVD	Collagen vascular disease

D

DAPI	4’,6 Diamidin-2-phenylindol
DIP	Desquamative interstitial pneumonia
DM	Myotonic Dystrophy
DMEM	Dulbecco’s Modified Eagle Medium
DMSO	Dimethylsulfoxid
DMPK	Dystophia myotonics protein kinase gene
DNA	Deoxyribonucleotid acid
DPLD	Diffuse parenchymal lung disease
dsRBP	Double stranded RNA binding domain
DTT	Dithiothreitol
DZL	Deutsches Zentrum für Lungen-Forschung

E

ECL	Enhanced chemi-luminescence
ECM	Extra cellular matrix
EDTA	Ethylenediamine-tetraacedic acid
eIF2alpha	Eukaryotic translation initiation factor 2
eIF4G	Eukaryotic translation initiation factor 4 G
ELISA	Enzyme linked immunosorbent assay
ER	Endoplasmic reticulum
ERS	European respiratory society
EAA	Exogenous allergic alveolitis

F

FCS	Fetal-calf-serum
FTLD	Frontaltemporal Lobar degeneration
FUS/TLS	Fused in sarcoma/translocated in liposarcoma
FVC	Forced volume vital capacity

G

G3BP1	Ras GTPase-activating protein-binding protein1
GAPDH	Glycerinaldehyd-3-phosphat-Dehydrogenase
GFP	Green fluorescent protein

H

H2O	Water
HCl	Hydrochloric acid
HEPES	2-(4,2-hydroxyethyl)-piperazinyl-1-Ethansulfonate
HIV	Human immunodeficiency virus
HRCT	High resolution computed tomography
HRP	Horseradish peroxidase
hRSV	Human respiratory syncytial virus

I

IBM	Inclusion body myositis
IDR	Intrinsically disorderes regions
IF	Immunofluorescence
IFN	Interferon
IHC	Immunohistochemnistry
IIP	Idiopathic interstitial pneumonias
ILD	Interstitial lung disease
IPF	Idiopathic pulmonary fibrosis
IVC	Intravacuolar compartment

K

kDa	Kilo Dalton
KH	K-homology domain

L

LAS X	Leica application suite advanced fluorescence
LCS	Low complexity sequences
LLPS	Liquid-liquid phase interactions

M

MBNL1	Muscleblind like splicing regulator 1
min	Minutes
miRNA	Micro RNA
MLE12	Mouse lung epithelial cells
MMP	Matrix metalloproteinases
mRNA	Messenger RNA
mRNP	Messenger RNP
MRTF	Myocardin-Related Transcription Factor
MSP	Multisystem proteinopathy
MUC5B	Mucin 5 B

N

NaCl	Sodium chloride
NaOH	Sodium hydroxide
NE	Nuclear extract
NSIP	Non-specific interstitial pneumonia
n.s.	Non significant

O

OPMD	Oculopharyngeal Muscular Dystrophy

P

P-bodies	Processing bodies

PABPC1	Polyadenylate-binding protein 1
PBS	Phosphate-buffered saline
PCLS	Precision cut lung slices
PCNA	Proliferting cell nuclear antigen
PDGF	Platelet derived growth factor
PGRN	Progranulin
PIC	Protease-inhibitor Cocktail
PMSF	Phenylmethylsulfonylfluorid
PQC	Protein quality control
PrLD	Prion like domains
pro SP-C	Pro Surfactat protein C
PVDF	Polyvinylidene fluoride

R

RBD	RNA-binding domain
RBP	RNA binding protein
RB-ILD	Respiratory bronchiolitis-interstitial lung disease
RNA	Ribonucleic acid
RNA PolI	RNA polymerase II
RNP	Ribonucleoprotein complexes
ROS	Reactive oxygen species
Rpm	Rounds per minute
RPMI	Roswell park memorial institure 1640 medium
RRM	RNA recognition motif
RT	Room temperature

S

s	Second
SD	Standard deviation
SDS	Sodium dodecyl sulfate
SDS-PAGE	SDSpolyacrylamide gel electrophoresis

SG	Stress granule
SLiMs	Short linear motifs
SMC	Smooth muscle cells
SMA	Spinal Muscular Atrophy
SNP	Single-nucleotid polymorphisms
Sp1	Specificity protein 1
SP-C	Surfactant protein C
SRF	Serum response factor
SVR	Systemic vascular resistance
SV40	Simian virus 40

T

TARDBP	Transactive response DNA binding protein 43
TBB	Transbronchial biopsy
TBST	Tris buffered saline with Tween 20
TDP43	TAR DNA binding protein 43 kDa
TEMED	N,N,N,N‘ -tetramethyl-ethane-1,2-diamine
TGFß	Transforming growth factor ß
TIA1	T-cell intracellular antigen-1
TOLLIP	Toll interacting protein
TRIS	Tris(hydroxymethyl)-aminomethan

U

UGMLC	University of Giessen and Marburg lung center
UIP	Usual interstitial pneumonia
UPS	Ubiquitin-proteasome system
USP10	Ubiquitin specific peptidase 10
UT	Untreated
UTR	Untranslated region

V

VATS	Video-associated thoracic surgery
Veh	Vehicle

W

WB	Western Blot

Z

ZnF	Zinc fingerdomain

V Summary

RNA binding proteins (RBPs) associate with target ribonucleic acids (RNAs) through conventional or unconventional RNA-binding domains to regulate messenger RNA (mRNA) biogenesis and metabolism. Under certain settings like cellular stress, membrane-free cytoplasmic aggregates, termed stress granules (SGs), are formed, which enclose RBPs and untranslated or stalled RNA transcripts. In organs with a high and complex RNA metabolism like the brain or the lungs, the task of RBPs and SGs becomes even more complex. The complex role of RBPs has been elegantly studied in the field of neurodegeneration, but their role in lung diseases remains poorly understood. Idiopathic pulmonary fibrosis (IPF) is a life-threatening, chronic lung disease that is characterized by alveolar epithelial cell injury and severe fibroblast proliferation, thus resulting in disturbed epithelial-mesenchymal crosstalk and, ultimately, fibrosis.

The goal of this study was to better understand the role of RBPs and SGs in lung fibrosis. For this, explanted lungs and interstitial fibroblasts isolated from IPF patients or healthy donors, mouse model of fibrosis as well as an *in vitro* amiodarone induced lung fibrosis model were employed. In general, a differential regulation of several RBPs including transactive response DNA binding protein 43 kDa (TDP43), fused in sarcoma/translocated in liposarcoma (FUS/TLS), serum response factor (SRF), muscleblind-like splicing regulator 1 (MBNL1) and polyadenylate-binding protein 1 (PABPC1) was encountered in IPF and in the amiodarone model. Of interest, some RBPs, namely FUS, TDP43 and PABPC1, were observed to be particularly increased in the interstitial fibroblasts of IPF patients. In addition to this, overexpression of FUS in healthy primary fibroblasts resulted in an increase in the cell proliferation marker proliferating cell nuclear antigen (PCNA), indicating that the increase in FUS is sufffcient to trigger their proliferation. Further, decreased staining for both FUS and PABPC1, was observed in IPF precision cut lung slices (PCLS) which were treated ex vivo with the anti-fibrotic drug pirfenidone. This indicated that pirfenidone may exert its anti-fibrotic effects, at least in part by targeting RBPs like FUS and PABPC1. Taken together, our study, for the first time, documents strict cell specific and altered expression and localization of RBPs and SG proteins in IPF. Our results also imply, that patient lungs and therapeutic targeting of RBPs may prove beneficial in IPF.

VI Zusammenfassung

RNA bindende Proteine verknüpfen sich mit ihren Ziel-RNAs über herkömmliche oder unkonventionelle RNA-Bindungsdomänen und regulieren hierüber die mRNA-Biogenese und den mRNA-Metabolismus. Unter bestimmten Bedingungen, wie z. B. zellulären Stress, bilden sich membranfreie cytoplasmatische Aggregate, sogenannte Stress Granula (SG), die RBPs und nicht-translatierte oder blockierte RNA-Transkripte einschließen. In Organen mit hohem und komplexem RNA-Metabolismus wie dem Gehirn oder der Lunge, sind die Aufgaben von RBPs und SGs noch komplexer. Die wichtige Rolle von RBPs wurde ausführlich im Gebiet der Neurodegeneration untersucht, ihre Rolle bei Lungenerkrankungen ist jedoch nach wie vor unbekannt. Die idiopathische pulmonale fibrose (IPF) ist eine lebensbedrohliche chronische Lungenerkrankung, die durch Verletzung des alveolären Epithels und starke Proliferation von Fibroblasten gekennzeichnet ist. Dies führt zu einem gestörten epithelialen-mesenchymalen Crosstalk und letztendlich zu Fibrose.

Das Ziel dieser Studie war es, den Einfluss von RBPs und SGs auf Lungenfibrose zu verstehen. Zu diesem Zweck wurden explantierte Lungen und extrahierte interstitielle Fibroblasten von IPF-Patienten und gesunden Spendern, ein Mausmodell der Lungenfibrose, sowie ein Modell der in vitro-Amiodaron-induzierten Lungenfibrose genutzt. Im Allgemeinen wurde eine unterschiedliche Regulation verschiedener RBPs, einschließlich TDP43, FUS, SRF, MBNL1 und PABPC1, im IPF und im Amiodaron-Modell festgestellt. Interessanterweise wurde beobachtet, dass die RBPs FUS, TDP43 und PABPC1 in interstitiellen Fibroblasten von IPF-Patienten besonders erhöht sind. Darüber hinaus führte die Überexpression von FUS in gesunden primären Fibroblasten zu einem Anstieg des Zellproliferationsmarkers PCNA, was darauf hinweist, dass der Anstieg von FUS ausreicht, um deren Proliferation auszulösen. Ferner wurde eine verringerte Färbung sowohl für FUS als auch für PABPC1 in IPF-precision cut lung slices (PCLS) beobachtet, die ex vivo mit dem Antifibrotikum Pirfenidon behandelt wurden. Dies deutete darauf hin, dass Pirfenidon seine antifibrotischen Wirkungen zumindest teilweise über eine Beeinflussung von FUS und PABPC1 ausüben kann. Zusammenfassend zeigt unsere Studie erstmals eine strikte, zellspezifisch veränderte Expression und Lokalisierung von RBPs und SG-Proteinen in IPF-Lungen. RBPs bieten sich daher als therapeutisches Ziel zur Beeinflussung des Verlaufs einer IPF an.

1. Introduction

1.1 Aims and Objectives

The complex role of RBPs and SGs has been elegantly studied in several human pathologies, but their role in lung diseases remains poorly understood. Especially under conditions of IFP, the regulation and role of RBPs and / or SGs is completely unclear. We therefore hypothesized that under conditions of IPF RBPs are differently regulated and may affect the cellular fate in IPF. To test this, we identified the following aims for this study:

1. To characterize known RBPs as well as SG proteins in lung fibrosis. For this, we first aimed to analyze the regulation of RBPs in the lung tissues of IPF versus donors, in primary fibroblasts of IPF and donor lungs, and also in animal models of lung fibrosis, especially the amiodarone induced model of lung fibrosis.

2. To perform gain and / or loss of function study of the altered RBP(s). Pending on the readouts obtained in 1, we aimed to either overexpress or knockdown the identified RBP(s) in *in vitro* models of lung fibrosis in order to understand the cellular fate as a result of such alterations, for example cell survival.

3. To understand if standard of care drugs for IPF may interact with RBPs. To study this, we aimed to treat precision cut lung slices of IPF patients with the known IPF standard of care drug, pirfenidone, and to identify its effects on the regulation of RBPs.

1.2 RNA-binding proteins (RBPs) & stress granules (SGs)

As the name suggests, RBPs uniquely interact with RNAs (Davidson, 1945) to control several facets of the RNA life cycle, thereby making them critical players in post-transcriptional events (Helder *et al*, 2016). Classically, two conserved domains have been ascribed to RBPs: the hydrophobic, glycine rich domain, which mediates reversible aggregation of these proteins, and RNA binding domains (RBD) that predominantly regulate their RNA binding. These RBDs recognize either a sequence or a structural motif to associate with their target mRNAs. Based on their RBDs, RBPs are further grouped as proteins with: 1. RNA recognition motif (RRM), 2. zinc-finger domain (ZnF), 3. K-homology (KH) domain and 4. double stranded RNA-binding domain (dsRBD) (Brinegar & Cooper, 2016; De Conti *et al*, 2017; Helder *et al.*, 2016). However, the functions of RBPs cannot be deduced based on the information of their binding sequences, as many RBPs display more than one RBD. There are certain auxillary domains that have been referred to as disordered protein regions that mediate both specific and non-specific interactions with RNA (De Conti *et al.*, 2017). This is supported by recent pioneering work where several RBPs, without the presence of a specific binding motif, have been identified by Castello & colleagues (Castello *et al*, 2013). In any case, the interaction of RBPs with RNAs (including coding, non-coding, untranslated or miRNAs (microRNA)) results in dynamic functional units called ribonucleoprotein (RNP) complexes. Through these RNP complexes, RBPs may either remain bound to the RNAs right from their synthesis to degradation or may be selectively bound to specific RNAs in a temporal fashion (Achsel *et al.*, 2016).

RBPs have diverse functions depending upon their cellular localization. In the nucleus, they regulate mRNA maturation that includes RNA splicing, RNA polymerase elongation, RNA helicase activity and nuclear export. In the cytoplasm RBPs regulate translation, silencing, RNA transport and degradation (Heyd & Lynch, 2011; Wolozin & Apicco, 2015). Pioneering studies in the past revealed that RBPs create RNPs out of mRNA - protein and protein - protein interactions to achieve their functions by forming discrete cytoplasmic granules which are the sites of transport and translational regulation. Depending upon the metabolic state of the cell, mRNA in these granules may be activated or directed for degradation. These could be the motile RNA granules which transport RNA (Bashkirov *et al*, 1997; Sheth & Parker, 2003b; van Dijk *et al*, 2002), stress granules (SGs) that are formed in response to stress and contain translation

initiation factors, RBPs, non-RBPs and untranslated RNA (Loschi *et al*, 2009; Thomas *et al*, 2005) or P-bodies (processing bodies) that contain a mRNA decay machinery like decapping enzymes and nonsense mediated decay enzymes (Loschi *et al.*, 2009).

SGs are assemblies of untranslating messenger ribonucleoproteins (mRNPs) that form in the cytoplasm and nucleus of eukaryotic cells (Protter & Parker, 2016) (Sheinberger & Shav-Tal, 2017). Cytoplasmatic SGs contain mRNAs stalled during the initiation of translation and proteins including numerous types of RBPs (Chen & Liu, 2017). They are non-membranous, liquid-liquid phase separations (LLPS) which are bound together through conventional protein-protein interactions, RNA binding domains from RBPs and interactions involving intrinsically disordered regions (IDR) of proteins (Protter & Parker, 2016) (Jain *et al*, 2016). SG assembly is a response to cellular stresses that represses mRNA translation like viral infections, heat, oxidation and starvation (Sheinberger & Shav-Tal, 2017) and they affect mRNA function and localization. This translational arrest leads to the accumulation of stalled translation preinitiation complexes (Kedersha *et al*, 2005) (Kedersha *et al*, 1999) (Panas *et al*, 2016) (Dang *et al*, 2006) (Mokas *et al*, 2009) thereby preventing the assembly of polysomes (Gebauer & Hentze, 2004).

There are three main functions of SGs:

Firstly, SGs allow cells to adapt to diverse environmental stressors and safeguard key cellular components (Cao *et al*, 2020). Furthermore, SGs contain a high local concentration of diverse proteins and mRNAs, which allows for the increased efficiency of certain reaction kinectics under stress conditions, in turn helping cells to survive. For instance, the concentration of mRNAs and translation factors in SGs may promote interaction and accelerate the formation of translation initiation complexes (Cao *et al.*, 2020) (Buchan *et al*, 2008).

Secondly, SGs play a role in signal transduction pathways in response to stress conditions. Several signaling factors are sequestered in SGs transiently in response to stress, affecting downstream signal transduction pathway (Kedersha *et al*, 2013).

The third function of SGs is temporary storage and protection of mRNAs and proteins from autophagy and proteasomal degradation under stress conditions (Cao *et al.*, 2020). This allows a rapid resumption of translation and other signaling pathways upon the release of the stress condition (Guzikowski *et al*, 2019) (Cao *et al.*, 2020).

The generation of SG's is based on a high concentration of macromolecules in order to reach a critical treshhold to start LLPS, thereby forming aggregates (Cao *et al.*, 2020). When liquid conglomerates convert into gel-like or solid-like fibrillar aggregates, the interaction of the components with the surrounding is significantly reduced (Alberti & Dormann, 2019; Molliex *et al*, 2015b) (Patel *et al*, 2015a). Such pathological assemblies, which arise in this way, can lead to several diseases including amyotrophic lateral sclerosis (ALS), Alzheimer's disease and Parkinson's disease (Alberti & Dormann, 2019; Falahati & Haji-Akbari, 2019). For instance, *in vitro* at physiological concentrations, the RBP FUS seperates into dynamic liquid compartments, in case of cellular stress its concentration is increased and the liquid phases transform into gel-like aggregates, thereby leading to a change in its properties (Cao *et al.*, 2020).

Under cellular stress, the nucleus exports nontranslating mRNPs including mRNA and translation initiation factors like eukaryotic translation initiation factor 4 G (eIF4G) and PAB1/PABP1 form physiological SGs into the cytoplasm. This process is driven by RBPs acting as primary nucleators such as Ras GTPase-activating protein-binding protein 1 (G3BP1) and T-cell intracellular antigen-1 (TIA1) and leading to a dynamic state where components of SGs dissociate from the complexes and cytoplasmic components bind to the SGs with a residence time of a few seconds (Sheinberger & Shav-Tal, 2017) (Chen & Liu, 2017). This fact contradicts the model of SGs as mRNP storage granules and rather indicates them as a dynamic point of maintainance from RNPs during stress conditions (Sheinberger & Shav-Tal, 2017). SG themselves persist for minutes to hours and their assembly takes more time than their disassembly. This equilibrium is maintained by multiple ATP (Adenosinetriphoshpate)-driven machineries (Jain *et al.*, 2016). For instance, ATP-driven disaggregases are needed, which dissolve SGs and prevents the fusion of P-bodies and SGs. P-bodies are also cytoplasmatic RNA granules (Aizer *et al*, 2008) (Aizer & Shav-Tal, 2008), which contain protein factors involved in mRNA degradation, translational repression and gene silencing (Zheng *et al*, 2008). Moreover DEAD-box helicases were found in the cores of SGs that are responsible for ATP-binding, ATP hydrolysis and RNA-binding (Cherry & Ananvoranich, 2014). Furthermore, they are important for SG assembly by increasing the binding affinity to eIF4, thereby repressing the translation (Hilliker *et al*, 2011). Another important role in the equilibrium of SGs is played by ATPases, which promote the targeting of SGs to autophagy (Buchan *et al*, 2013).

Severe oxidative stress (ROS), ageing and cellular surveillance systems influence SG clearance even in resistant cells like neurons and muscle cells. It is well-known that oxidative stress leads to the oxidation of proteins and in fact to changes in their tertiary structure and protein aggregation (Squier, 2001) (Mirzaei & Regnier, 2008). Simultaneously, early stage protein aggregates generate hydrogen peroxide and other ROS (Tabner *et al*, 2005) which leads to a circle of oxidation and SG assembly. Persistent oxidative stress induces the Oligomerization of pathological RBPs like TDP43 and FUS and they are recruited into SGs, where their transition to pathological amyloid-like SG is enhanced (Chen & Liu, 2017) (Figure 1).

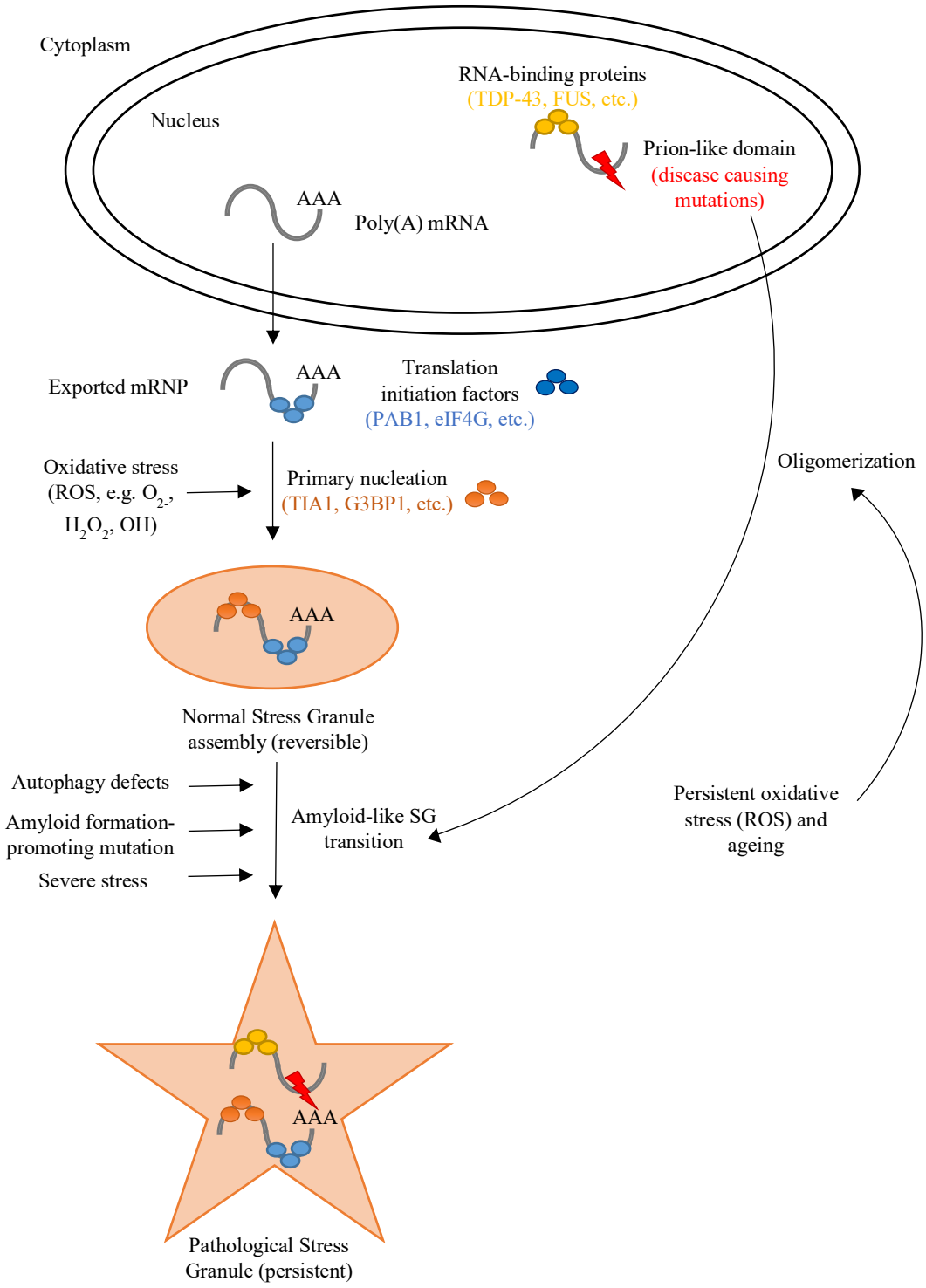

Figure 1: Assembly of physiological SGs and transformation into pathological SGs due to persistant oxidative stress combined with autophagy defects and amyloid formation-promoting mutations (modified from Chen & Liu, 2017).

1.2.1 SG and autophagy

Autophagy is a lysosome dependent cellular quality control mechanism. Proteins and organelles are targeted to lysosomal degradation via double-membraned structures called autophagosomes (Buchan *et al.*, 2013). Likewise, SGs and P-bodies can be targeted to vacuoles/lysosomes for degradation by autophagy, this process is referred to as granulophagy (Buchan *et al.*, 2013). Stress granule accumulation can be caused by mutations which inhibit autophagy at stages prior to an autophagosome-vacuolar membrane fusion. Such view is consistent with a continuous SG clearance by an autophagic process. Moreover, several mutations that disrupt autophagy lead to an increase in SGs, which are then usually associated with P-bodies (Buchan *et al.*, 2013). Buchan et al observed the accumulation of PAB1-GFP and Edc3-mCh (P-body marker) in an intravacuolar compartment (IVC) in an autophagy-disrupted mutant (atg15 Δ mutant). Atg15 is a vacuolar lipase involved in opening of vesicles targeted to the vacuole from autophagic trafficking pathways (Teter *et al*, 2001). Consequently, these results support the view that SG and P-bodies accumulate in the cytosol of strains defective in autophagy (Buchan *et al.*, 2013).

There are several mechanisms that regulate the clearance of P-bodies and SGs. First, the translation initiation can reduce P-bodies and SGs by promoting the return of mRNAs to translation (Bhattacharyya *et al*, 2006; Brengues *et al*, 2005). Second, decapping and 5‘ to 3‘ degradation can reduce the mRNAs present within P-bodies (Sheth & Parker, 2003a). Third, targeting of SGs and possibly P-bodies to autophagy regulates the clearance of these structures (Buchan *et al.*, 2013). Since these pathways are dependent on each other, decrease in one of these pathways increases the other. Buchan et al confirmed that a decrease in decapping or 5‘ to 3‘ exonucleolytic degradation that leads to the accumulation of P-bodies, SGs and a pool of non-degraded mRNAs results in an increased flux of mRNPs into the autophagy pathway (Buchan *et al.*, 2013; Buchan *et al.*, 2008; Sheth & Parker, 2003a).

Normally mRNPs can return to translation from SGs and might play an important role especially durig prolonged cellular stress. This is however not the case when SGs and P-bodies are targeted to autophagy. The mRNPs within them cannot return to translation once their autophagy is initiated (Buchan *et al.*, 2013).

These observations imply that aberrant forms of SGs, which accumulate in some degenerative diseases such as ALS (Amyotrophic lateral sclerosis), FTLD (frontotemporal lobar degeneration), IBM (inclusion body myositis) and MSP (multisystem proteinopathy), may also be cleared by targeting them to the lysosomal pathway for degradation. TDP43 is the most consistenly observed component of pathological cytoplasmatic inclusions in ALS, FTLD and MSP and is preferentially cleared by autophagy (Wang *et al*, 2012; Wang *et al*, 2010). Consequently, mechanisms to enhance the autophagy of SG and related RNPs may have potential as therapies to treat various degenerative diseases (Buchan *et al.*, 2013, Cao *et al.*, 2020). The hypothesis that ALS, FTLD and some related pathologies are driven by hyper-formation or stabilization of SGs is strengthened by these findings. Mutations in the SG components TDP43, FUS and Atx2 enhance their self-assembly or aggregation and may be causative for these diseases in addition to causing the accumulation of SG and related RNPs (Dewey *et al*, 2012; Ito & Suzuki, 2011; Kim *et al*, 2013).

1.2.2 SG and ageing

The regulation of SGs also plays a role in the process of ageing. Ageing is a ubiquitious, irreversible process which predominantly can include different pathomechanisms: genomic instability, telomere attrition, epigenetic alterations, loss of proteostasis, deregulated nutrient sensing, mitochondrial dysfunction, cellular senescence, stem cell exhaustion and altered intercellular communication (López-Otín *et al*, 2013). The classic SG proteins PAB1 and TIAR-2 can form aggregates in aged *C. elegans* and higher levels of SG component aggregation is associated with smaller animal size, reduced fitness and a shorter lifespan (Lechler & David, 2017). Based on this, it has been suggested that SG protein aggregaton may accelerate ageing and reduce lifespan. Oligomeric aggregates disturb cellular processes, as they trigger aggegration of other normally folded monomeric proteins, sequester cell membrane or organelles, and are more effectively transported from initially affected brain regions to other regions, compared with fibrillar aggregates (Cao *et al.*, 2020; Jay *et al*, 2005; Langer *et al*, 2011). In addition some cytosolic amyloid-like protein aggregates such as TDP43 have been shown to disturb nuclear integrity and nucleocytoplasmic transport by sequestering nucleo-cytoplasmatic transporters (Cao *et al.*, 2020; Gasset-Rosa *et al*, 2017; Woerner

et al, 2016). A consequence of these mechanisms can potentially be an acceleration of ageing and the onset of neurodegenrative diseases.

Another aspect of ageing is that cells enter into a senescene state, which means that they are in cell cycle arrest (López-Otín *et al.*, 2013). It has been revealed, that cellular senescence impairs the proper formation of both canonical and non-canonical SGs in kidney cells (Moujaber *et al*, 2017). The depletion of transcription factor Sp1 (specificity protein 1) leads to reduced canonical SG formation by a modified abundance of the SG-nucleating proteins G3BP1 and TIA1/TIAR (Moujaber *et al.*, 2017). This suggests that the transcription factor Sp1 as an essential SG protein can work as a direct ageing related target when cells enter into the senesence state. This can cause significant deficiencies in SG production (Cao *et al.*, 2020).

Ageing is associated with a reduction in the ability to regulate gene expression and protein homeostasis (Figure 2, b) (Cao *et al.*, 2020). Walther et al. report that the nematode *C. elegans* shows extensive proteome remodeling and imbalance during ageing, with a large amount of proteins increasing or decreasing, in addition to widespread protein aggregation and impaired SG formation (Walther *et al*, 2015). Under these conditions, cells are frequently exposed to chronic stress, such as constant oxidative stress (Denoth Lippuner *et al*, 2014). Oxidative stress leads to the the induction of SG formation (Figure 2, c) and is a key factor of neurodegenerative disorders (Federico *et al*, 2012; Gandhi & Abramov, 2012; Patten *et al*, 2010). During ageing, mitochondrial structure and function changes dramatically (Hughes & Gottschling, 2012; Lam *et al*, 2011; McFaline-Figueroa *et al*, 2011; Scheckhuber *et al*, 2007; Veatch *et al*, 2009). Mitochondria produce the majority of the cell's ATP via oxidative phosphorylation, thus mitochondrial dysfunction is known to impact energy production and normal metabolism. Recent studies showed that SG assembly, dynamics, disassembly, and clearance occur in an energy-consuming manner (Buchan *et al.*, 2013; Cherkasov *et al*, 2013; Jain *et al.*, 2016; Kroschwald *et al*, 2015; Loschi *et al.*, 2009). Therefore, it is speculated that when cells are young, their active mitochondrial metabolism supports the assembly and health dynamics of SGs in the cell (Figure 2, d) (Cao *et al.*, 2020).

The protein quality control (PQC) system is an integrated network of chaperones, the ubiquitin-proteasome-system (UPS) and autophagy, which selectively degrades

misfolded proteins and dysfunctional organelles (Amm *et al*, 2014; Boya *et al*, 2013). Ageing leads to disruption of the PQC system and the protein homeostasis (Josefson *et al*, 2017). It has been shown that there is an age-dependent decrease in the amount of proteasomes or UPS subunits, as well as proteasomal activity during the ageing process (figure 2, e) (Baraibar & Friguet, 2012; Bulteau *et al*, 2002; Kastle & Grune, 2011; Saez & Vilchez, 2014). Inhibition of the UPS induces SG formation, although this is not because of the failure of degradation of SG assembly factors (Cao *et al.*, 2020; Mazroui *et al*, 2007).

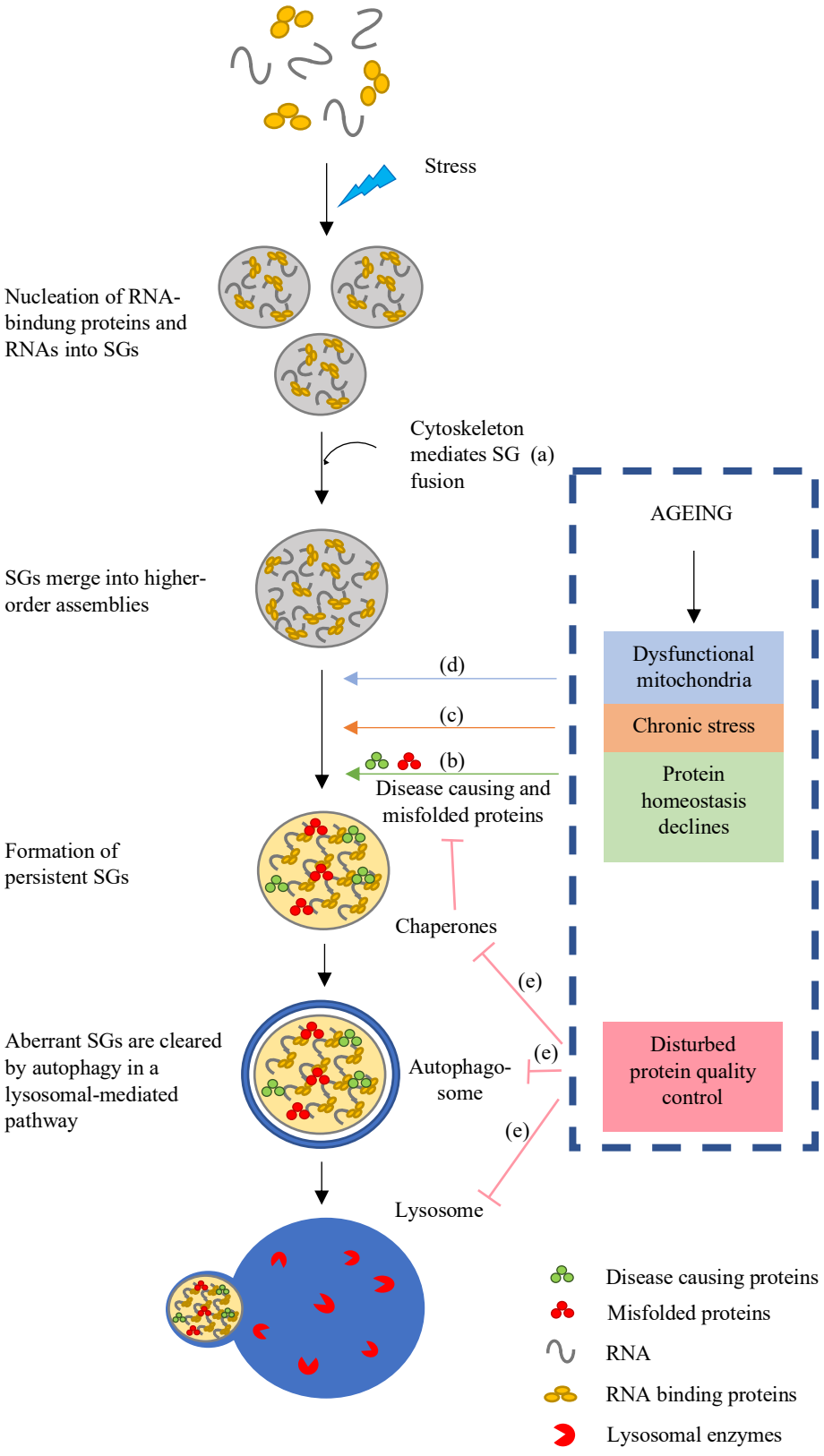

Figure 2: Effects of ageing on SG assembly, dynamics and clearance. As a response to stress RBPs and RNAs form SGs mediated by a cytoskeleton system-dependent manner (a). Ageing

related circumstances may lead to limited control of this process and aberrant SGs (b-d). Under normal conditions aberrant SGs can be cleared by autophagy, but an age disturbed protein quality control system can have a negative effect on the removal of aberrant SGs (e) (modified from Cao *et al.*, 2020).

1.2.3 Structure and formation of SG

SGs are not uniform structures, they contain internal sub-structures with higher concentrations of proteins and mRNAs (Jain *et al.*, 2016), which are called “cores”. They are sorrounded by a less concentrated and more dynamic shell, which ensures the rapid exchange with the cytoplasm, while the core region is less dynamic. Studies revealed that the core regions are 200nm in diameter and constitute higher levels of G3BP1, PABPC1 and polyA RNA (Jain *et al.*, 2016) than the shell. SG can be described as a network of multivalent weak interactions and are defined by the on-off rates of their components. As previously described, the shell regions have a high exchange rate with the cytoplasm or P-bodies and these fast off-rates lead to liquid assemblies, whereas the core structure with the more stable elements have solid phases. The formation of SGs occurs through the cross-linking of untranslated mRNAs, which provides a scaffold for multiple RBPs (Protter & Parker, 2016). RBPs have different possibilities to interact with mRNAs, one pathologically significant binding is the one through intrinsically disordered regions (IDR), also described as low complexity sequences (LCS) which contain prion-like domains (PrLD). Their amino acid composition is similar to fungal prion proteins with high cross-beta zipper forming abilities (Decker *et al*, 2007) (Kato *et al*, 2012). This has particularly been shown in the human TIA1 protein (Gilks *et al*, 2004), affecting its IDR regions and other RNP granules (Hanazawa *et al*, 2011). The mechanism behind the promiscious interactions of IDRs can be described with various backgrounds. The first variant refers to Short Linear Motifs (SLiMs), which can get access through IDRs. SLiMs are short protein sequences that typically fit into bindig sites on other well-folded domains, investigated at P-bodies (Jonas & Izaurralde, 2013). Moreover, IDRs can build weak interactions between each other, this is shown for the RBP FUS (Patel *et al*, 2015b) and leads to a liquid-liquid-phase (LLPS) interaction. This interaction is initially dynamic and liquid-like but over the time high concentration of IDRs within the LLPS can lead to stronger interactions, like amyloid-like structures (Lin *et al*, 2015) (Molliex *et al*, 2015a) (Patel *et al.*, 2015b)

(Zhang *et al*, 2015a) (Xiang *et al*, 2015). Besides, IDRs can contain regions which directly bind to RNA (Lin *et al.*, 2015) (Molliex *et al.*, 2015a).

SG assembly consists of multiple steps and can be controlled by post-translational modifications and RNP remodelling as shown in defects in the CCT (chaperonin containing tailless complex) in yeast, leading to a higher number of SGs. The CCT complex limits nucleation by remodeling interactions between mRNPs or by limiting misfolded proteins and if this complex is inhibited more SG assemble (Jain *et al.*, 2016) (Cherkasov *et al.*, 2013) (Wallace *et al*, 2015) (Kroschwald *et al.*, 2015) (Cherkasov *et al.*, 2013). The size of SG increases over time while the number of SGs per cell decreases caused by fusion events (Fournier *et al*, 2010), this merging-step is microtubule dependent (Chernov *et al*, 2009) (Loschi *et al.*, 2009) (Nadezhdina *et al*, 2010).

1.2.4 Stress granule markers

SG constituents and SG formation differ depending on the type of stress. For instance, SGs induced by glucose starvation contain eukaryotic initiation factor 4 (eIF4E), mRNAs and the poly(A)-binding protein 1 (PAB1) (Chen & Liu, 2017) (Brengues & Parker, 2007) (Buchan *et al*, 2008), whereas oxidative stress induced SG have the SG-nucleating protein TIA-1 as a major component (Chen & Liu, 2017) (Arimoto-Matsuzaki *et al*, 2016). But beside the SG inducing effects, oxidative stress may also supress SG formation (Chen & Liu, 2017) by oxidating TIA-1. Hydrogen peroxide directly oxidizes this RBP, abolishing its interaction with target mRNA's and hence suppressing SG assembly (Gilks *et al.*, 2004). The two SG components USP10 (Ubiquitin specific peptidase 10), an antioxidant ezyme, and its cofactor G3BP1 are responsible for the antioxidant activity of SGs (Chen & Liu, 2017). Under steady state conditions, G3BP1 can mask USP10 activity. Under oxidative stress conditions, however, G3BP1 is inactivated, thereby activating USP10 and thus results in a decrease in ROS production and apoptosis. Moreover, USP10 interacts with proteins like PABPs which are localized at polysomes (Chen & Liu, 2017) (Sowa *et al*, 2009) and is thus most likely involved in redox control by influencing the fate of the responsible mRNAs.

1.2.5 RBPs and SGs in disease

RBPs are critical players in mRNA maturation, translation and degradation. Under healthy situations, specific RBPs are destined to bind to drive nonsense mediated decay, thereby preventing toxic protein buildup. The pathological role of RBPs has been best described in neurodegenerative diseases, followed by cancer. Several RBPs have been indicated to aggregate in different neurodegenerative diseases. Classical RBPs namely TDP-43 (Gebauer *et al.*, 2004) and FUS/TLS (Kedersha *et al.*, 2009) belong to the group of best studied proteins. These proteins have diverse RNA targets that are involved in critical cellular functions and are currently being considered as targetable options for neurodegeneration (Cao et al., 2020) (Buchan *et al.,* 2008). In addition, accumulation of TDP-43 inclusions in amyotrophic lateral sclerosis (ALS) as well as in frontotemporal lobar degeneration (FTLD) has been shown to be associated with SGs (Gebauer *et al.*, 2004) (Kedersha *et al.*, 2009) (Li *et al*, 2013) (Ramaswami *et al*, 2013) (Klar *et al*, 2013). In these diseases, SG markers (TIA1, G3BP1, PABP) colocalized with pathological lesions (Kedersha *et al.*, 1999) (Kedersha *et al*, 2000) (Tourriere *et al*, 2003). Persistence of SGs, due to stable, irreversible beta-amyloid structures built by the prion-like domains, and the acccumulation of these hyper-stable SGs can trigger cell death by altering the regulation of RNA biogenesis and function, misregulation of signaling pathways and transport of mRNPs (Ramaswami *et al.*, 2013) (Freibaum *et al*, 2015) (Ling *et al*, 2013) (Zhang *et al*, 2015b). In ALS and FTLD, SGs can be located by visualizing TDP43 positive lesions (Liu-Yesucevitz *et al*, 2010), that aggregate because of the loss-of-function mutation of PGRN (progranulin) (Kumar-Singh, 2011).

SGs are also involved in tumor progression (Anderson *et al*, 2015). Formation of ‚pro-survival' SGs in cancer cells result in their resistance to chemotherapy (Fournier *et al.*, 2010) (Anderson *et al.*, 2015) (Arimoto *et al*, 2008) (Fujimura *et al*, 2012) (Woldemichael *et al*, 2012) (Mason *et al*, 2011) (Kaehler *et al*, 2014). For instance, cells treated with Borezomib (against multiple myeloma) show a high number of SGs and a strong resistance to apoptosis. Furthermore, SG assembly interferes with radiotherapy by inhibiting the translation of angiogenic factors in hypoxic tumor cells (Moeller *et al*, 2004). This also leads to enhanced metastasis (Somasekharan *et al*, 2015). Besides chemotherapeutic stress, SGs also appear in response to viral infection (Onomoto *et al*, 2014). For example, HIV2 (Human immunodeficiency virus) induces SG formation and its genomic RNA is stored in SGs until virus packaging commences

(Soto-Rifo *et al*, 2014). Another virus that interacts with SGs is hRSV (human respiratory syncytial virus) (Santangelo *et al*, 2009).

Based on several intersections between SGs and failure of treatments, therapies to reverse pathological SGs and to perhaps delay the progression of disease are currently developed (Wolozin, 2012) (Vanderweyde *et al*, 2012). In this regard, the first approach was to target the SG pathway by inhibiting eIF2alpha phosphorylation during neurodegeneration (Moreno *et al*, 2012). Besides this, TDP43 aggregates were endeavored to reduce (Boyd *et al*, 2014) oxidative stress and to increase the antioxidant answer (Fujita *et al*, 2012).

1.3 Idiopathic pulmonary fibrosis

1.3.1 Interstitial lung diseases

Interstitial lung diseases (ILDs) or diffuse parenchymal lung diseases (DPLDs) classify more than 200 pulmonary parenchymal disorders, with the majority classified as rare diseases (Flaherty *et al*, 2017; Mikolasch & Porter, 2014). All three compartements of the lung, the pulmonary interstitium, the alveolar epithelium and the capillary endothelium are affected by ILDs. The characteristic feature of ILDs is the increased connective tissue production leading to fibrosis, reduced lung compliance and impaired gas exchange (Chapman, 2004; Maher, 2012; Kramer, 2017). ILDs represent an important cause of morbidity and mortality worldwide, with respiratory failure being the most common cause for fatal outcome of the disorder. In the late stages of the disease patients develop a cor pulmonale (American Thoracic Society, 2002; Kramer, 2017). Figure 3 shows an overview of the general classification of ILDs.

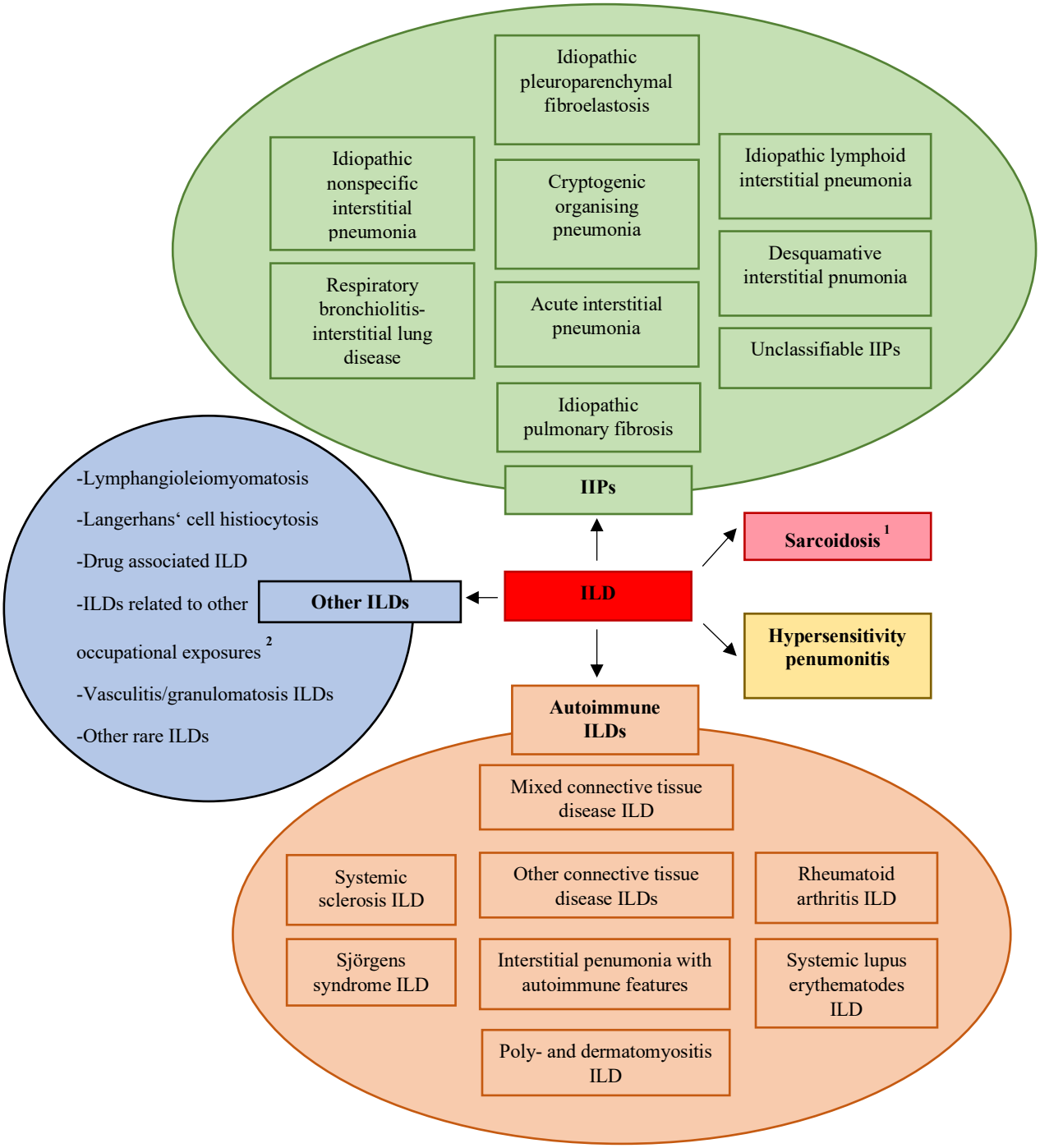

Figure 3: Types of ILDs. IIPs: idiopathic interstitial pneumonias. 1: stage IV sarcoidosis only, 2: e.g., asbestosis, silicosis (modified from Cottin *et al*, 2018).

The herterogenity of the disease leads to a high complexity of ILD classification. Some ILDs lack a well-defined cause, other IIPs could arise from an obvious origin, e.g.

inhalational (e.g., asbestosis), drug induced (e.g., amiodarone) or granulomatous (e.g., sarcoidosis) etiology. ILDs are also frequently observed in association with systemic disorders such as vasculitis, reno-pulmonary syndromes and collagen vascular diseases (CVD) (Flaherty *et al.*, 2017; Kramer, 2017). The classification of Idiopathic Interstitial Pneumonias (IIPs) combines clinical, imaging and histopathological information and distinguishes between major IIPs, rare IIPs and unclassificable IIPs. The major IIPs usually have a progressive-fibrosing phenotype and include idiopathic pulmonary fibrosis (IPF), non-specific interstitial pneumonia (NSIP), smoking related IPs comprising respiratory bronchiolitis-interstitial lung disease (RB-ILD) and desquamative interstitial pneumonia (DIP). Additionally, acute/subacute IIPs exist including cryptogenic organizing pneumonia (COP) and acute interstitial pneumonia (AIP) (American Thoracic Society, 2002; Kramer, 2017).

It is demanding to make a precise diagnosis of ILDs and disease progression is often difficult to prognosticate (Cottin *et al.*, 2018). Multiple clinical and pathophysiological features are shared between IPF and other fibrosing ILDs that may present a progressive phenotype (Kreuter *et al*, 2017; Solomon *et al*, 2013; Wells *et al*, 2018). The fibrotic commonalities of ILDs suggest a potential for a common, antifibrotic treatment modality. Some ILDs show a combination of inflammation and fibrosis and therefore offer for an additional immunomodulatory therapy, the efficacy of which greatly varies between conditions. The existant therapies most likely stabilize and slow down disease progression, for example in NSIP and connective tissue disease-associated ILD (CTD-ILD) (Flaherty *et al.*, 2017), but resolution of ILD may also be seen. Pulmonary fibrosis is regularly associated with disease progression, and prognosis is then limited (Cottin *et al.*, 2018).

A multidisciplinary approach is required for safe setting of the diagnosis of ILDs, usually involving pulmonologists, radiologists and pathologists (De Sadeleer *et al*, 2018). Finding a diagnosis includes clinical presentation, specific history assessment, smoking status, lung function evaluation, serological test results, imaging and, in some cases, a lung biopsy (Martinez *et al*, 2017; Raghu *et al*, 2011b; Travis *et al*, 2013). Most often, the initial diagnosis is made using a high-resolution computed tomography (HRCT). Here ground-glass opacities in absence of traction bronchiectasis show high inflammatory activity. Trough serological testing it can be figured out, whether there is an underlying autoimmune disease or autoreactive component (Raghu *et al.*, 2011b). In

a minority of cases flexible bronchioscopy with bronchoalveolar lavage (BAL) and transbronchial biopsy (TBB) are performed. As goldstandard, Video-associated thoracic surgery (VATS) may be performed. VATS bears the risk of complications, including acute exacerbations of the underlying disease. New methods exist, such as transbronchial cryobiopsy which may be associated with reduced risks. Even though it may not be required in definite IPF, bronchoalveolar lavage (BAL) can be useful in diagnosing IPF (Raghu *et al.*, 2011b). Pulmonary function tests and blood gas analysis are often unable to provide precise information in terms of differential diagnosis, because all ILDs with fibrosis have a restrictive lung capacity and abnormal gas exchange (Buzan & Pop, 2015, Cottin *et al.*, 2018). Nevertheless, the severity of the disease and the prognosis can be better evaluated with those tests (du Bois *et al*, 2011; Flaherty *et al*, 2003; Gimenez *et al*, 2018; Jegal *et al*, 2005; Park *et al*, 2009) and lung function tests (particulary forced volme vital capacity (FVC)) are regularly used to monitor disease progression (Buzan & Pop, 2015). Table 1 shows the important subtypes of idiopathic intersitial pneumonias and their different clinical courses and diagnostic criteria.

Subtype	**IPF**	**DIP**	**RB-ILD**	**AIP**	**NSIP**
Progress	slow	slow	slow	acute	slow to acute
Nicotine consumption relevant	yes	yes	yes, always	no	no
BAL	Neutrophilia	Normal or unspecific	Normal or Neutrophilia	Neutrophilia	Neutrophilia and/or Lymphocytosis
HR-CT results *localisation*	Peripheral, basal, subpleural	Peripheral, basal	diffuse	diffuse	Peripheral, basal, subpleural
Ground-glass opacity in HR-CT	barely	yes	spotty	yes	yes
Response to steroids	low	yes	yes	low	yes
Mean survival time	2-3 years	12 years	No information	1-2 month	17 years

Differential-diagnosis	Sarcoidosis, collagenosis, exogenous allergic alveolitis (EAA)	EAA, Pneumocystis-jiroveci-pneumonia, RB-ILD	DIP, NSIP, EAA	Pneumonia, pulmonary edema, ARDS, eosinophilic penumonia	UIP, EAA, DIP

Table 1: Important subtypes of idiopathic interstitial pneumonia and their differences (modified from Hellmich, 2017).

1.3.2 Idiopathic Pulmonary Fibrosis: Definition and Epidemiology

Idiopathic pulmonary fibrosis (IPF) is a chronic, progressive disease of the lung parenchyma (Raghu *et al*, 2015) (Wilson & Wynn, 2009) (King *et al*, 2011). It is the most common type of idiopatic intersitital pneumonias (Hutchinson *et al*, 2015) with a mean survival rate of 2 to 3 years after diagnosis in absence of treatment (Raghu *et al.*, 2015) (King *et al.*, 2011). The incidence of IPF varies between 4,6 cases per 100.000 people per year (study from England (Gribbin *et al*, 2006)) and 6,8 – 16,3 patients per 100.000 people per year (study from USA (Raghu *et al*, 2006)). The incidence seems to be lower in Asia and South Africa, where it is estimated to range between 0,5 and 4,2 cases per 100.000 individuals per year. The disease is more common in men and people older than 50 years (median age at diagnosis around 65 years (Raghu *et al*, 2011a) (Raghu *et al.*, 2006)) and is associated with a positive smoking history (Raghu *et al.*, 2015) (Wilson & Wynn, 2009) (King *et al.*, 2011). The prevalence ranges between 2 to 29 cases per 100.000 people (Raghu *et al.*, 2015).

1.3.3 Clinical appearance

Clinical signs of IPF are characterized by chronic dyspnea and dry cough. On physical examination, inspiratory crackles can be auscultated over the lung bases in 90% of the cases and at the inspection of the extremities, clubbed fingers and other dyspnea signs like cyanosis can be seen in 30% of the cases (King *et al*, 2001). Pulmonary function tests reveal that IPF is a restrictive disease, with a decreased total lung capacity, decreased vital capacity, decreased compliance and is accompanied by abnormal gas exchange (lowered capacity for carbon monoxide diffusion) (Raghu, 2011). If

pulmonary function tests are performed in early diesease or in cases with coexisting emphysema which pseudonormalize volume, normal spirometry and plethysmography results come up and only an isolated reduction in diffusion is displayed. The diagnosis is often made in advanced states of IPF. Progression of the disease my be individually different: In some cases a high rate of exacerbations is observed and in other cases there is slow progression (Raghu *et al.*, 2015) (King *et al.*, 2011). After the onset of fibrosis, a progressive deterioration of the status of health appears until death due to respiratory failure or complications of comorbidities.

A high-risk group for rapid progression wih frequent exacerbations are men with a positive smoking history. This group amounts 5-20% of patients and severe hypoxaemia, with many newly appeared alveolar infiltrates, can be observed in case of exacerbation (Raghu *et al.*, 2015) (King *et al.*, 2011). Acute exacerbations with severe respiratory deterioration often occur together with fever and influenza like symptoms, which are idiopathic and not explainable by infections or other comorbidities (Collard *et al*, 2007). During an acute exacerbation new bilateral diffuse ground-glass opacities arise and previous symptoms deteriorate.

To confirm IPF, imaging via high-resolution computed tomography (HRCT) is performed. Signs which affirm the diagnosis IPF are subepithelial, basal retractions, traction bronchiectasis and clusters of subpleural, multilayer, cystic airspaces of similar diameters (3-10mm); defined as honeycombing. These hallmark characteristics, also called definite usual interstitial pneumonia (UIP) pattern, are predominantly found in the bilateral, peripheral and basal regions (Raghu *et al.*, 2011a) (Hansell *et al*, 2008) (Travis *et al.*, 2013) (Hunninghake *et al*, 2003). If still unconclusive, a histopathological investigation of tissue from 2 to 3 lung lobes is usually considered. Histologically, also a UIP pattern is observed, where regions of patchy interstitial fibrosis are found adjacent to healthy appearing areas and destruction of alveolar architecture. A typical histopathological feature of UIP are fibroblastic foci. There are no known biomarkers which prove the presence of IPF (Xaubet *et al*, 2017).

1.3.4 Pathophysiology of IPF

The cause of IPF remains unknown, but it is thought to be a consequence of multiple interacting genetic and environmental risk factors and repetitive local micro-injuries. In

the following course of events, aberrant epithelial-fibroblast communication is initiated, with the induction of matrix-producing myofibroblasts and extracellular matrix accumulation, resulting in a remodeling of the lung interstitium (Richeldi *et al.*, 2017) (figure 4).

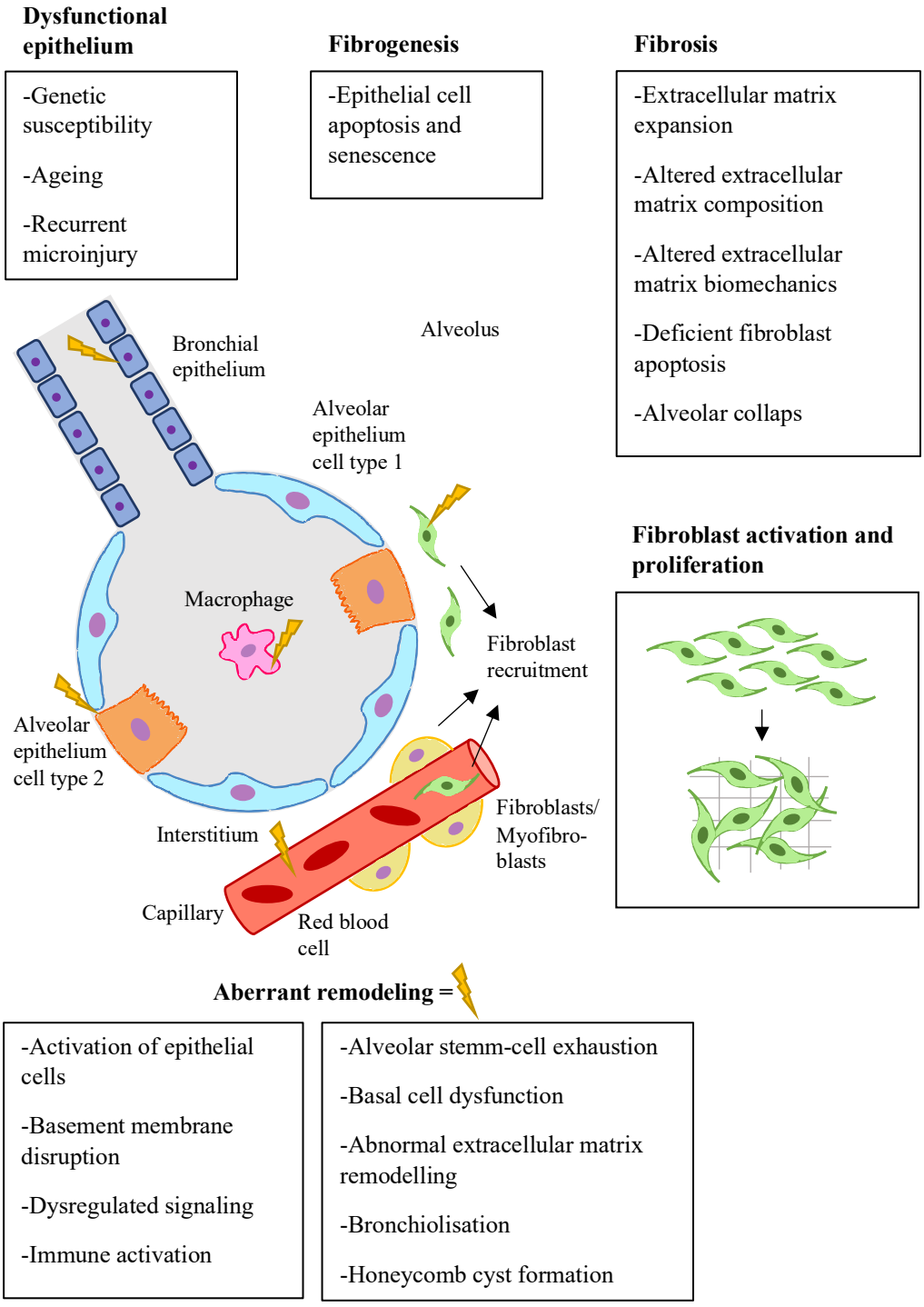

Figure 4: Pathophysiology of IPF including dysfunctional epithelium, fibrogenesis, fibrosis and aberrant remodelling (modified from Richeldi *et al.*, 2017).

Inflammatory processes can also be seen but they are usually mild and the interstitial infiltration of lymphocytes is not causative for the severe symptomes of IPF and for disease progression (Raghu *et al.*, 2015) (Wilson & Wynn, 2009) (King *et al.*, 2011). Causative factors are rathrer particulate inhalation (cigarette smoke, metal and wood dusts, agricultue and farming, viruses (Raghu *et al.*, 2011a) (Hubbard, 2001) (Taskar & Coultas, 2006)) and genetic susceptibility (Raghu *et al.*, 2011a) (Armanios *et al*, 2007; Cogan *et al*, 2015; Kropski *et al*, 2012; Nogee *et al*, 2001; Stuart *et al*, 2015; Tsakiri *et al*, 2007; Wang *et al*, 2009). Genetic polymorphisms were found to increase the risk of IPF. The development of IPF is associated with mutations in surfactant protein C, surfactant protein A2, and genes that stabilize telomere length. Deficiency of surfactat protein C could lead to recurrent atelectasis, lung injury, and inflammation (Nogee *et al*, 2001). Taken together, these mutations cause a small proportion of the population risk of IPF (Seibold *et al*, 2011). Moreover single-nucleotid polymorphisms (SNPs) of MUC5B (Mucin 5 B) and TOLLIP (Toll interacting protein) (both located on chromosome 11) are more often found in IPF lungs than in healthy donor lungs (minor allele of MUC5B detected in 38% among IPF lungs and 9% among controls) (Seibold *et al*, 2011). Bonella et al. investigated that the minor allele of TOLLIP indicates a worse survival and more rapid disease progression of IPF (Bonella et al, 2021).

Maladaptive repair processes

As described in the chapter above, injuries of the lung require effective repair processes to ensure its physiological functions. In case of IPF, chronic dysregulation of alveolar epithelial cells Type 2 (AECII) lead to maladaptive repair processes, since these cells also function as stem cells and are responsible for the renewal of AECI cells during homoeostasis or injury (Desai *et al*, 2014) (Rock *et al*, 2011). Moreover, abnormal AECII are found especially attached to the typical fibroblast foci (Selman *et al*, 2001) and both, fibroblasts and myofibroblasts are subepithelially located at the transition between healthy lung tissue and fibrotic parts (Raghu *et al.*, 2015) (Scotton & Chambers, 2007) (King *et al.*, 2011). In particular, there is premature shortening of AECII telomers and a resistance against apoptosis, which consequently leads to remodeling and fibrosis in mouse models (Naikawadi *et al*, 2016) (Alder *et al*, 2008) (Kropski *et al*, 2015). Activated dysregulated AECII secrete fibrogenic growth factors and cytokines like Transforming Groth Factor ß (TGFß) and Platelet Derived Growth

Factor (PDGF) consequently, which leads to aberrant epithelial mesenchymal cross-talk and ultimately results in the recruitment and activation of myofibroblasts (Horowitz & Thannickal, 2006). Myofibroblasts play a central role in the pathogenesis of IPF since they produce a large amount of extracellular proteins, especially myofibrils. The extracellular matrix depots transform into scar tissue which further disrupts gas exchange and the normal alveolar architecture (King *et al.*, 2011). Recruitment of myofibroblasts is implemented largely through transdifferentiation from a local resident mesenchymal cellpool called lipofibroblasts; to a minor degree also by recruition of lung interstitium pericytes, circulating fibrocytes; epithelial-mesenchymal transition and endothelial-mesenchymal transition (Rock *et al.*, 2011). Another central process leading to IPF is the bronchiolization of alveolar tissue. Basal cells, which are stem cells located in the conducting airways are suspected to play an important role in this process especially when the alveolar progenitors are exhausted. In response to the damage of the alveolar epithelium they activate developmental pathways (Chilosi *et al*, 2003) which result in re-epithelisation of alveolar tissue (Boers *et al*, 1998) (Hong *et al*, 2004) (Chilosi *et al*, 2002) (Korfei *et al*, 2015).

1.3.5 Therapy

Depending on the stage of the disease there are different types of therapy (Fig 5). Antifibrotic treatment with one of the authorized drugs Nintedanib or Pirfenidone nowadays represent the most important medical treatment modality, which slows down disease progression and prolonges survival times. At later stages palliative care becomes more important. Lung transplantation should be offered to suitable conditions early, but is undertaken only in a minority of subjects (Anstrom *et al*, 2012) (Noth *et al*, 2012).

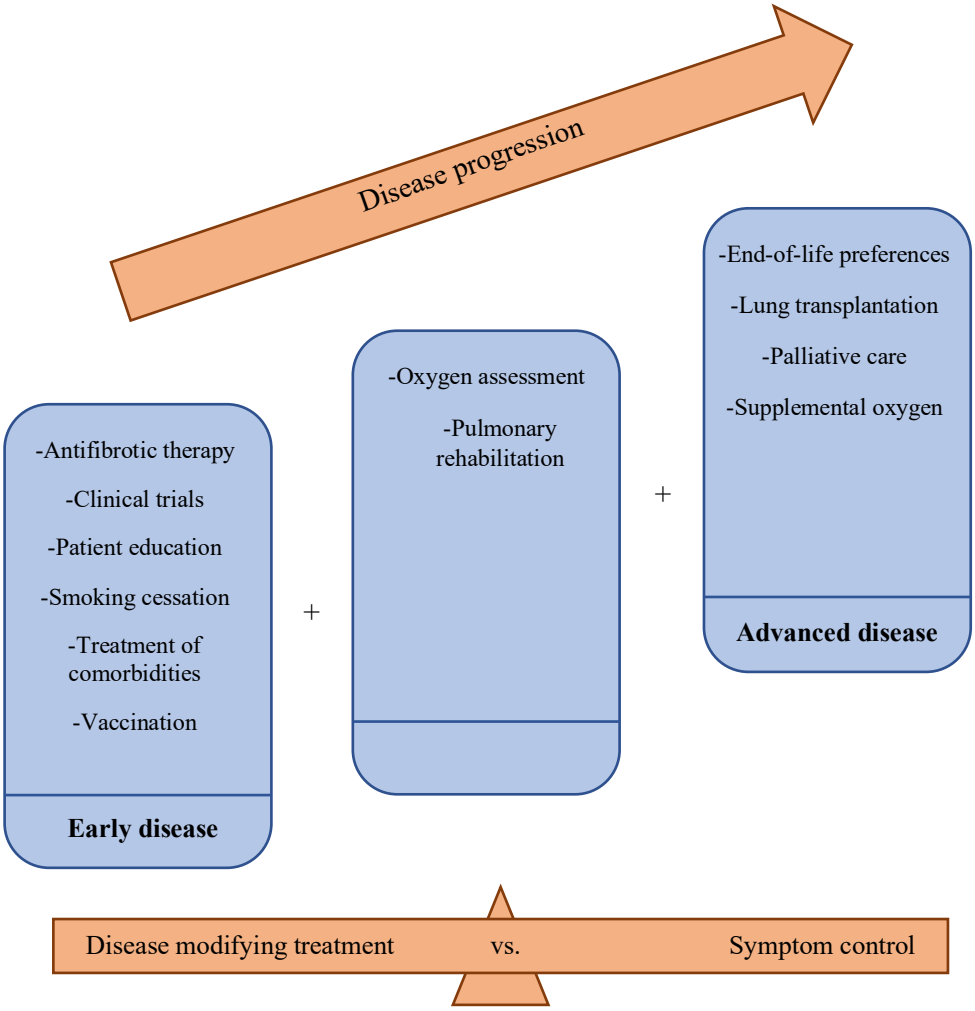

Figure 5: Therapy of IPF depends on the progression of the disease (modified from Richeldi *et al.*, 2017)

Nintadanib is a tyrosine kinase inhibitor, which suppresses multiple signaling receptors like the fibroblast growth factor receptor, platelet-derived growth factor receptor and the vascular endothelial growth factor receptor (Hilberg *et al*, 2008) (Chaudhary *et al*, 2007). The precise mechanism of Pirfenidone is not fully understood yet. However, it is an orally admistered pyridine and shows combined anti-inflammatory, anti-oxidant and anti-fibrotic effects, broadly explained by the regulation of TGFß in vitro and inhibition of fibroblast- and collagen synthesis in animal models (Schaefer *et al*, 2011). Both drugs have similiar effects on the rate of decline in forced vital capacity over 1 year and reduction in mortality (Richeldi *et al*, 2014) (King *et al*, 2014) (Noble *et al*, 2011). Moreover, both therapies have acceptable tolerability and require regular monitoring of liver function. To slow down the irreversible destruction of lung tissue, the disease modifying therapy is started as early as possible.

Besides the treatment of the lung fibrosis itself, complications like pulmonary hypertension are under discussion for treatment. However, there is no clinical evidence yet showing a therapeutic effect of pulmonary vasoactive drugs in IPF, with the exeption of inhaled Iloprost in advanced IPF. However, long term oxygen therapy is recommended (Hellmich, 2017).

A radical treatment is performing a lung transplantation, which has a 5 year post-transplantation survival rate of about 50% (Raghu *et al.*, 2011a) (Kistler *et al*, 2014). There are many comorbidities which develop as a result of the pathogenesis of IPF which may exclude transplantation, therefore this possibility is considered early in disease. Another column of disease treatment is symptom focused therapy. This includes opiates, which may reduce anxiety, dyspnea and cough (Bajwah *et al*, 2013) and other therapies including pulmonary rehabilitation (Ryerson *et al*, 2014), education programmes, supplemental oxygen therapy and palliative care (Richeldi *et al.*, 2017).

2. Material and Methods

2.1 Material

2.1.1 Equipments

Instrument	**Manufacturer**
Analytical balance	IKA®
Cell culture hood	Heraeus-Thermo scientific
Cell culture plates (10cm)	Satstedt, Germany
Cell culture plates (6 well)	Sarstedt, Germany
Centrifuge (table top)	Hettich 200
8-well chamber slides	VWR
Cooling centrifuge	Hettichmikro 200R
Centrifuge (rotina 380R)	Hettich
Falcon tubes	BD Falcon, USA
Glass slides for IHC	Langenbrinck, Germany
Cell culture incubator, Hera cell, 150i	Thermo scientific
Magnetic stirrer	Heidolph, Germany
Cell Scraper	Sarstedt, Germany
Plate reader for determination of protein concentration	Tecan
SDS gel apparatus	Keutz labor technic
Transfer chamber	Bio-rad
Chemiluminischence imager	INTAS, Germany
Imager-Software	INTAS, Germany
PVDF transfer membrane	Thermoscientific
Water bath	Julabo
Thermo mixer	IKA®
Shaker	Grant-bio
Light-microscope	Nikon eclipse Ts-100
pH-Meter	Hanna instruments
IHC slide scanner	Hamamatsu

Fluorescence microscope	Leica, Germany
Vortex machine	VWR, Germany
Precellys vials and Bulk Beads	Peqlab, Germany
Homogenizor	Peqlab, Germany
Pipette	Eppendorf, Germany
Pipette boy	Eppendorf, Germany
Pipette tips	Biozym, Germany
NDP view software	Hamamatsu Photonics, Germany
Image J software	National institute of health, USA
Graph Pad Prism	Graphpad software, Inc.
Leica application suite Advanced Fluorescence (LAS AF) software	Leica, Germany
Spin down	VWR, Germany

Table 2: Instruments/Manufacturer

2.1.2 Reagents

2-(4,2-hydroxyethyl)-piperazinyl-1-Ethansulfonate (HEPES)	Sigma Aldrich, Germany
2-amio-2-hydroxymethyl-1,3-propanediol (TRIS)	Roth, Germany
2-mercaptoethanol	Sigma Aldrich, Germany
Acrylamide solution, Rotiphorese Gel 30	Roth, Germany
Agarose (DNA electrophoresis)	Carl Roth
Ammonium persulfate (APS)	Roth, Germany
Amiodarone	Sigma Aldrich, Germany
Bleomycin	Hexal
Bovine Serum Albumine (BSA)	Roth, Germany
Dimethyl-Sulfoxide (DMSO)	Sigma Aldrich, Germany
D-MEM-F12 medium (Dubecco's modified eagle's medium)	GIBCO Invitrogen, Germany
Dulbecco's phosphate buffered saline (PBS)	PAA, Austria
Ethanol 70%, 95%, 100%	Fischer scientific, Germany

Ethylenediamine-tetraacedic acid (EDTA)	Sigma Aldrich, Germany
Fetal calf serum (FCS)	Roth, Germany
Glycerol mountig medium	Dako cytomation, Gemany
Glycerol	Roth, Germany
Haemalaun	Roth, Germany
Hydrochloric acid (HCl) 32%	Roth, Germany
Methanol	Fuka Chemie, Switzerland
Milk powder	Sigma Aldrich, Germany
NaCl (Sodium chloride)	Roth, Germany
Normal donkey serum	Johnson Immuno
N,N,N',N'-tetramethyl-1,2-diaminomethane (TEMED)	Sigma Aldrich, Germany
Penicillin/Streptomycin	PAA, Austria
Pierce ® BCA protein Assay Kit	Thermo scientific, USA
PMSF (Phenylmethylsulfonylfluorid, Proteinase Inhibitor)	SERVA Electrophoresis GmbH, Germany
Protease inhibitor cocktail complete	Merck
Sodium dodecyl sulfate (SDS)	Sigma Aldrich, Germany
Sodium hydroxide (NaOH)	Sigma Aldrich, Germany
Triton-X-100	Sigma Aldrich, Germany
Trypsin/EDTA	PAA, Austria
Tween 20	Sigma Aldrich, Germany

Table 3: Chemicals and Reagents

2.1.3 Antibodys

Primary:

Primary antibody	**origin**	**dilution**	**Company/catalog number**
TDP43	rabbit	1:100 (IHC, IF)	Cell Signaling, A260
	rabbit	1:1000 (WB)	Protein Tech, 10782-2-AP
	rabbit	1:500 (WB)	Sigma, SAB420223
FUS	mouse	1:50 (IHC)	Santa Cruz, 4H11

	rabbit	1:250 (WB), 1:50 (IF)	Thermo Fisher, PA5-27531
SRF	rabbit	1:500 (WB), 1:250 (IF, IHC)	Invitrogen, 720240
MBNL1	rabbit	1:50 (IF)	Genetex, GTX33335
	mouse	1:50 (WB)	Santa Cruz, Sc47740HRP
PABC1	rabbit	1:50 (WB)	Proteintech, 10970-1-AP
TIA1-HRP	mouse	1:100 (WB)	Santa Cruz, sc166247
GAPDH (14C10)	rabbit	1:30.000 (WB)	Cell signaling, 2118s
ß-Actin	rabbit	1:30.000 (WB)	Abcam, ab8227
pro SP-C	rabbit	1:500 (IF, IHC)	Millipore, AB3786
Alpha-SMA	rabbit	1:100 (IHC)	Abcam, ab5694
Lamin B1	chicken	1:300 (WB)	Abcam, ab90169
LAMP1	rabbit	1:50 (IF)	Abcam, ab24170

Table 4: Primary antibodies

Secondary:

Secondary antibody	**origin**	**dilution**	**Company**
Polyclonal Rabbit anti Mouse, HRP	rabbit	1:2000	Dako, Denmark
Polyclonal Swine anti Rabbit, HRP	swine	1:2000	Dako, Denmark

Table 5: Secondary antibodies

2.1.4 Buffer

-Protein extraction: 50 mM Tris, pH=7,5

5 mM EDTA

150 mM NaCl

1% (w/v) Triton x-100

0,5% (w/v) Na-Deoxycholat

1 mM PMSF

-Western Blot analysis:

- Seperating Gel buffer: 1,125M Tris
  - pH 8,8
  - 30% Saccharose

- Stacking Gel buffer: 0,625M Tris
  - pH 6,8

- SDS Running buffer (PAGE): 25 mM Tris
  - 192 mM Glycin
  - 0,1% SDS

- 4x SDS-loading buffer: 5 g SDS
  - 40 ml glycerin
  - 25 ml stacking gel buffer
  - 0,01 g bromophenolblue

  For a final volume of 100 ml

- Transfer buffer: 20 mM Tris
  - 159 mM Glycine
  - 20% MeOH

- Wash-buffer (TBS-T 10x): 1M Tris
  - 4M NaCl
  - 1% Tween-20
  - pH 7,5

- Block solution: Skim Milk powder 5%
    - TBS-T 1x

- Stripping buffer: TBS-T 1x
    - 2% SDS
    - 100 mM ß-Mercaptoethanol

-IH and IF:

- Citrate buffer: 2,94 g Trisodium citrate dihydrate
    - 1000 ml H2O dest
    - pH 6
    - 0,5% [v/v] Tween-20

2.1.5 Gels

Separating Gel

	8%	9%	10%	12%	15%
Rotiphorese	5,31 ml	6,0 ml	6,66 ml	8 ml	10 ml
Dest. H2O	7,74 ml	7,06 ml	6,4 ml	5,06 ml	3,06 ml
10% SDS	200 µl	200 µl	200 µl	200 µl	200 µl
Separating gelbuffer	6,66 ml	6,66 ml	6,66 ml	6,66 ml	6,66 ml
10% APS	100 µl	100 µl	100 µl	100 µl	100 µl
Temed	40 µl	40 µl	20 µl	20 µl	20 µl

Table 6: Separating Gel

Stacking Gel

Rotiphorese	1,33 ml
Dest. H2O	6,57 ml
10% SDS	100 µl
Stacking-buffer	2 ml
10% APS	100 µl
Temed	10 µl

Table 7: Stacking Gel

2.1.6 Kits

Product	**Manufacturer**
Zytochem AP fast red kit, broad spectrum	Zytomed systems, Berlin, Germany
BCA protein assay kit	Pierce, Germany
Nuclear and cytosolic extraction kit	Invitrogen

Table 8: Kits

2.2 Methods

2.2.1 Human lung tissue and primary cells

Lung tissue samples were attained from 11 patients with sporadic IPF (mean age ± SD: 57.64 ± 7.3 years) and 10 non-diseased control subjects (organ donors, mean age ± SD: 49.42 ± 16.4 years) under informed consent (European IPF Registry and Biobank, V54 – 19 c 20 15 (1) GI 20/20 Nr. 109/2011). Explanted lungs were obtained from the Department of Thoracic surgery, Vienna, sampled and stored at the biobank of the Universities of Giessen & Marburg Lung Center (UGMLC), Gießen. All IPF cases were diagnosed as stated by the American Thoracic Society/European Respiratory Society consensus criteria (2000). The study protocol was approved by the Ethics Committee of the Justus-Liebig-University School of Medicine (111/08 and 58/15). Primary human lung fibroblasts were isolated from explanted IPF (n=5) and control lungs (n=5) followed by an outgrowth technique as described before (Conte *et al*, 2013) and were cultured in Dulbecco's Modified Eagle Medium (DMEM F12) supplemented with 10% FCS, 1% pencillin/ streptomycin, 1% L-Glutamine and 1% non-essential amino acids. All experiments with primary cells were carried with cells between passages 3 and 5.

2.2.2 Precision cut lung slices (PCLS)

About 2-3 PCLS from each IPF patient were pooled and PCLS from three IPF patients were used. Fresh 300 µm thick PCLS were received from the UGMLC biobank from three IPF patients (Mean age of 56.0 ± 8.2 years (SD)). PCLS were maintained in culture medium containing phenol red free RPMI (Roswell park memorial institure 1640 medium), 10% FCS, 1% pencillin / streptomycin. 1 M Pirfenidone (Sigma) stock solution was prepared in sterile filtered DMSO (Dimethylsulfoxid). Each PCLS was treated with vehicle (DMSO) or with 2.7 mM Pirfenidone every day for 48 hours. On the third day, PCLS were fixed in formalin and embedded in paraffin. Embedded blocks were sectioned (3 µm thickness) using a microtome.

2.2.3 Mice

Intratracheal administration of vehicle or amiodarone (0.8 mg/kg body weight, Sigma-Aldrich, Germany) was performed in C57BL/6 mice as established in our lab and as

described before (Mahavadi *et al*, 2014). The treatment of the mice was performed with standard lab procedures as described before (Mahavadi *et al*, 2010). The study protocol was approved by both the University Animal Care Committee and the Federal Authorities for Animal Research of the Regierungspraesidium Giessen (Hessen, Germany) (Proposal Nr. GI 20/20-Nr. 109/2011).

2.2.4 Cell culture

Mouse lung epithelial cells (MLE12) were cultered in DMEM-F12 medium supplied with 10 nM Hydrocortisone, 10 nM Hydrobeta estradiole, 50 µg/ml Insulin, 10 µg/ml Transferrin, 30 nM Na-Selentine, 10 nM HEPES, 2 mM L-Glutamine, 2% FCS and Penstrep. They were grown in an incubator with 95-100% air-humudity and 5% CO2 at 37°C. Upon reaching confluency, cells were washed with 1xPBS to remove magnesium since this inhibits the action of trypsin. Next, trypsin was added and the cell plates were incubated for 2 min in 37°C to enable the detachment of the cells. Afterwards trypsin was removed and 2 mL of fresh culture medium was added. By pipetting the medium up and down, cells were stripped and transferred into a falcon and were freshly plated depending on the desired dilution.

2.2.5 Treatment of MLE12 cells with amiodarone

MLE 12 cells were treated with 10 mg/ mL (14.6 nM) amiodarone. For this, 5 mg of amiodarone hydrochloride (Sigma) was dissolved in 5 mL sterile cell culture grade aqua dest as described before (Mahavadi *et al.*, 2014). The tube was then warmed to 65°C for 10 minutes and the final volume was made up to 50 mL using warm growth medium and vortexed. Vehicle was prepared in the same way with the exception of amiodarone. 1 mL of this stock solution was added to a 10 cm culture dish with MLE12 cells containing 9 mL medium. Cells were then harvested at the indicated time points.

2.2.6 Protein extraction and quantifiction from cells

After treatments, cells were shockfrozen and stored at -80°C. To extract proteins, protein extraction buffer was prepared with fresh phenylmethylsulfonyl fluoride (PMSF) (1:100). Cells were scraped and crude lysates were transferred to Eppendorf tubes. In order to shear the DNA, the crude lysates were sonicated followed by

centrifugation at 15000 RPM for 15 min at 4°C. The supernatant was collected in a new tube and the pellet was discarded. Protein concentration was determined by Bicinchoninic acid (BCA) method, a colorimetric detection system using cuprous cations. Formation of BCA and copper complexes results in a linear absorbance at 562 nm that increases with increased protein concentration. A serial dilution was created using bovine serum albumine (BSA). A standard curve was created using 2000 µg/ml BSA, follwed by 1500 µg/ml, 1000 µg/ml, 750 µg/ml, 500 µg/ml, 250 µg/ml, 125 µg/ml, 62,5 µg/ml, 31,25 µg/ml, 15,625 µg/ml and 7,813 µg/ml. The protein probes were diluted 1:10 in NaCl and were pipetted in duplicates in a 96 well plate besides the BSA solutions. After adding 200 µl of the BCA working reagent (1:50) the probes were incubated for 30 min at 37°C and the absorbance was measured at 565 nm in an ELISA (Enzyme-linkedmmunosorbent Assay) plate reader. With the aid of the standard curve, the corresponding protein concentrations were calculated.

2.2.7 Nuclear and cytosloic fractions from cells

Following vehicle/amiodarone treatments, cells were scraped on ice and transfered into a falcon tube. Tubes were centrifuged for 5 min at 4°C at 1000 rpm. The pellet was resuspended in 1.5 ml icecold PBS and followed by centrifugation for 5 min at 4°C with 1000 rpm. The supernatant was discarded and the pellet was stored in -80°C. The next day, the nuclear and cytosolic fractioning kit (Invitrogen) was used and further steps were carried according to the manufacturer's instructions. Briefly, in the first step, NE1 (nuclear extract) was 1:10 diluted in A. dest. together with 1 µl DTT (Dithiothreitol) and 1 µl PIC (protease inhibitor cocktail Complete ™). The pellet was resuspended in 100 µl of this buffer and incubated on ice for 10 min. Next, the sample was vortexed for 10 s and centrifuged at 12000 rpm and the supernatant was transferred into a new tube which is the cytosolic fraction. The pellet was resolved in NE2 buffer and was kept for 15 min on ice. Next, the sample was vortexed every 3 min for 5 s. Nuclear fraction was enriched by centrifuging this sample at 14000 rpm at 4°C.

2.2.8 Protein extraction from human lungs and mouse lungs

Frozen lung tissue in liquid nitrogen was cut and filled into precellys vials together with Bulk Beads and buffer consisting of protein extraction buffer and PMSF. The vials were

placed into a homogenisator which downsizes the lung tissue-particles. To ensure that the cell walls and the DNA were destroyed, an additional treatment with the sonicator was performed. The samples were then centrifuged at 4°C for 10 min at 15000 rpm and the supernatant was saved two times and inbetween again centrifuged with the same settings. Before using the lysates for Western Blots, protein concentration was measured with the BCA method.

2.2.9 Polyacrlyamide Gel Electrophoresis of Protein (SDS-Page)

Lung- or cell-homogenates were mixed in ratio 1:3 with buffer containing 10% ß-Mercaptoethanol to reduce disulfide bridges to thiols and 4x SDS-loading buffer to charge the polypeptides negatively. Proteins were denaturated by heating up to 98°C for 12 min and afterwards collected by brief centrifugation and stored in -20°C. Now the protein extracts were able to be seperated by SDS polyacrylamide gelelctrophoresis. The negative charged polypeptides migrated to the positive electrode and the mobility of the polypeptides increased linearly according to the protein size. Consequently the pieces with a smaller molecular weight went further than the ones with a higher molecular weight. After the stacking and seperating gels were prepared, samples were loaded and electrophoresis was performed. In the presence of SDS running buffer and at 95 V, proteins migrated and were stopped when the bromphenolblue reached the bottom of the seperating gel.

2.2.10 Immunoblotting

After separating the proteins in the SDS polyacryamide gel, they transferred to a polyvinylidene fluoride (PVDF) membrane. The transfer was prepared by activating PVDF membrane with methanol and stacking the transfer equipment onto the electroblotting chamber. The first two layers were Whatmann 3 mM filter paper, followed by activated PVDF membrane. Both were washed with transfer buffer and encased with a sponge. The next layer was formed by the gel and two other sheets of filter paper, also washed with transfer buffer. Immunoblotting was performed at a constant voltage of 100 V for 90 min at 4°C. Afterwards, the membrane was blocked with 5% milkbuffer (blocking solution) for 1 h at RT (room temperature) and then incubated overnight at 4°C with the primary antibody diluted in 5% milkbuffer. The

next day the membrane was washed 4 times with 1x TBST for 15 min each, before it was incubated with the respective secondary antibody at RT for 1h. It was washed 4 times for 15 min with 1xTBST again and then the polypeptide bands were detected by ECL (Enhanced Chemi-luminescence) treatment. Therefore, the membrane was exposed to ECL films in the dark and bands on the film were visualized by dipping them in developing and fixing solutions. If necessary, the membranes were stripped and re-probed by washing them 2 times in 1xTBST for each 5 min and then putting them into 0,2M NaOH solution 2 times for each 15 min. Afterwards the membranes were cleaned with A. dest and then blocked again for 1 h in blocking solution and then the appropiate first antibody was added and they were treated like described above.

2.2.11 Densitometry

Densitometry was performed with Image J, Excel and Graph Pad Prism. Image J was used to measure the size of the bands and the results were transferred to Excel where the average of one group was built in relation to GAPDH values. To visualize the data Graph Pad Prism was used by employing Mann-Whitney U-test or Kruskal-Wallis post test.

2.2.12 Immunohistochemistry

Immunohistochemistry (IHC) was performed in order to visualize the location and the amount of the proteins of interest directly on the sections. This involved working with labeled antibodys, which enter specific antigen-antibody interactions that are visualized by a marker. Serial sections have been used, where the same cells are represented and stained at different sections, which allows a control of the expression of the cell type and the protein of interest (dertermine AECll cells: pro-SP-C, fibroblasts: alpha-SMA).

For all the immunohistochemical stainings Zytochem-AP fast red kit from the company Zytomed Systems (Berlin, Germany) was used. The paraffin embedded sections of lung tissue had been entparaffinized and rehydrated after they were heated to 60°C for 90 min. Therefore, the sections had been immersed for 10 min in a Xylol-bath and afterwards in a descendig alcohol series consisting of 99,6% Ethanol, 96% Ethanol, 80% Ethanol, 70% Ethanol, 50% Ethanol each for 3 min. Sections were washed in 1x PBS to remove traces of alcohol and antigen retrieval was performed by heating up the

sections with a microwave while they stood in the citrate buffer. Following this, the sections were blocked for 10 min with blocking solution and washed before and afterwards with 1xPBS. The primary antibody dilutions were prepared in 3% BSA solution and additionally a negative control was prepared, where the primary antibody was omitted and only the BSA solution was applied. The sections were incubated with the primary antibody overnight at 4°C in a humid chamber. Before the secondary bioethinylated antibody was added, the sections needed to be washed 5x with PBS. After 10 min incubation at RT they were washed and an enzyme conjugate (streptavidin/alcalic phosphate conjugate) was dropped on the tissue and washed away after 10min with 1xPBS. For developing, developing tablets from the Zytochem-AP fast red kit were solved in substrate buffer (naphtol phosphate buffer) and this solution was applicated on each section. The development of a colourbuilding in the dark was constantly monitored under the light microscope. The reaction was stopped for all of the sections by putting them into A. dest. when a sufficient colour was registered in one of the sections. This required between 3 and 15 min depending on which first antibody was used. Counterstaining with Haemalaun for 2 min was done to stain the nuclei, followed by washing the slides under running tap water. The sections were fixed with mounting medium and then were allowed to dry.

2.2.13 Immuofluorescence mikroscopy

The aim of immunofluorescence microscopy is to portray the localisation of proteins in the cell. For closer analysis we did costainings with the protein of interst and a marker (alpha-smooth muscle actin) for fibroblasts.

Random IPF and Donor sections or IPF PCLS sections were used and they were treated the same way as described in the immunohistochemnistry protocol until the the antigen induced heat retrieval. Afterwards the cells were blocked for 30 min with 5% donkey serum at RT and were then washed 3 times with 1xPBS. The second blocking step was performed with 3% BSA for 1 h at RT and then the first antibody was diluted in 3% BSA and was afterwards added overnight at 4°C. At the next day the sections were washed properly 5 times with 1xPBS and then treated with secondary fluorescing antibody (Alexa Flur 555 nm, 488 nm) and then incubated for 1 h in the dark. The slides were washed again with 1xPBS and then the sections were fixed with VECTASHIELD

mounting medium, that contains DAPI and stains the nuclei. For analysis Leica Application Suite Advanced Fluorescence (LAS X) software was used.

2.2.14 Transfection of primary fibroblasts

Interstitial fibroblasts were available from the UGMLC biobank. Cells were cultured and upon reaching confluency, transfection of empty GFP plasmid or FUS-GFP was performed using Xtreme gene DNA transfection reagent (Sigma) as per manufacturer's instructions. Transfection mixture was prepared using 2 µL of transfection reagent and 2 µg of plasmid in 100 µL serum free medium mixed gently and was incubated at room temperature for 15 minutes. The transfection mix was then added in a drop wise manner in respective wells containing 2 mL of culture medium, then cells were harvested 24 hours post-transfection.

Turbo-GFP tagged human FUS plasmid (Ref. sequence: NM_004960.2, NP_004951.1) was ordered from Origene. Plasmid purification was performed using endotoxin free plasmid purification kit from Qiagen.

2.2.15 Mikroskopy

For Immunfluorescence images the Leica M205 FA fluorescent stereoscope (Leica Microsystems) equipped with a Leica DFC360 FX camera was used. We were capturing the images using an 60x objective lens. Afterwards Immunofluorescence images were analyzed with Leica Application Suite Advanced Fluorescence (LAS AF) software, version 4.3. For IPF fibroblast immunofluorescence we used n=5 slides for each protein of interest and alpha SMA as a costaining. We performed Pirfenidone IPF PCLS IF and used n=2-3 slides. For every slide we took at least 3 fields of views and used the most representative one for our results.

IHC slides were microskoped and scanned with Hamamatsu scanner (Nanozoomer 2.0 RS; HamamatsuPhotonics, HamamatsuCity, Japan). For Donor and IPF tissue and AD and vehicle treated mice we used the material of each n=5-6 patients/mice. We captured images with the magnification x 400 and then used NDP.view 2.0 software for analyzing the images.

2.2.16 Statistics

For statistical comparison all data are expressed as means, ± SD. For every analysis there were at least 2 independent experiments performed. The programs ImageJ and GraphPadPrism 5.0 were used. Statistical significance was applied using one-way Anova followed by Kruskal-Wallis post test for comparison between multiple groups and Mann–Whitney U test for comparing two groups. P value summary: *P≤.5, **P≤0.01, ***P≤0.001.

3. Results

3.1 Investigating expression of RBPs in healthy and fibrous lung tissue

Firstly, we prepared total homogenates of lungs from donors as well as IPF lungs. Denatured lung homogenates were then subjected to western blotting for known RBPs: SRF, FUS, MBNL1, TDP43, PABPC1, and SG markers: TIA-1 and G3BP1. Significant differences in the levels of these proteins were not observed between donor and IPF lung tissues (Figure 6).

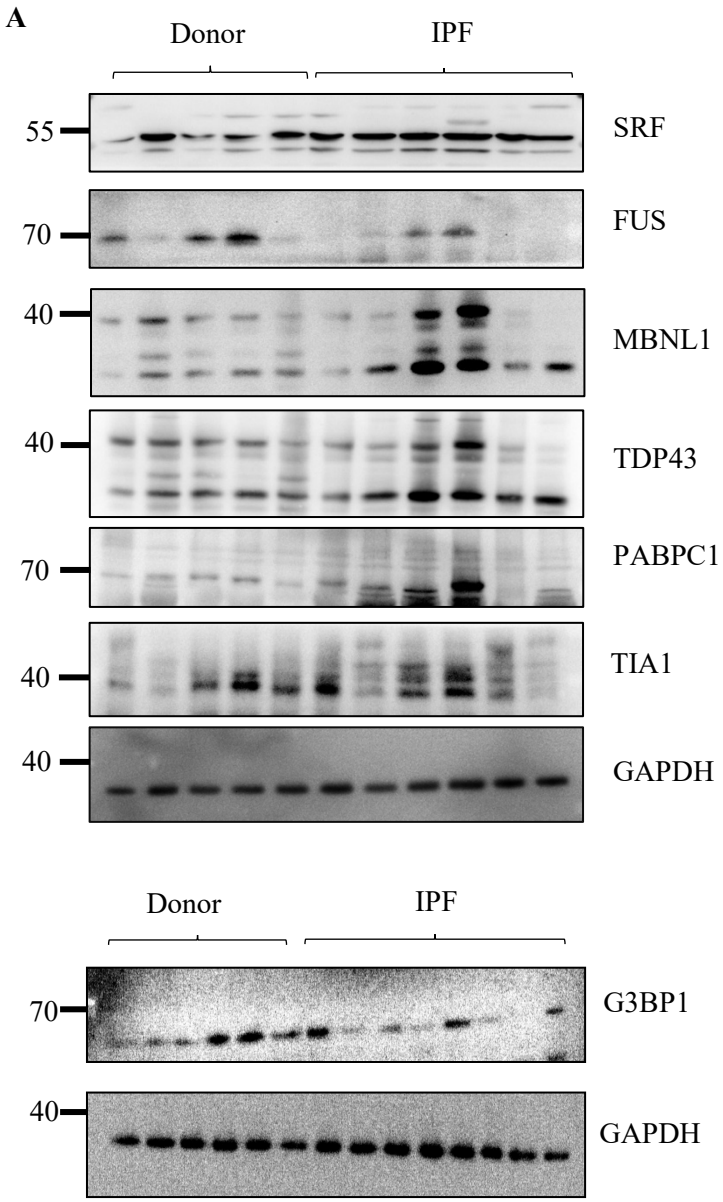

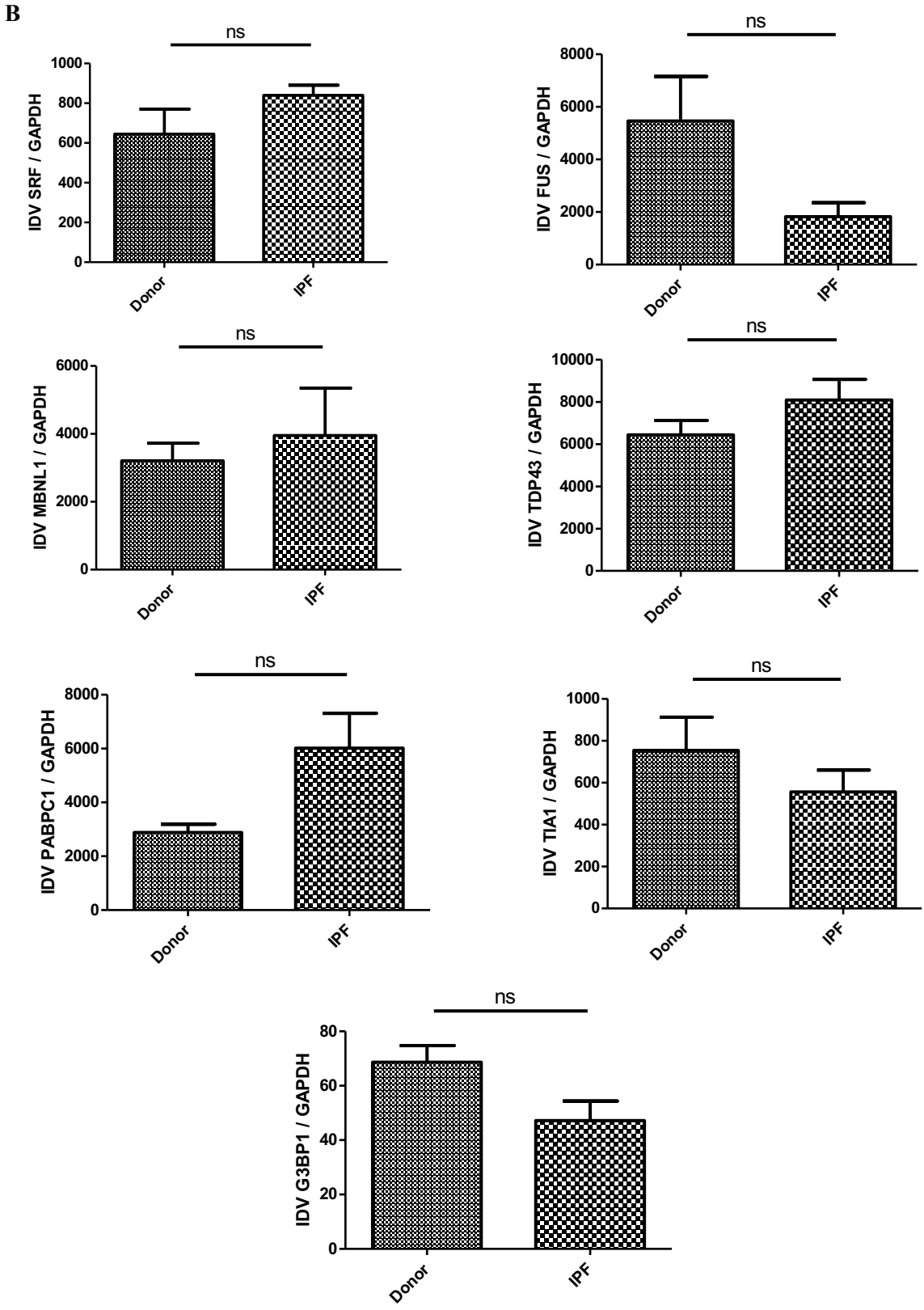

Figure 6: RBPs are not significantly elevated in human lungs from IPF patients
(A) Representative Western Blot images for SRF, FUS, MBNL1, TDP43, PABPC1, TIA1 (IPF n=6 and Donor n=5), G3BP1 and GAPDH as a loading control (IPF n=8 and Donor n=6) from human lung homogenates. (B) Densitometry analysis of RBP and GAPDH (loading control). Target protein*100/GAPDH ratio was calculated and depicted as bar graphs. **p < 0,01, *p < 0,05, ns – no significance.

3.2 RBP homeostasis is also altered in AECll cells of IPF patients

We then asked if altered RBP homoestasis is also observed in other important cell types like the AECII of IPF patients. For this, we performed immunohistochemistry for specific RBPs and SG-markers as well as for the AECII marker, pro SP-C on serial lung sections of IPF and organ donors. We observed a prominent nuclear as well as cytoplasmic staining for TDP43 in IPF versus Donor AECII (Figure 7A, B). FUS protein, on the other hand, was only slightly increased in AECII and fibroblasts of IPF patients (Figure 8A, B). SRF is not altered in AECII of IPF patients compared to Donors (Figure 9A, B). Results until this point indicate that RBP homeostasis is disturbed in both, fibroblasts a well as in the AECII of IPF patient lungs.

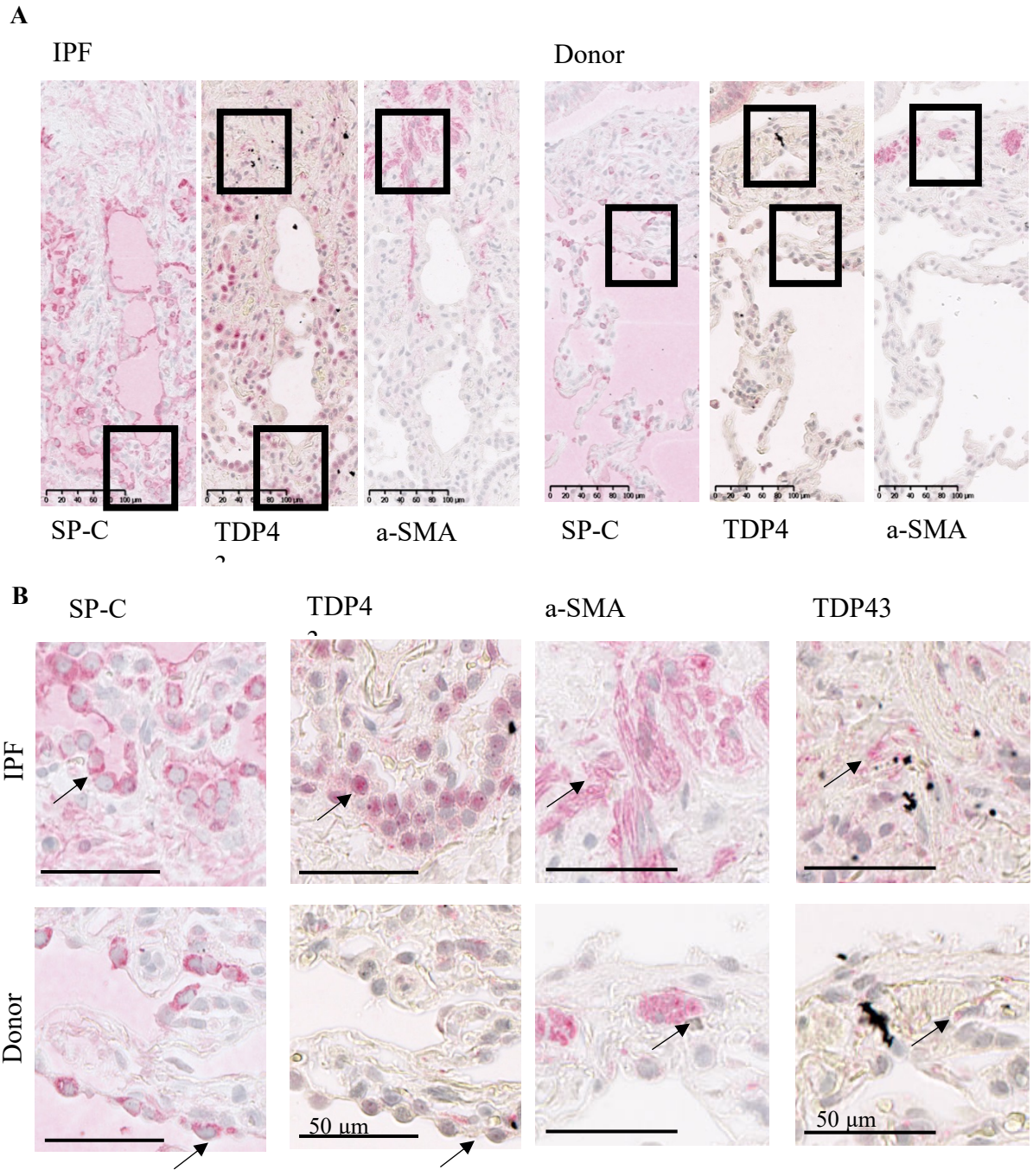

Figure 7: TDP43 is increased in AECII and fibroblasts of IPF patients
Immunohistochemical analysis of serial sections of IPF and donor lungs. (A) Overview of IPF and Donor sections. Scale bar=100 µm (B) Figure of representative cells, in the upper row IPF cells and in the lower row Donor cells. SP-C staining indicates AECll and a-SMA fibroblasts and arrows highlight representative cells on serial sections. Scale bar= 50 µm, n=5 Donors, n=6 IPF patients. Original magnification: x40

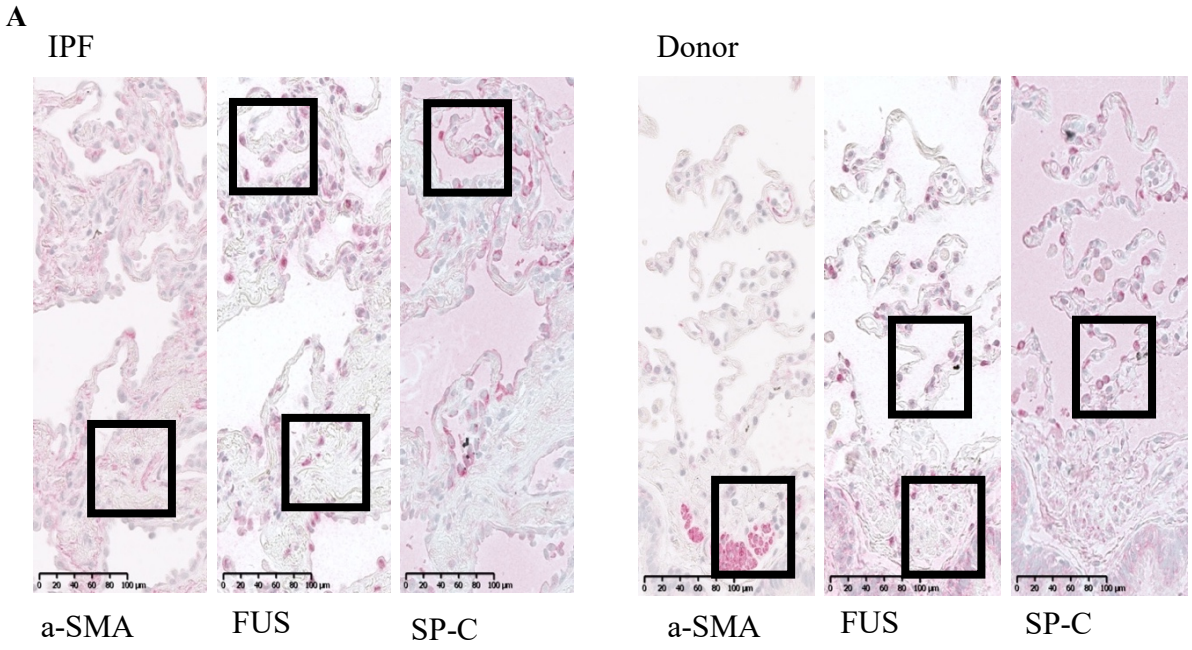

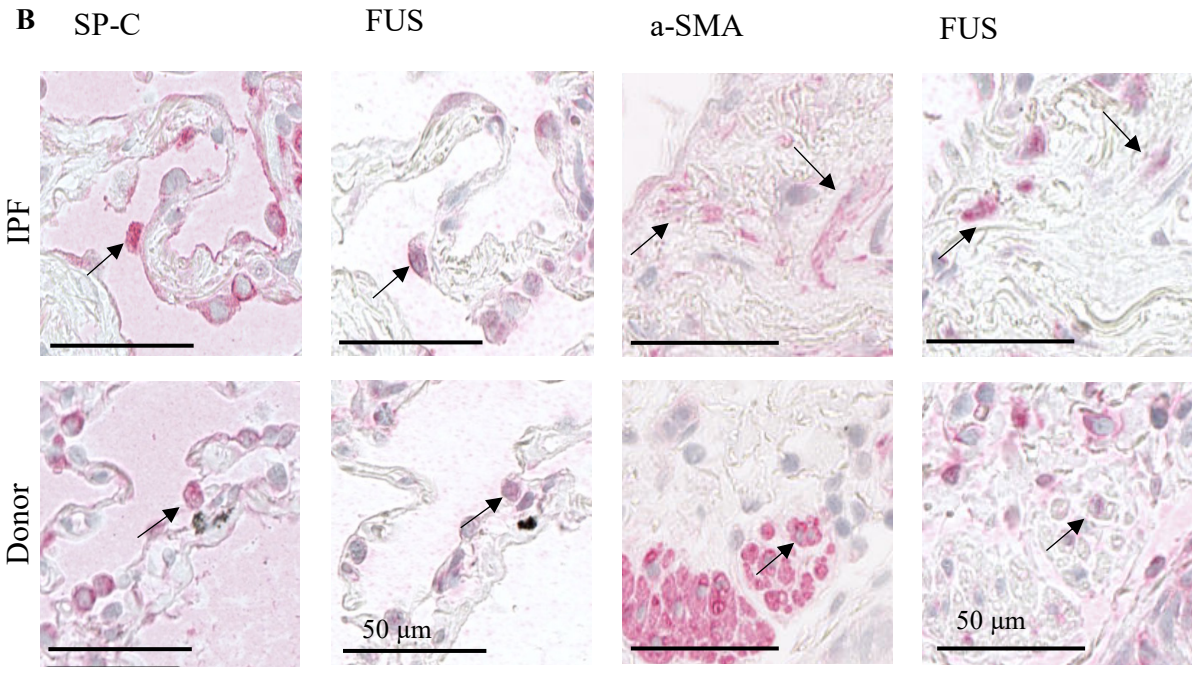

Figure 8: FUS is slightly increased in AECII and in fibroblasts of IPF patients.
Immunohistochemnical analysis of serial sections of IPF and Donor lungs. (A) Overview of IPF and Donor sections. Scale bar=100 µm (B) Figure of representive cells, in the upper row IPF cells and in the lower row Donor cells. SP-C staining indicates AECll and a-SMA fibroblasts and arrows highlight representative cells of the serial sections. Scale bar= 50 µm, n=5 Donors, n=6 IPF patients. Original magnification: x40

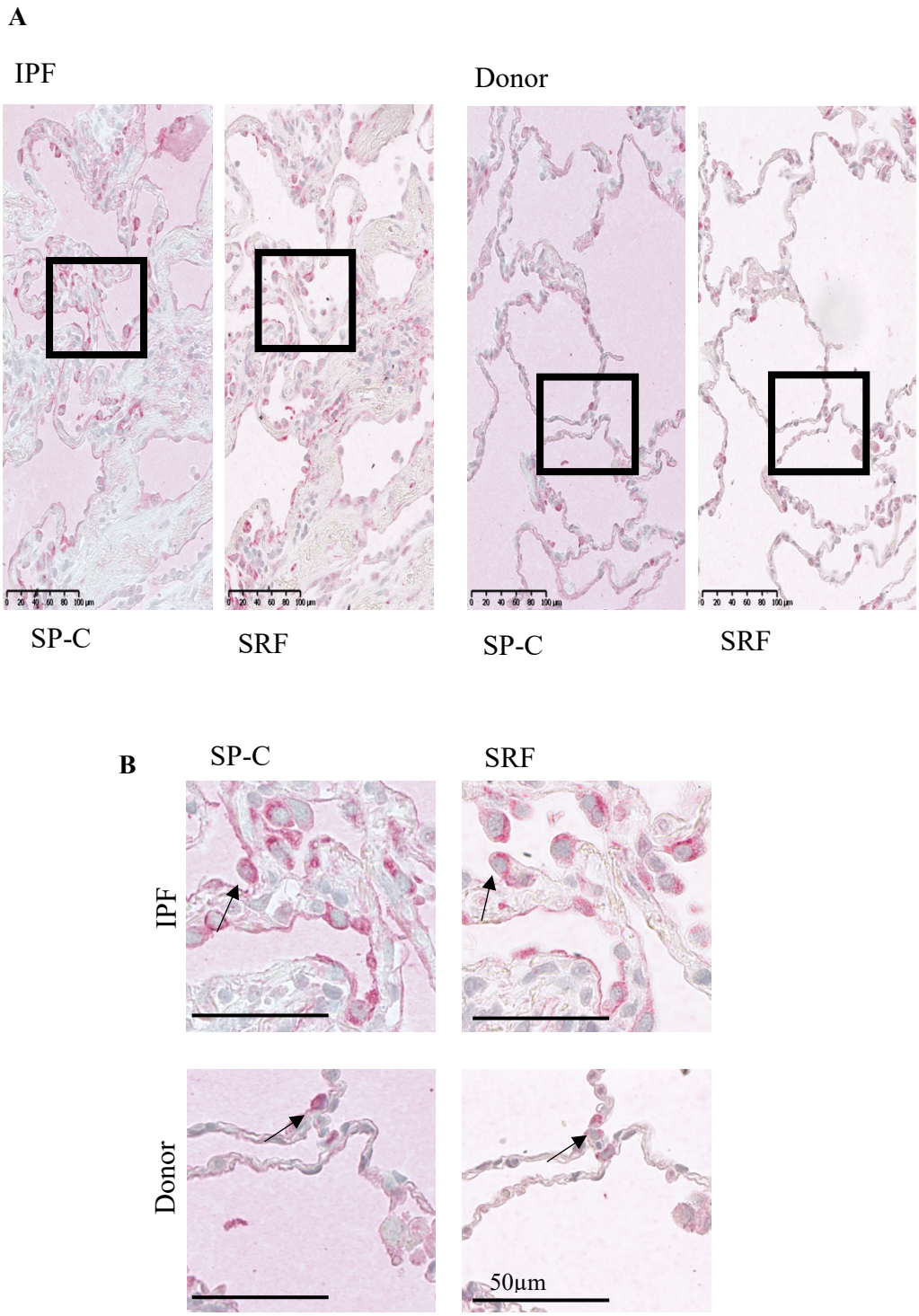

Figure 9: SRF is not altered in AECII of IPF patients compared to Donors.
Immunohistochemnical analysis of serial sections of IPF and Donor lungs. (A) Overview of IPF and Donor sections. Scale bar=100 µm (B) Figure of representive cells, in the upper row IPF cells and in the lower row Donor cells. SP-C staining indicates AECll and arrows highlight representative cells of the serial sections. Scale bar= 50 µm, n=5 Donors, n=6 IPF patients. Original magnification: x40

3.3 RBPs and stress granule markers are elevated in human fibroblasts from IPF patients

We next sought to study how RBPs or SGs are regulated in a cell specific manner under IPF conditions. To study this, we performed western blots for RBPs, namely SRF, FUS, TDP43, PABPC1, MBNL1 and TIA1 in lysates prepared from interstitial lung fibroblasts of IPF patients as well as from organ donors (Figure 10). Out of all these RBPs analyzed, we observed a significant increase in FUS, TDP43 as well as PABPC1 in IPF fibroblasts as compared to donor fibroblasts (Figure 10A, quantification Figure 10C). We next performed immunofuorescence for the RPBs alongside with α-smooth muscle actin (α-SMA), a marker for activated fibroblasts. We observed prominent staining for both FUS (Figure 11B), PABPC1 (Figure 12B) as well as TDP43 (Figure 16B) in α-SMA fibroblasts of IPF patient lungs as compared to the fibroblasts of donor lungs. In fact, in IPF patient fibroblasts, we observed increased nuclear and cytoplasmic FUS deposition, enhanced cytoplasmic staining for PABPC1 and increased nuclear staining for TDP43. Mislocalization of RBPs, especially FUS protein to the cytoplasm clearly indicates there is an imbalance in RBP homeostasis in IPF fibroblasts. Immuno staining for other major RBPs namely SRF, MBNL1 or G3BP1 did not show prominent stainings in IPF patient lung fibroblasts (Figure 13B, 14B, 15B).

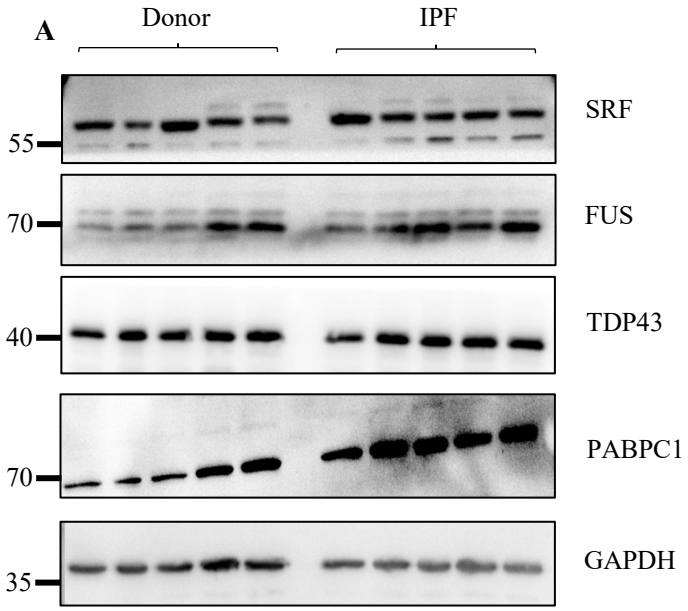

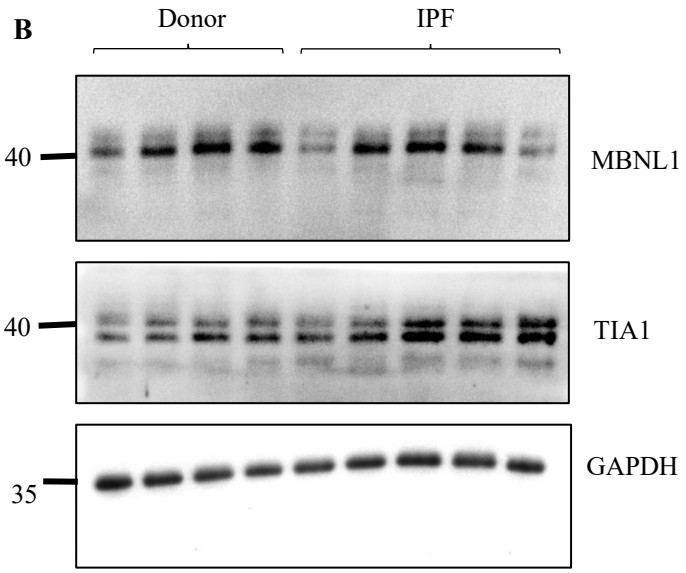
B
Donor
IPF
40
MBNL1
40
TIA1
35
GAPDH

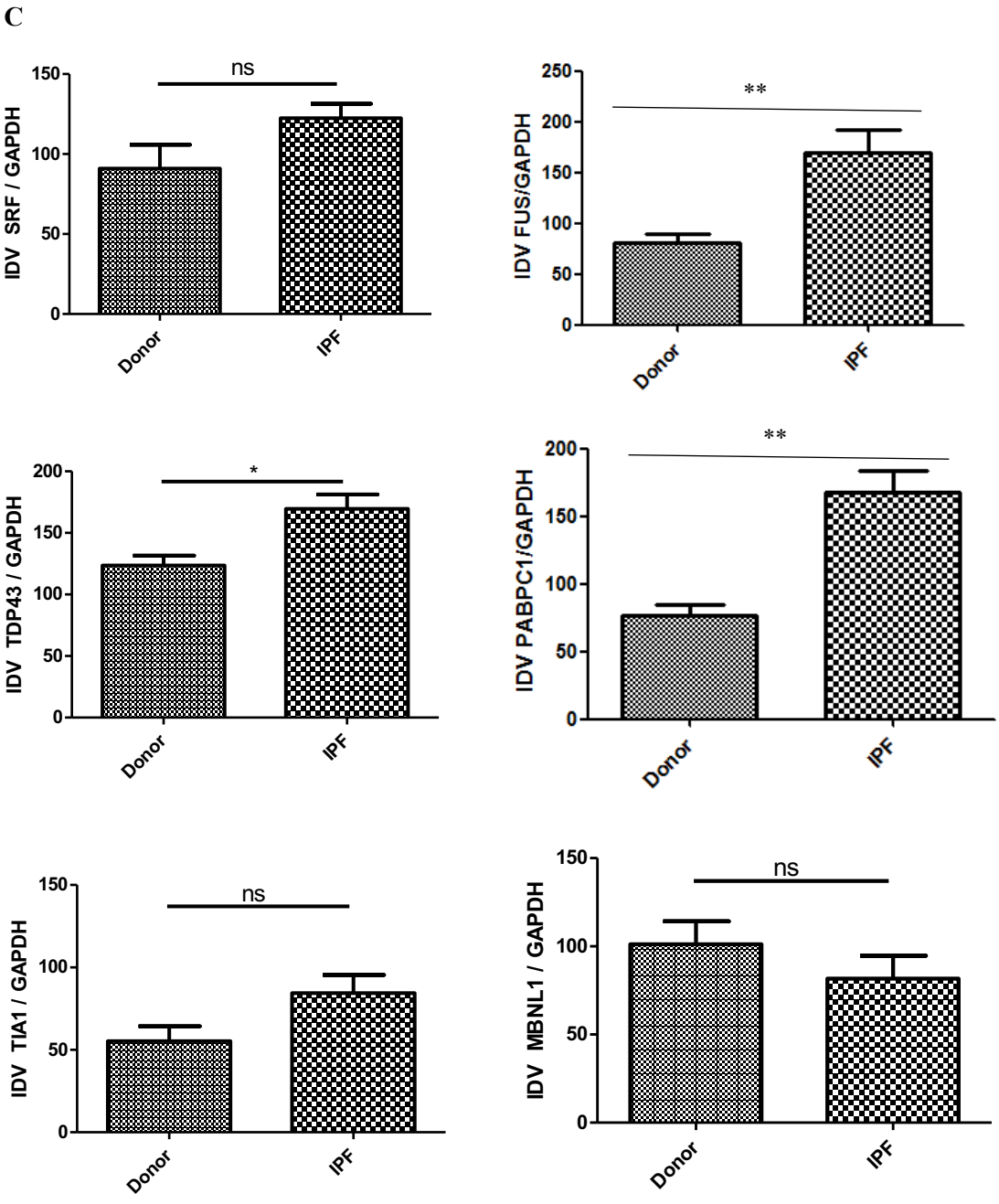
C
IDV SRF / GAPDH
ns
IDV FUS/GAPDH
**
IDV TDP43 / GAPDH
*
IDV PABPC1/GAPDH
**
IDV TIA1 / GAPDH
ns
IDV MBNL1 / GAPDH
ns
Donor
IPF

Figure 10: RBPs and SG markers are increased in fibroblasts from IPF patients
(A) Representative Western Blot images for SRF, FUS, TDP43, PABPC1 (IPF (n=5) and Donor (n=5)), (B) Representative Western Blot images for MBNL1, TIA1 (IPF (n=5) and Donor (n=4)) and GAPDH (loading control) from isolated fibroblasts of IPF and Donor lungs. (C) Densitometry analysis of RBP and GAPDH (loading control). Target protein*100/GAPDH ratio was calculated and depicted as bar graphs. **p < 0,01, *p < 0,05, ns – no significance.

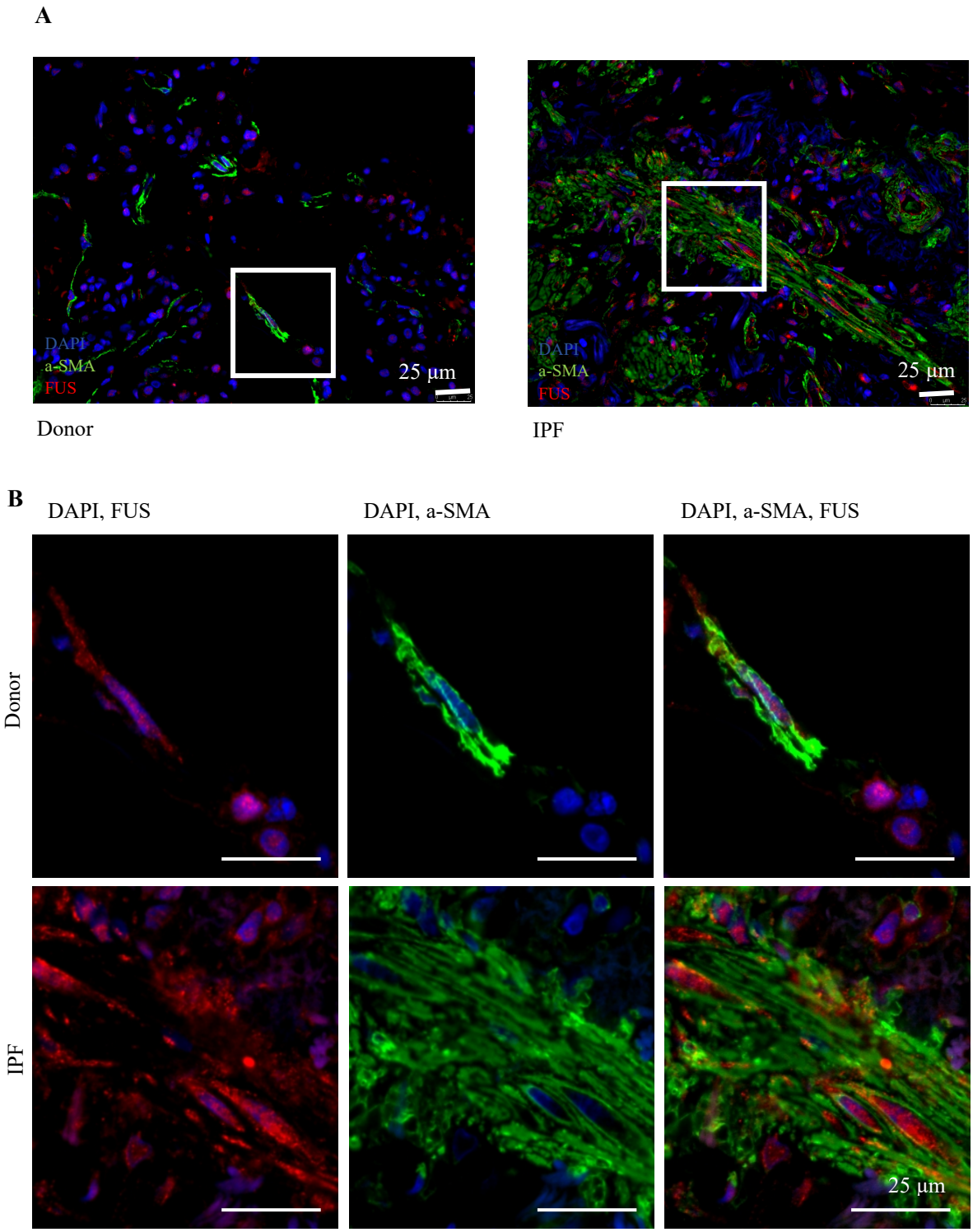

Figure 11: FUS is increased in fibroblasts from IPF patients and is located in the cytoplasm and the nucleus of fibroblasts in fibrotic lungs
(A) Overview of IPF and Donor sections. Scale bar=25 µm (B) Immunofluorescence analysis of Donor (upper row) and IPF lungs (lower row). Costaining of a-SMA (green) to indicate fibroblasts and FUS (red). Nuclei are stained with DAPI (blue). Scale bar=25 µm.

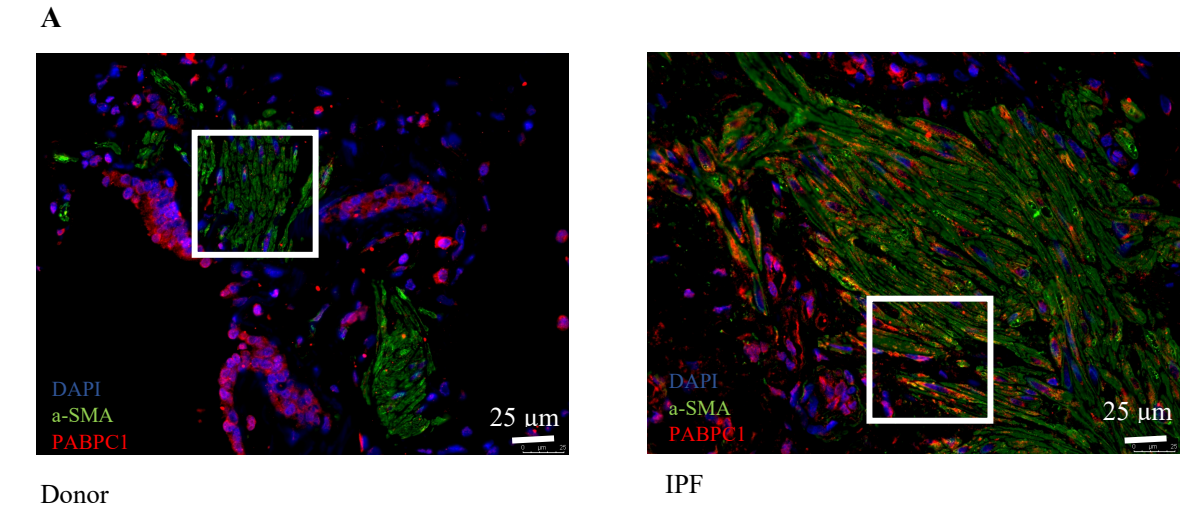

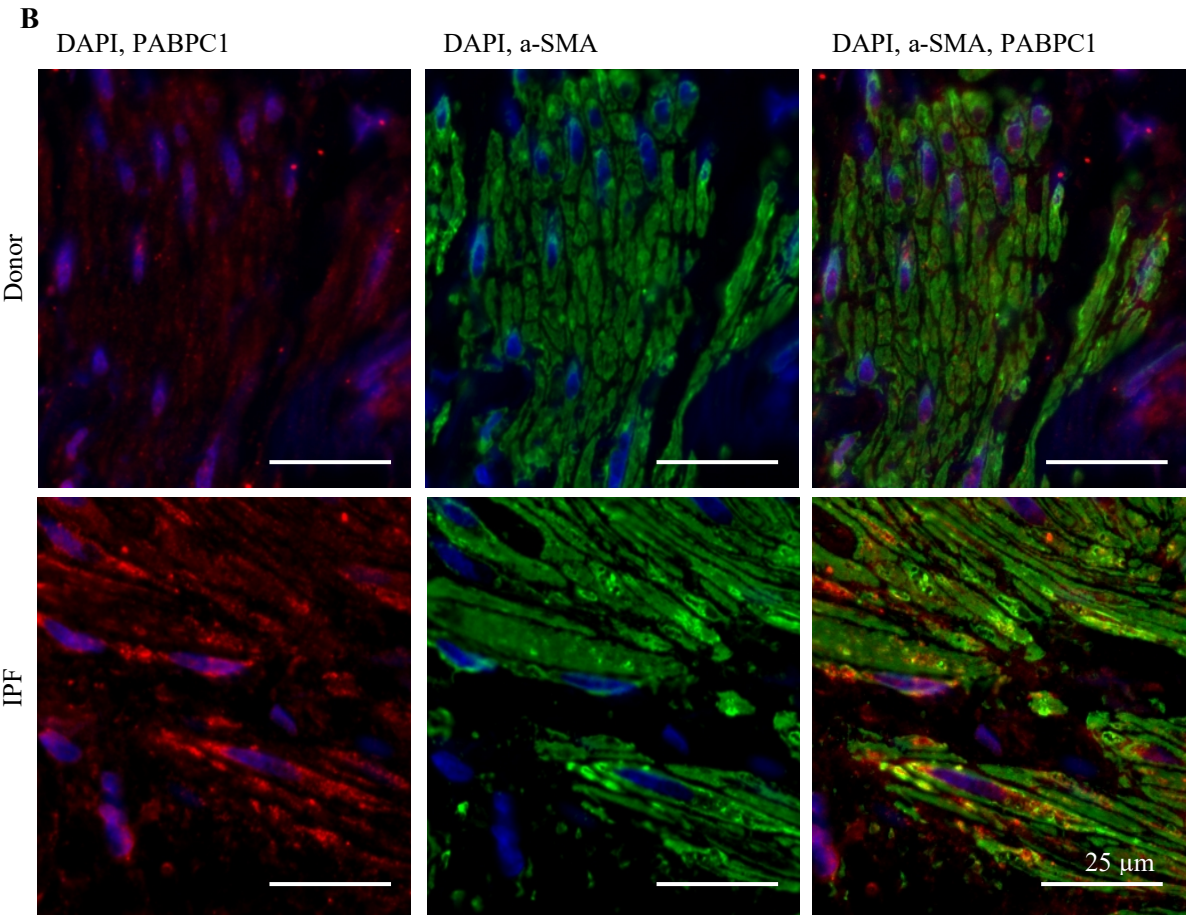

Figure 12: PABPC1 is extensively increased in fibroblasts from IPF patients and is located mostly in the cytoplasm of fibroblasts in fibrotic lungs
(A) Overview of IPF and Donor sections. Scale bar=25 µm (B) Immunofluorescence analysis of Donor (upper row) and IPF lungs (lower row). Costaining of a-SMA (green) to indicate fibroblasts and PABPC1 (red). Nuclei are stained with DAPI (blue). Scale bar=25 µm.

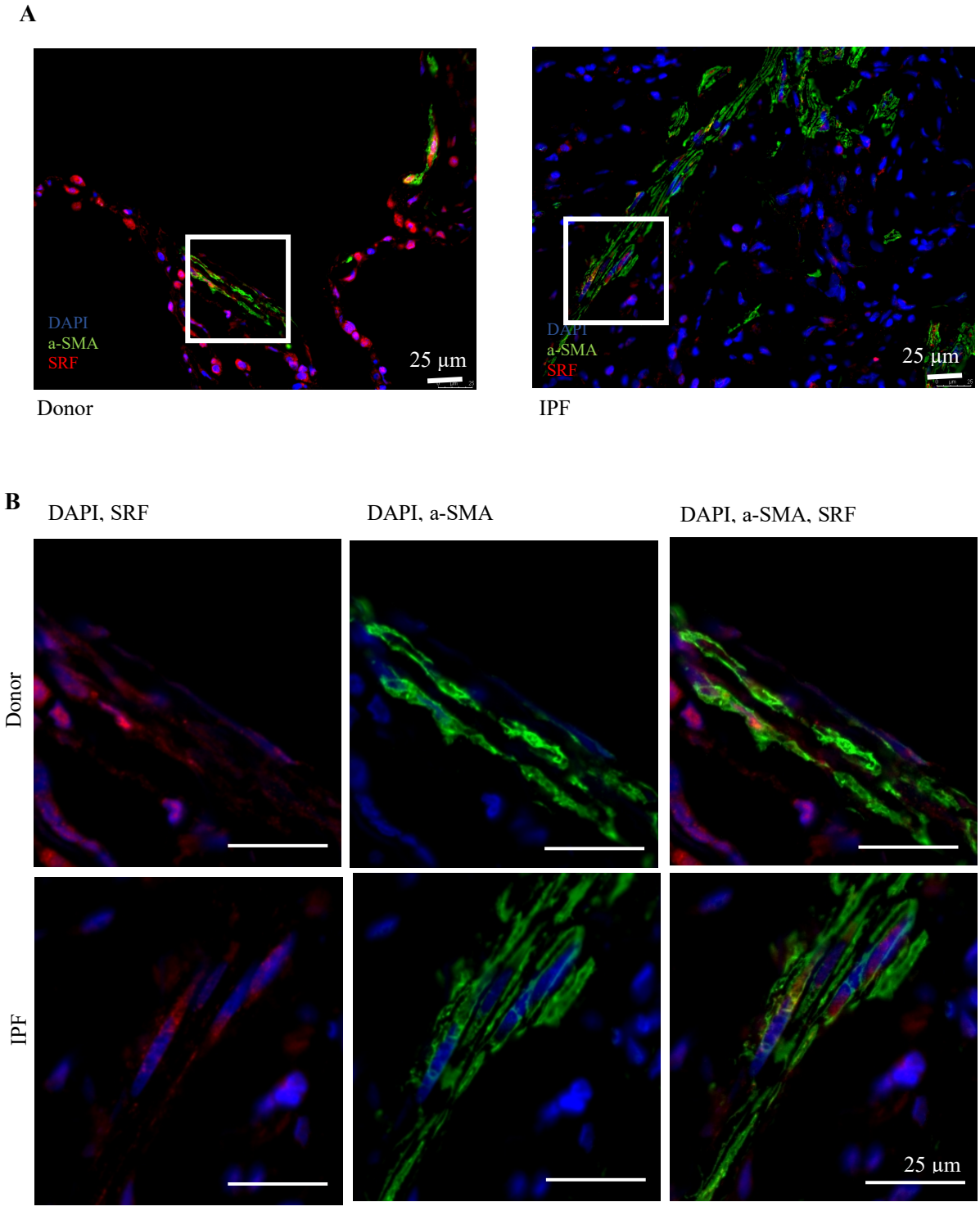

Figure 13: SRF is not significantly increased in fibroblasts from IPF patients and is located in the cytoplasm and partly in the nucleus of fibroblasts in fibrotic lungs
(A) Overview of IPF and Donor sections. Scale bar=25 µm (B) Immunofluorescence analysis of Donor (upper row) and IPF lungs (lower row). Costaining of a-SMA (green) to indicate fibroblasts and SRF (red). Nuclei are stained with DAPI (blue). Scale bar=25 µm.

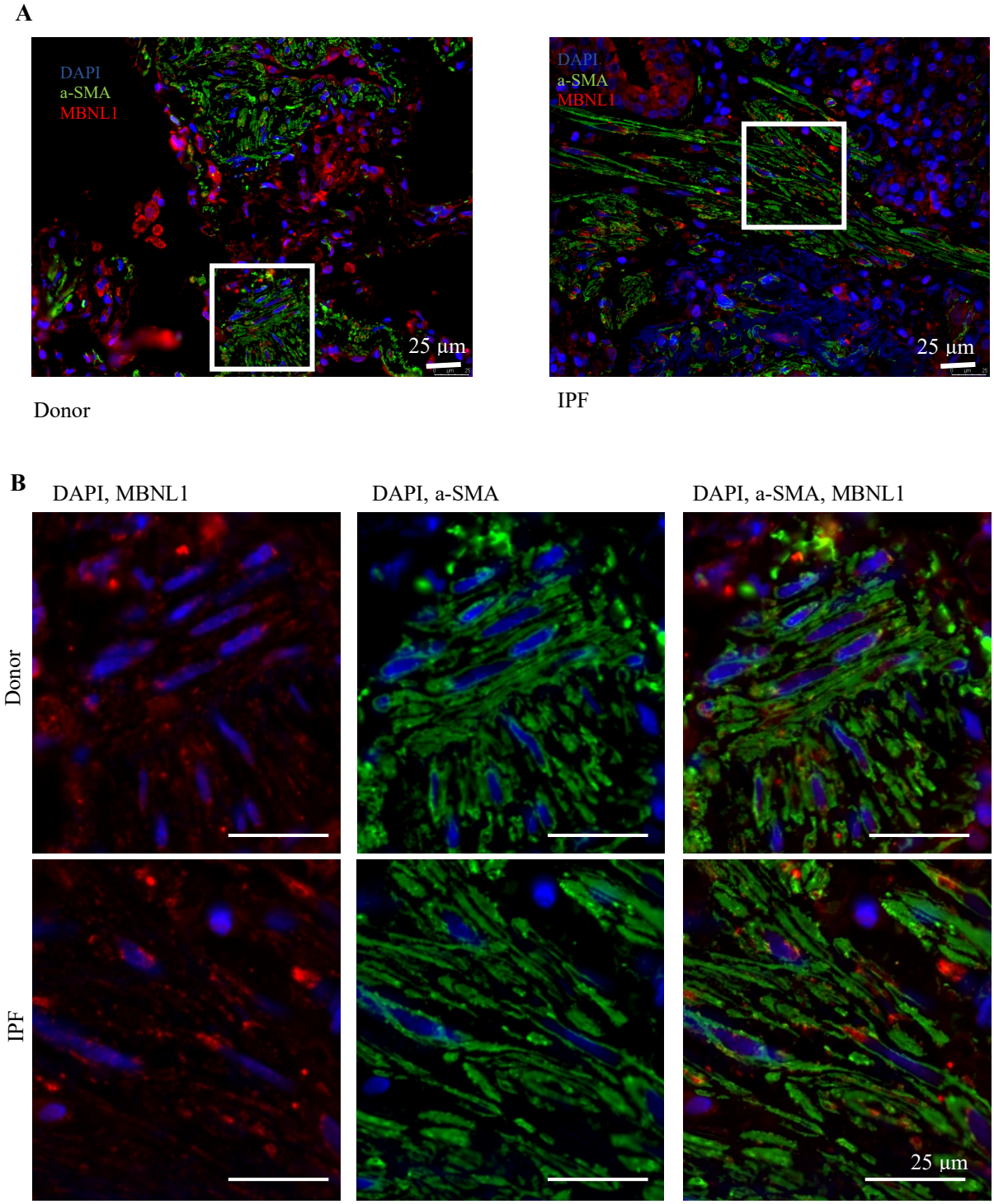

Figure 14: MBNL1 is not significantly increased in fibroblasts from IPF patients and is located mostly in the cytoplasm of fibroblasts in fibrotic lungs
(A) Overview of IPF and Donor sections. Scale bar=25 n (B) Immunofluorescence analysis of Donor (upper row) and IPF lungs (lower row). Costaining of a-SMA (green) to indicate fibroblasts and MBNL1 (red). Nuclei are stained with DAPI (blue). Scale bar=25 µm.

A

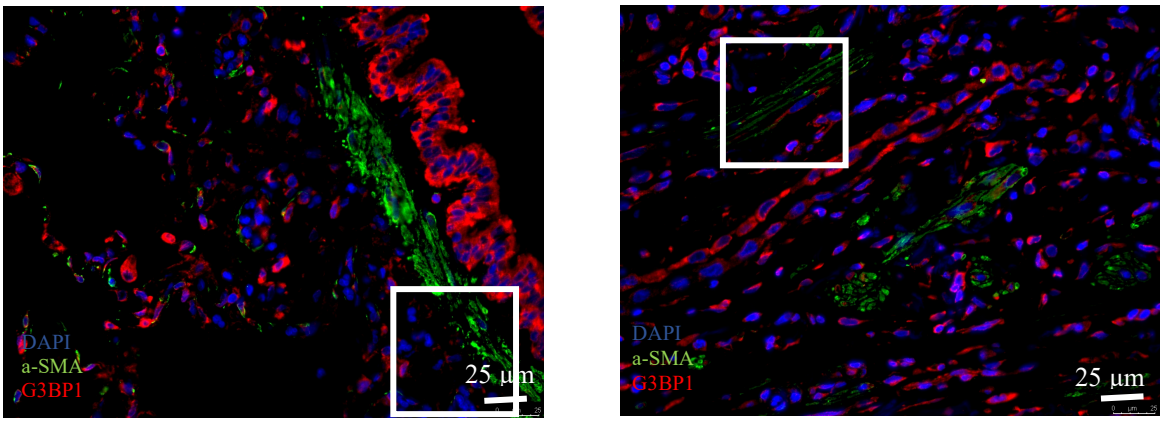

Donor IPF

B

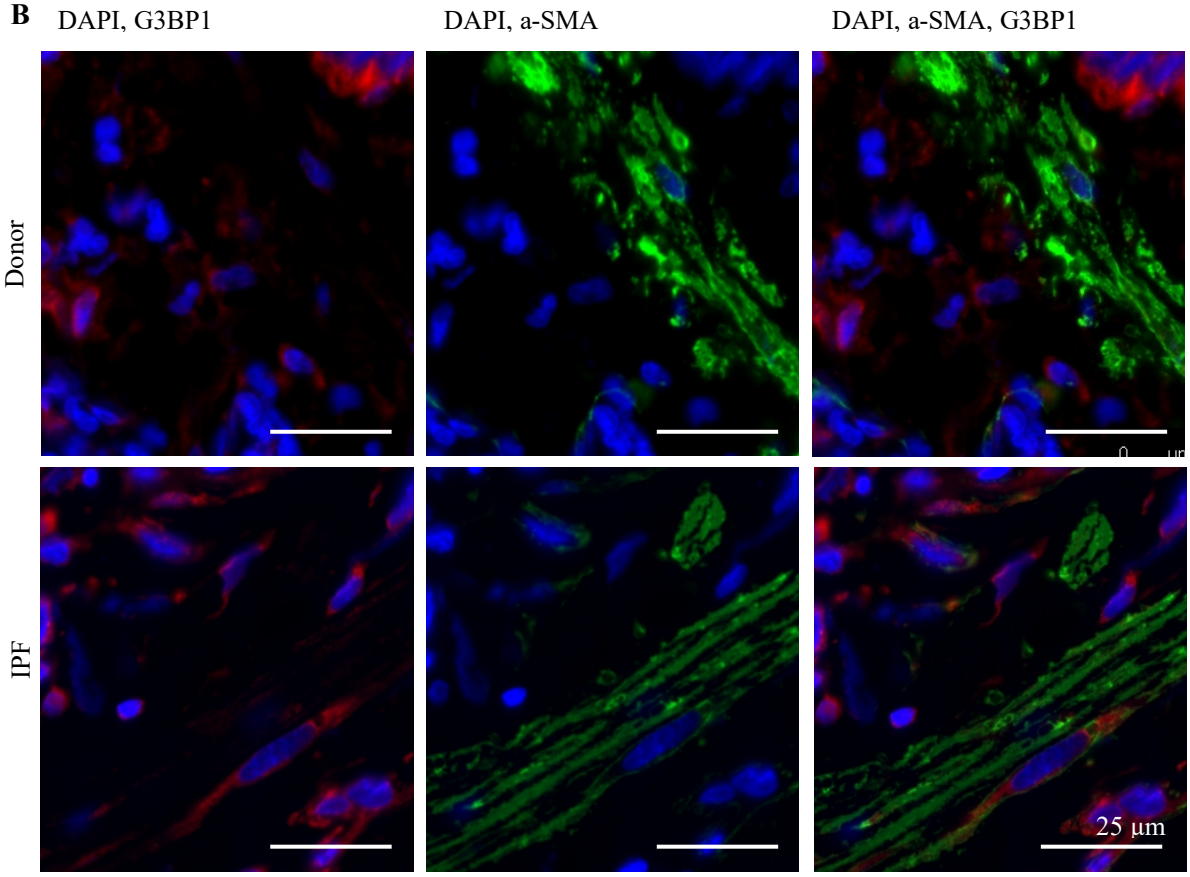

Figure 15: G3BP1 is not significantly increased in fibroblasts from IPF patients and is located in the cytoplasm of fibroblasts in fibrotic lungs
(A) Overview of IPF and Donor sections. Scale bar=25 µm (B) Immunofluorescence analysis of Donor (upper row) and IPF lungs (lower row). Costaining of a-SMA (green) to indicate fibroblasts and PABPC1 (red). Nuclei are stained with DAPI (blue). Scale bar=25 µm.

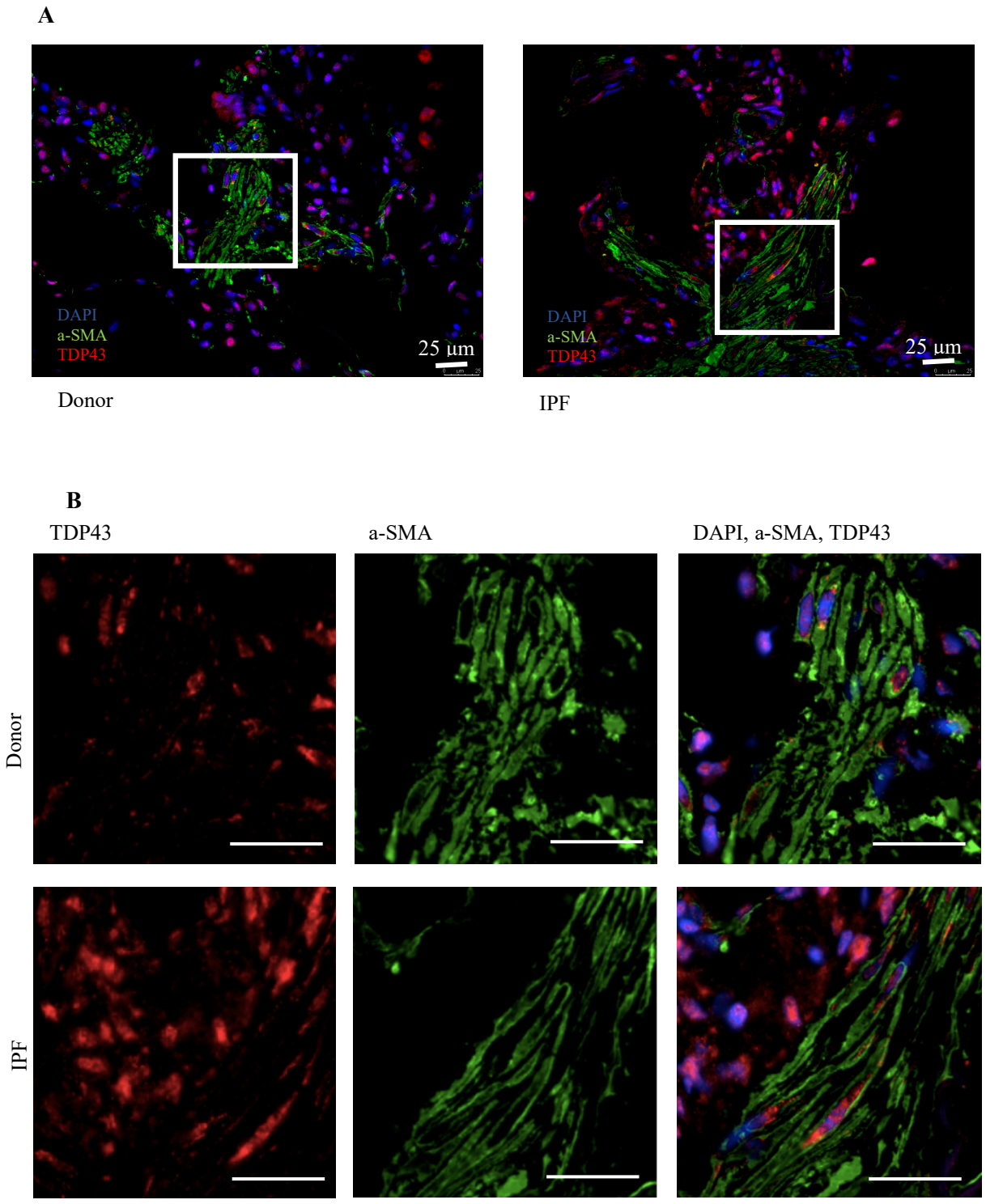

Figure 16: TDP43 is increased in fibroblasts from IPF patients and is located mostly in the nucleus of fibroblasts in fibrotic lungs

(A) Overview of IPF and Donor sections. Scale bar=25 µm (B) Immunofluorescence analysis of Donor (upper row) and IPF lungs (lower row). Costaining of a-SMA (green) to indicate fibroblasts and TDP43 (red). Nuclei are stained with DAPI (blue). Scale bar=25 µm.

3.4 RBPs are elevated in amiodarone (AD) induced fibrous mouse lungs and are located in AECll

In order to better understand the changes in RBP regulation as encountered in human IPF we conducted additional investigations in established animal models of lung fibrosis. For this purpose, we used the murine AD model of lung fibrosis established in our group. Vehicle or AD was administered to C57BL/6 mice intratracheally, every fifth day, as described before (Mahavadi *et al.*, 2014). Mice were harvested at days 7, 14, 21 and 28 post AD treatment or 28 days post vehicle treatment that served as controls. Lungs were either formalin fixed and embedded in formalin for histological assessment or were shock frozen for molecular and biochemical analysis. Shock frozen lungs were homogenized and the protein concentration was determined. Western blots analysis of the total lung homogenates revealed significantly elevated levels of SRF in AD treated mice at day 7 until day 28 as compared to vehicle treated mice (Figure 17A, quantification in B). On the other hand, TDP43, PABPC1, FUS and MBNL1 did not show considerable differences in protein levels between AD and vehicle treated mice (Figure 17A, B). Immunohistochemistry on serial lung sections of AD and vehicle treated mice lungs showed that MBNL1 is located in fibroblasts (shown by a-SMA) and increased in fibrotic lungs (Figure 19A, B) and revealed a positive stianing for TDP43 in AECII as shown by pro SP-C staining (Figure 18A, B, C) and in fibroblasts (shown by a-SMA) fully supporting our observations from the IPF lungs.

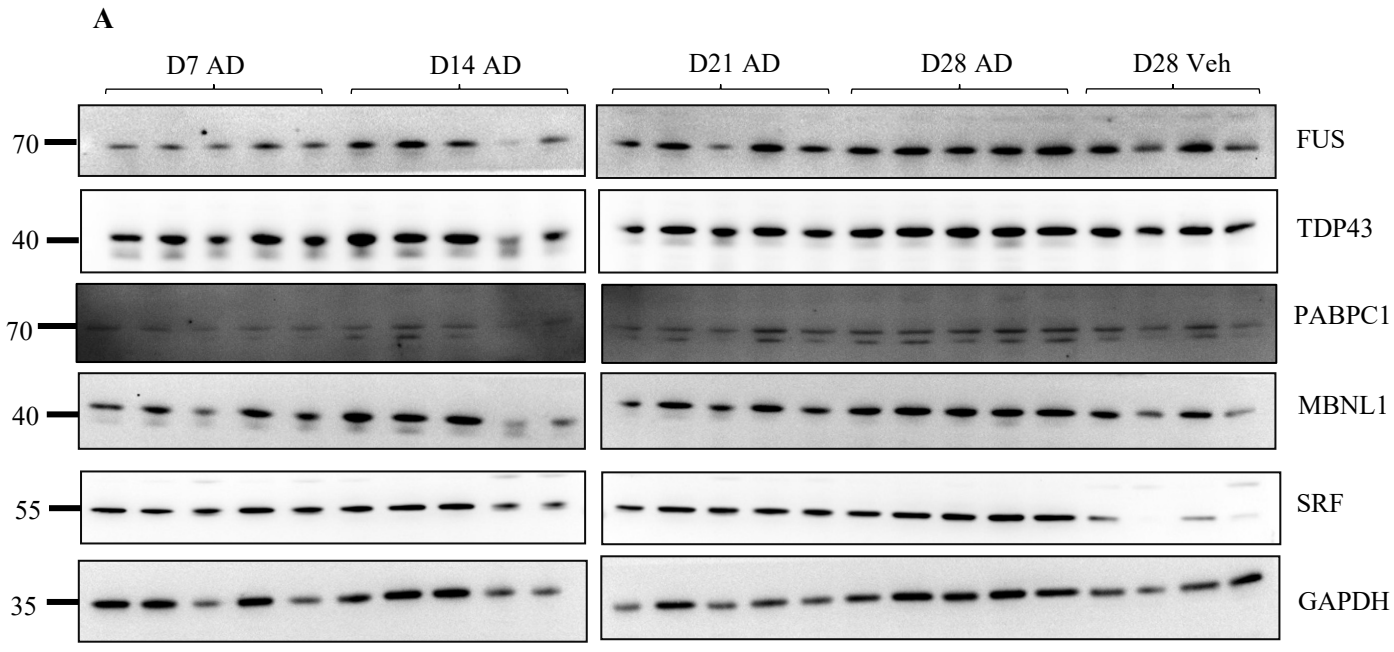

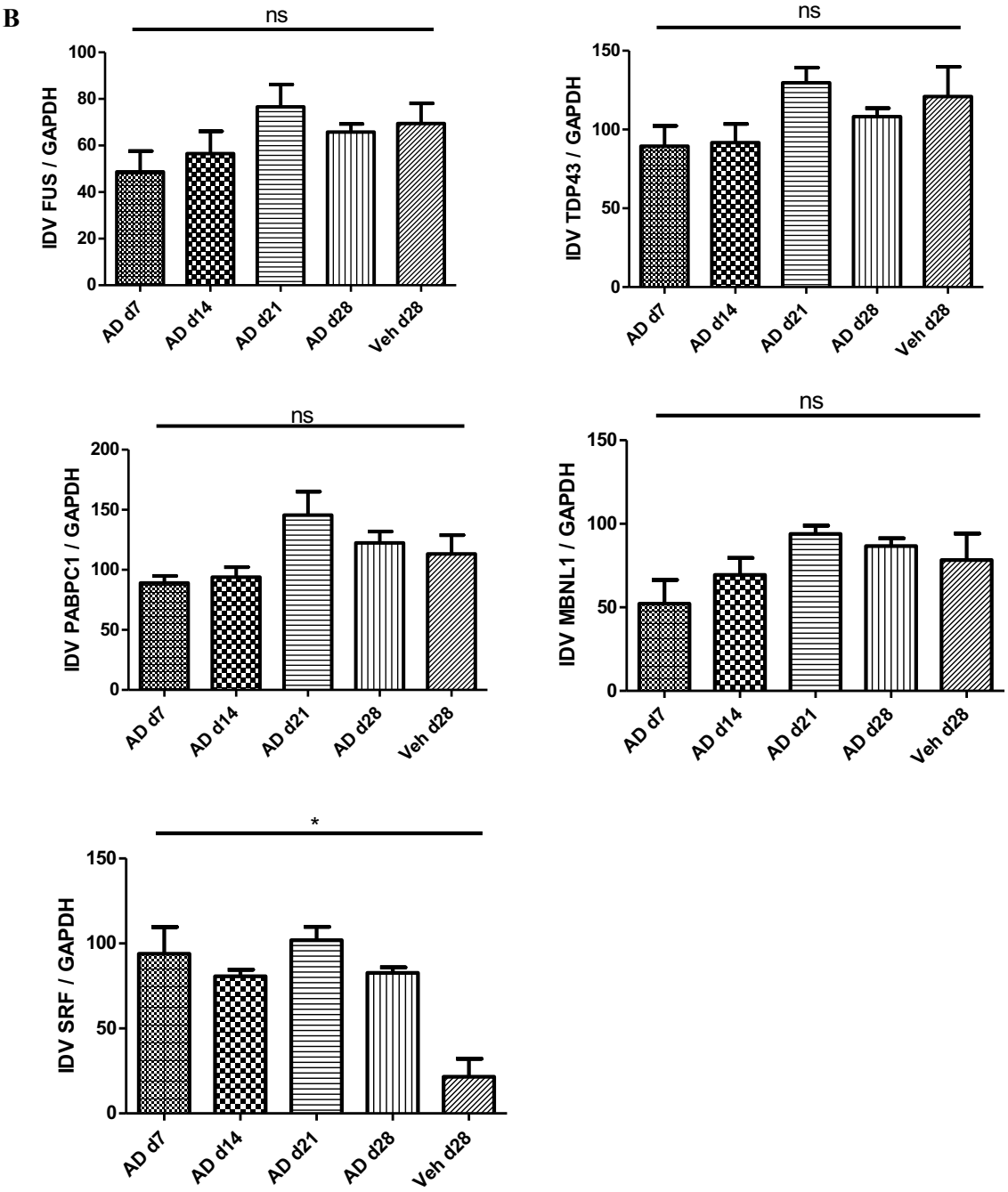

Figure 17: Levels of SRF differ from healthy vehicle lungs to AD indued fibrotic mice lungs

(A) Representative Western Blot images for SRF, FUS, TDP43, MBNL1, PABPC1 and GAPDH (loading control) from AD induced fibrotic mice lungs. Exposure time of AD was 7 days, 14 days (upper row of the bands), 21 days, 28 days and the vehicle exposure time was also 28 days (lower row of bands). Each AD exposure time was performed with n=5 mice and the vehicle treatment were completed with n=4 mice. (B) Densitometry analysis of RBP and GAPDH (loading control). Target protein*100/GAPDH ratio was calculated and depicted as bar graphs. **p < 0,01, *p < 0,05, ns – no significane.

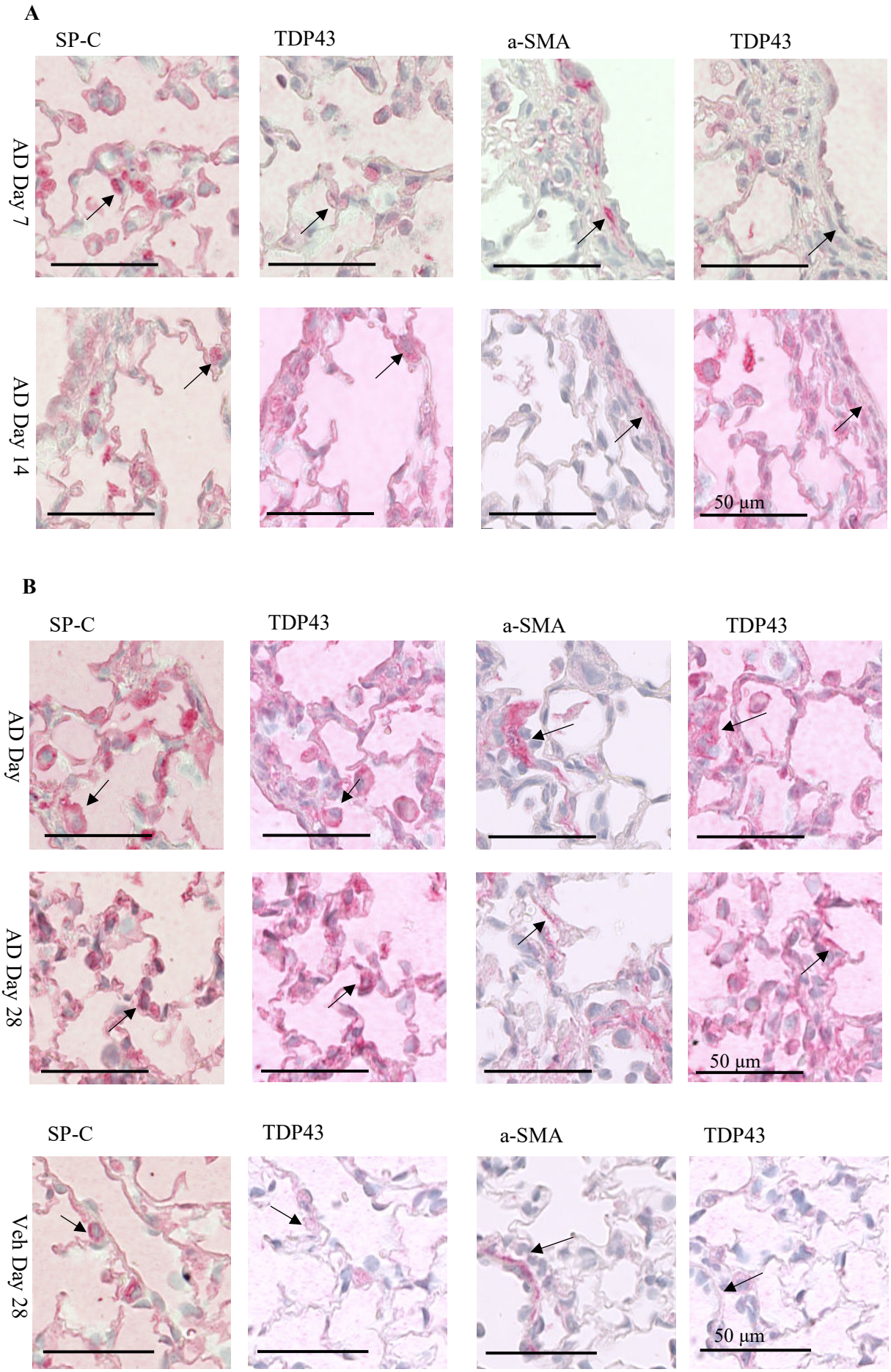
A
SP-C
TDP43
a-SMA
TDP43
AD Day 7
AD Day 14
50 µm
B
SP-C
TDP43
a-SMA
TDP43
AD Day
AD Day 28
50 µm
SP-C
TDP43
a-SMA
TDP43
Veh Day 28
50 µm

C

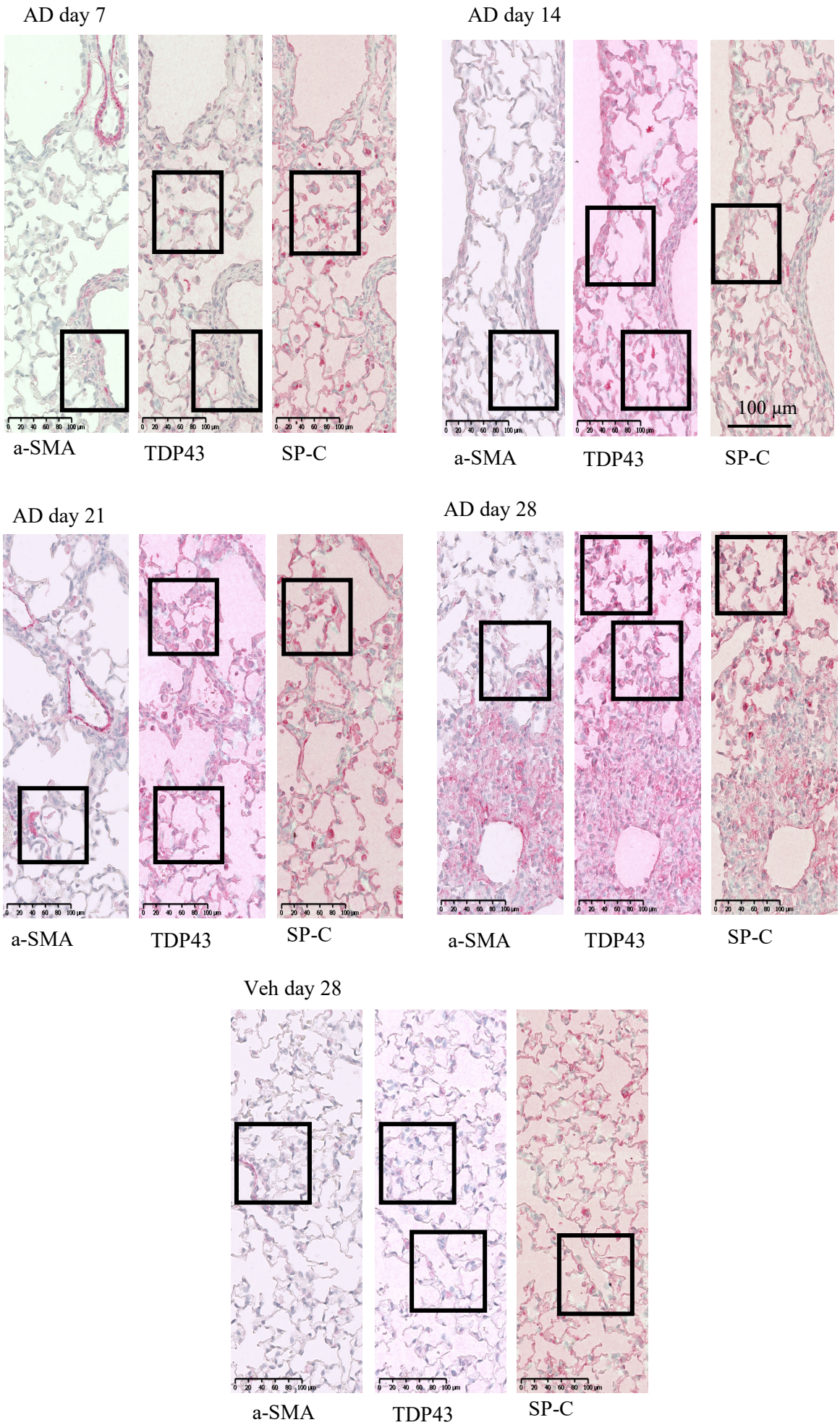
AD day 7
AD day 14
AD day 21
AD day 28
Veh day 28
100 µm
a-SMA
TDP43
SP-C

Figure 18: TDP43 is located in AEC ll and in fibroblasts and is increased in fibrotic lungs
Immunohistochemnical analysis of serial sections of AD and Vehicle treated lungs. (A) Figure of representive cells, in the upper row cells with 7 days of AD treatment and in the lower row cells with 14 days of AD treatment. (B) Figure of representive cells, in the first row cells with 21 days of AD treatment and in the second row cells with 28 days of AD treatment and in the third row cells with 28 days of vehicle treatment. SP-C staining indicates AECll and a-SMA staining fibroblasts. Arrows highlight representative cells of the serial sections. Scale bar= 50 µm, each exposure time of AD/Veh n=5. Original magnification: x40 (C) Overview of AD and Vehicle treated sections. Scale bar=100 µm

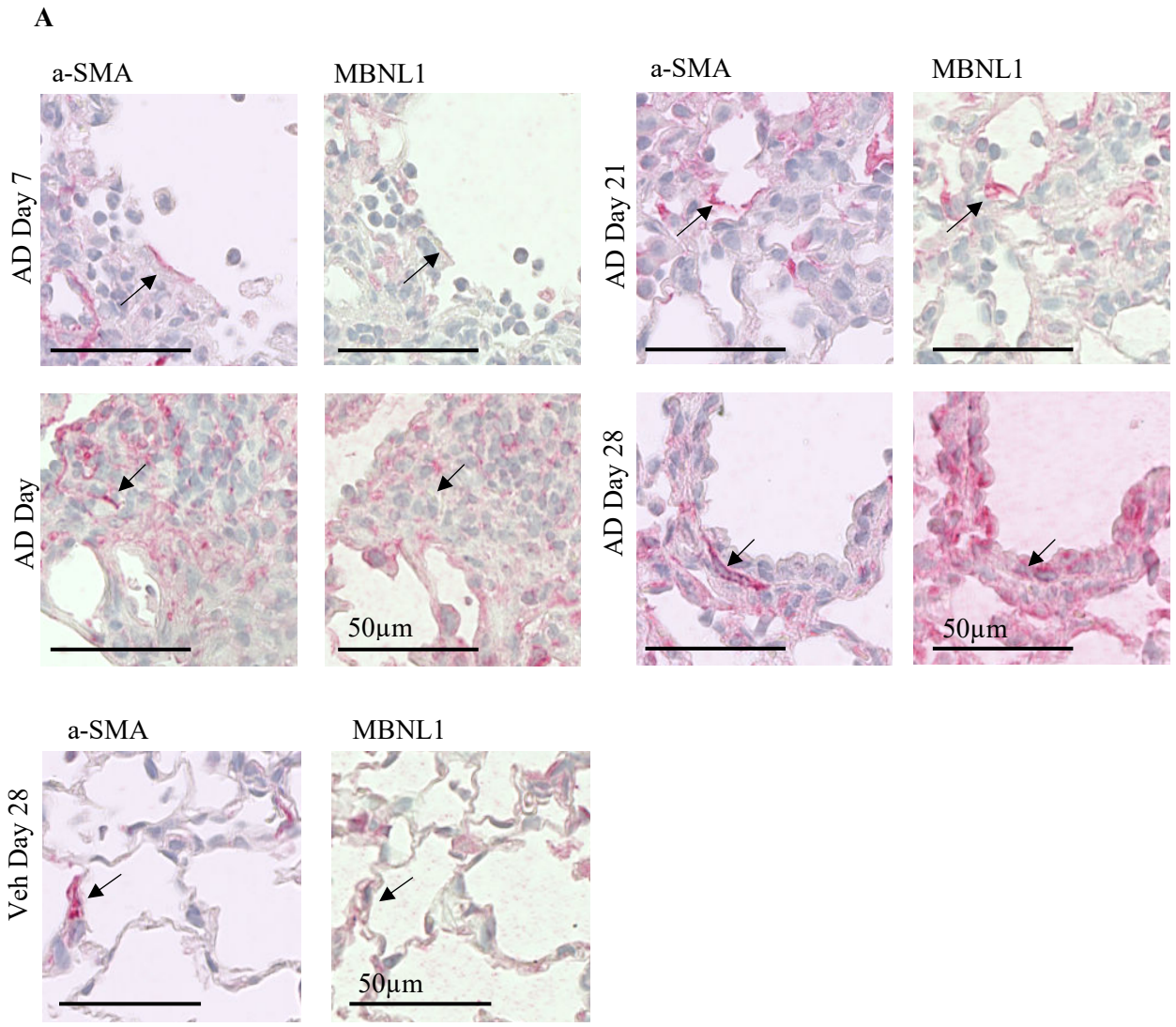

B

AD day 7

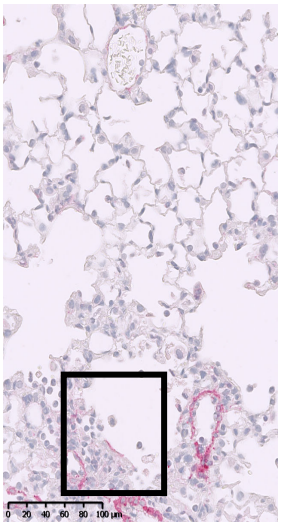

a-SMA

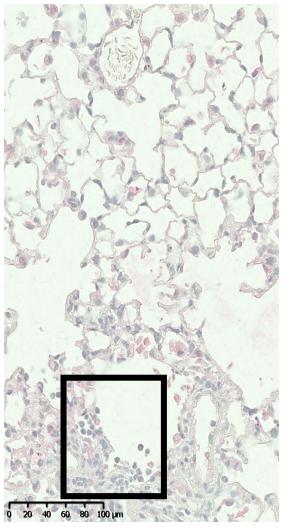

MBNL1

AD day 14

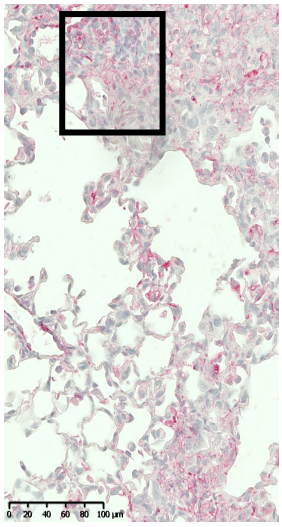

a-SMA

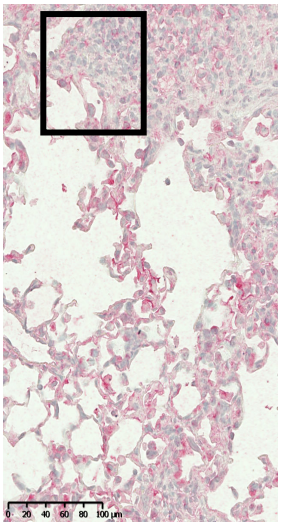

MBNL1

AD day 21

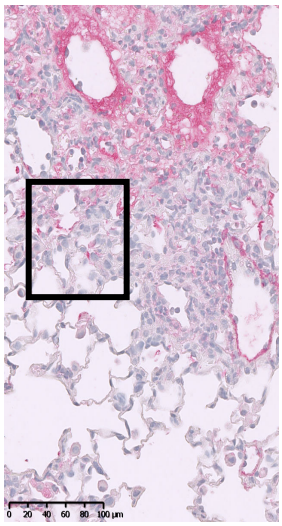

a-SMA

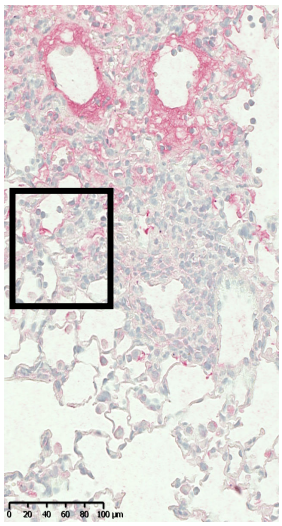

MBNL1

AD day 28

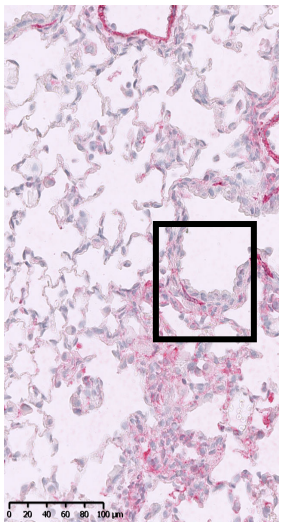

a-SMA

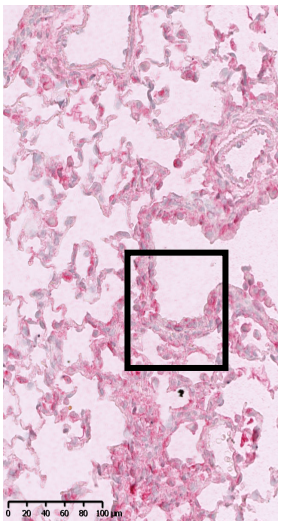

MBNL1

Veh day 28

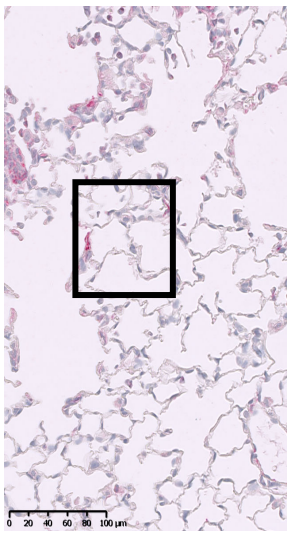

a-SMA

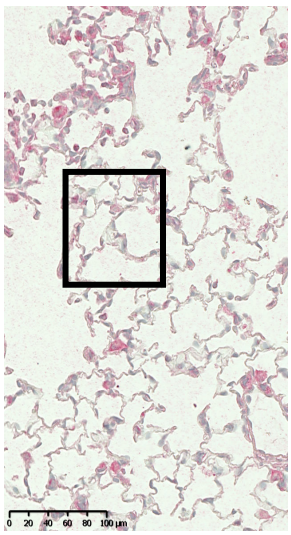

MBNL1

Figure 19: MBNL1 is located in fibroblasts and is increased in fibrotic lungs
Immunohistochemnical analysis of serial sections of AD and Vehicle treated lungs. (A) Figure of representive cells, on the left side cells with 7 and 14 days of AD treatment and on the right side cells with 21 and 28 days of AD treatment and in the third row cells with 28 days of vehicle treatment. a-SMA staining indicates fibroblasts. Arrows highlight representative cells of the serial sections. Scale bar= 50 µm, each exposure time of AD/Veh n=5. Original magnification: x40 (B) Overview of AD and Vehicle treated sections. Scale bar=100 µm

3.5 RBPs and stress granule markers show no difference in AD treated MLE12 cells and vehicle treated ones

Further, *in vitro*, mouse lung epithelial cells (MLE12) were treated with AD or vehicle for 4, 8, 16 and 24 hours. Western blots for RBPs revealed no differences between AD and vehicle treated cells in total cell lysates (Figure 20A). Since phenotypic changes in AD treated cells were already observed from 30 mins of AD treatment (Unpublished), we were questioning whether RBPs may be differentially regulated at early time points. For this, we treated MLE12 cells with AD or vehicle for 30 mins, 1, 2 or 3 hrs and analyzed RBPs via western blotting (Figure 20B). Interestingly, RBPS regulation did not differ between AD and vehicle treated cells. First, we performed the experiments with n = 1 to see if there was a tendency for the RBPs to increase in the amiodaron treated cells. Since there was no sign of any change here, we dispensed with a larger sample size and further statistical analyzes and concentrated on further experiments.

We further performed nuclear and cytosolic extracts from MLE12 cells treated with AD or vehicle. The enrichment of fractions was confirmed by western blotting for GAPDH for cytosol and Lamin for the nucleus. However, differences in the protein levels of RBPs were not observed between AD and vehicle treated groups (Figure 21A, B).

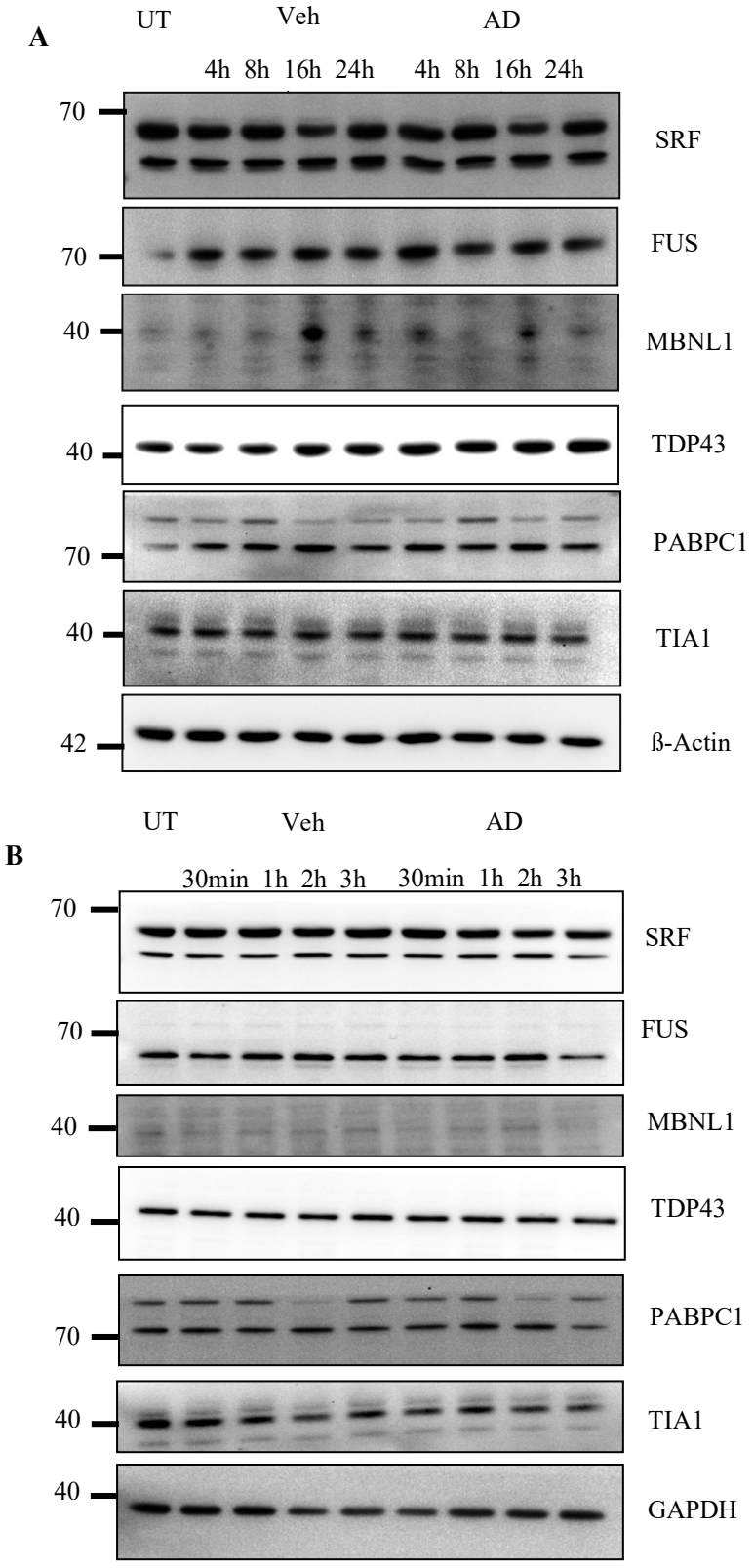

Figure 20: Levels of RBPs remain unaltered in AD treated cells *in vitro*
(A) Representative Western Blot images for SRF, FUS, TDP43, MBNL1, PABPC1, TIA1, ß-Actin (loading control) from AD treated, vehicle treated and untreated MLE 12 cells. Exposure time of AD and vehicle solution was 4 h, 8 h, 16 h and 24 h. (B) Representative Western Blot images for SRF, FUS, TDP43, MBNL1, PABPC1, TIA1, GAPDH (loading control) from AD treated, vehicle treated and untreated MLE 12 cells. Exposure time of AD and vehicle solution was 30 min, 1 h, 2 h and 3 h.

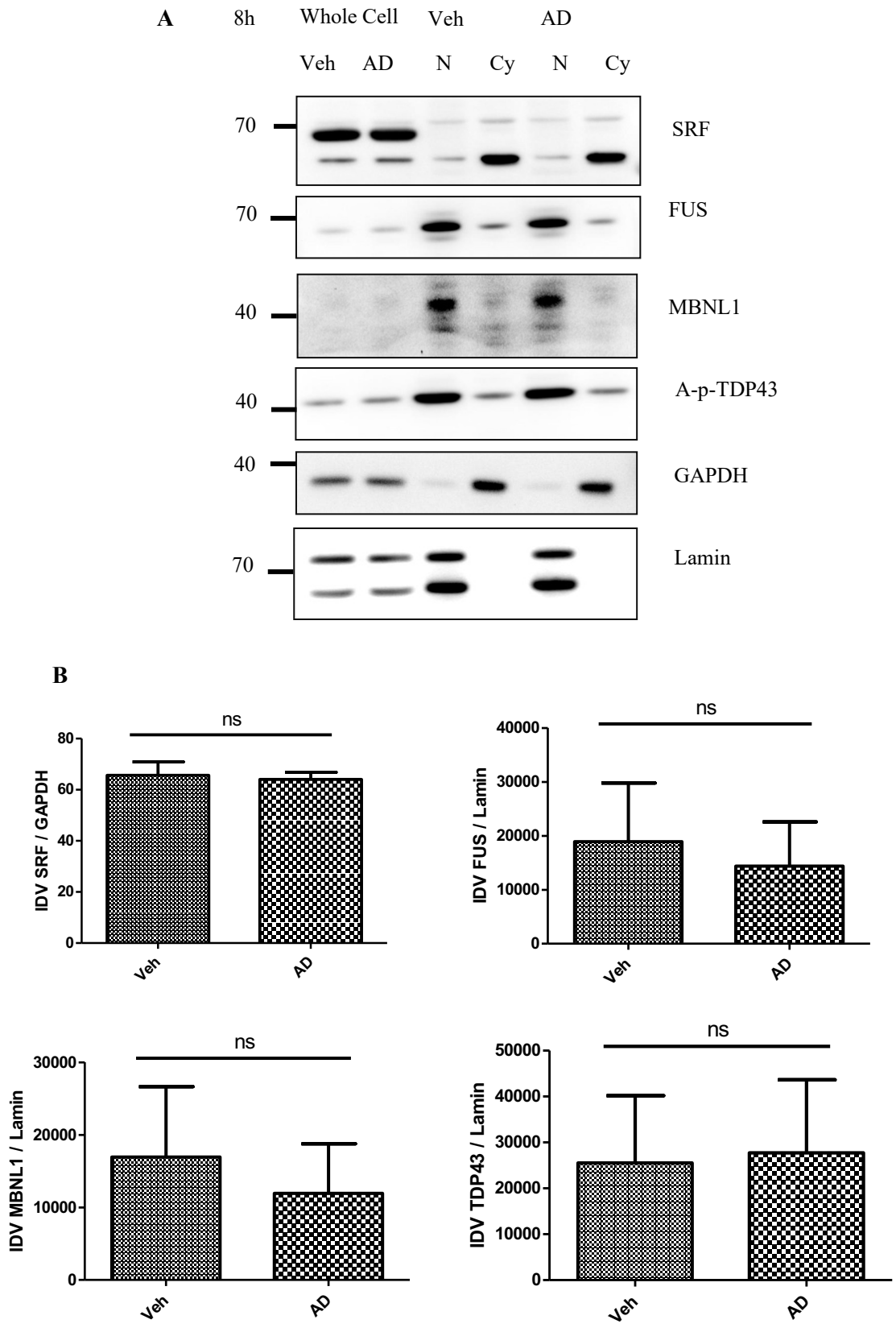

Figure 21: Distribution of RBPs in nucleus and cytoplasm of Veh or AD treated cells
(A) Representative Western Blot images for SRF, FUS, TDP43, MBNL1 from AD treated and vehicle treated cells and whole cell lysates as a control. GAPDH functions as a marker for the cytosolic fraction and Lamin for the nuclear fraction. Exposure time of AD and vehicle solution was 8 h. (B) Densitometry analysis of RBP and GAPDH/Lamin (loading control). Target protein*100/GAPDH ratio was calculated and depicted as bar graphs. **p < 0,01, *p < 0,05, ns – no significance.

3.6 FUS overexpression drives fibroblast proliferation

Since we observed an increase in FUS expression in IPF fibroblasts, we asked if FUS overexpression alone could influence the fate of this cell type. For this, we overexpressed empty GFP or turboGFP tagged human FUS in donor primary lung fibroblasts. Upon transfection, fibroblasts overexpressing FUS showed a significant increase in the proliferation marker, PCNA (proliferting cell nuclear antigen) (Figure 22A, B), suggesting that overexpression of FUS alone in healthy fibroblasts is sufficient to increase their proliferation.

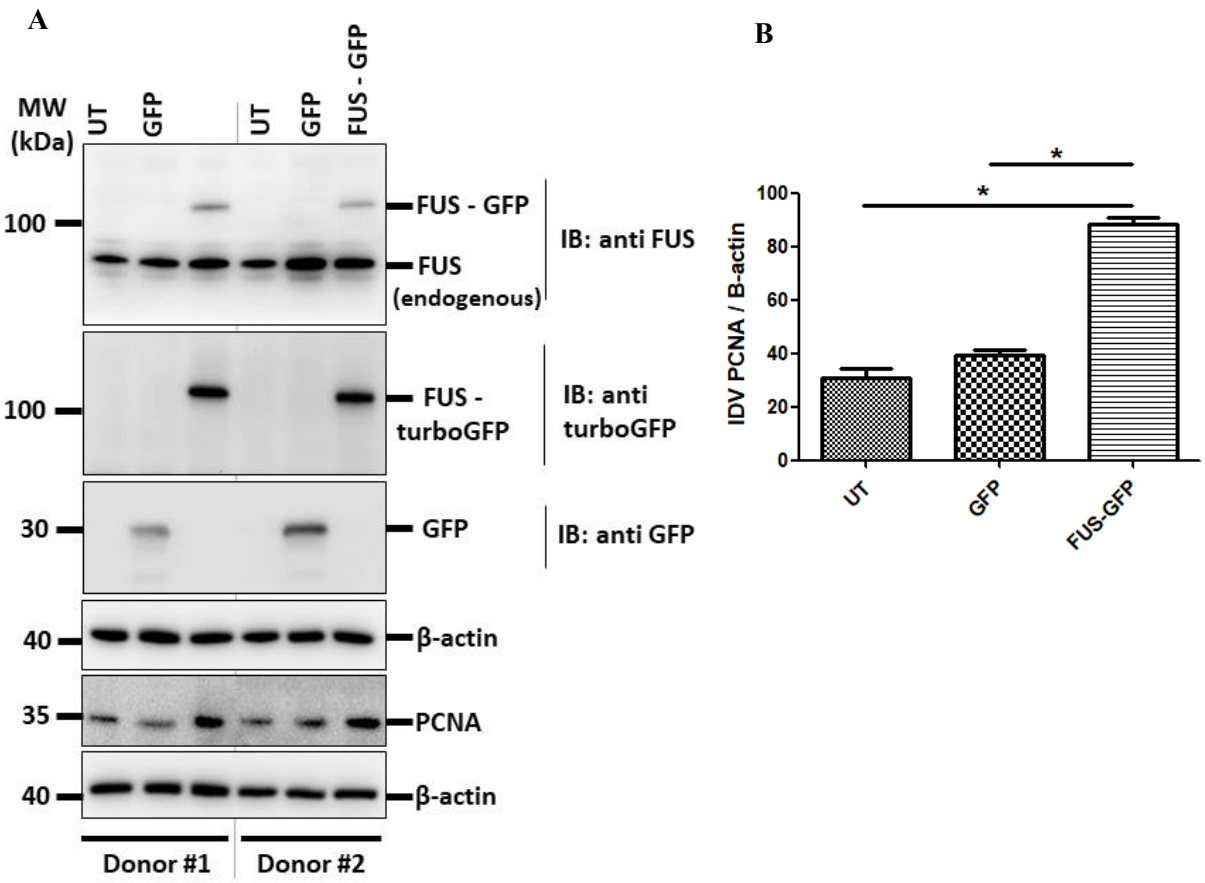

Figure 22: Overexpression of FUS drives fibroblast proliferation. (A) Primary interstitial fibroblasts from healthy donor lungs were left untransfected or transfected with empty GFP or FUS-turbo GFP for 24 hours. Cells were lysed and subjected to western blotting for the indicated proteins. (B) Densitometric quantification of PCNA is shown. Analysis was performed from two independent experiments from interstitial fibroblasts of two donor lungs. *P<0.05.

3.7 Pirfenidone treatment leads to a decrease of RBPs and SG markers in fibroblasts of fibrotic lungs

Pirfenidone is a potent, clinically prescribed anti-fibrotic drug. It is known to suppress lung fibrosis in IPF patients in part by attenuating the transcription of pro collagen, TGF-β mediated extra cellular matrix (ECM) deposition and fibroblast migration. We investigated whether pirfenidone exerts its anti fibrotic effects via influencing FUS, PABPC1 and SRF protein levels and thereby affecting the function of its target mRNAs. For this, we undertook *ex vivo* studies emplying precision cut lung slices (PCLS) from IPF lungs. As described in the methods section, we cultured 300 µm IPF lung sections and incubated them with vehicle (DMSO) or with 2.7 mM pirfenidone for 48 hours. Following this, we fixed treated PCLS in formalin and embedded them in paraffin. 5 µm sections were generated and immunofluorescence staining was performed for FUS as well as for PABPC1. Pirfenidone treatment shows no decrease in the staining for SRF in fibroblasts in human lung PCLS slides (Figure 25 A, B). As indicated in Figure 23 and Figure 24, pirfenidone treatment resulted in a decrease in the staining for FUS as well as PABPC1 proteins, indicating that the anti-fibrotic activity elicited by pirfenidone is, in part, mediated by the RBPs FUS and PABPC1, which, in turn, affects its binding affinity to its target RNAs in IPF fibroblasts.

A

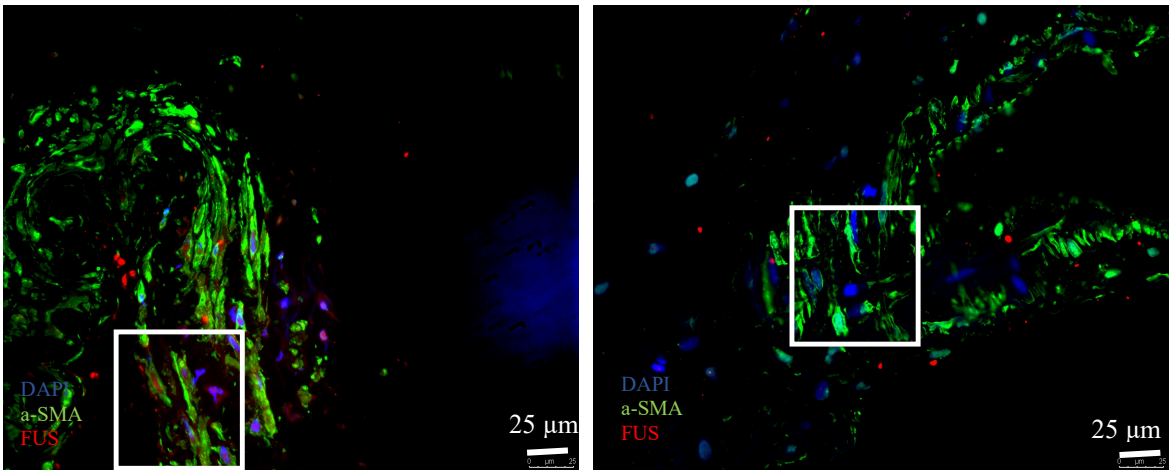

Untreated Pirfenidone

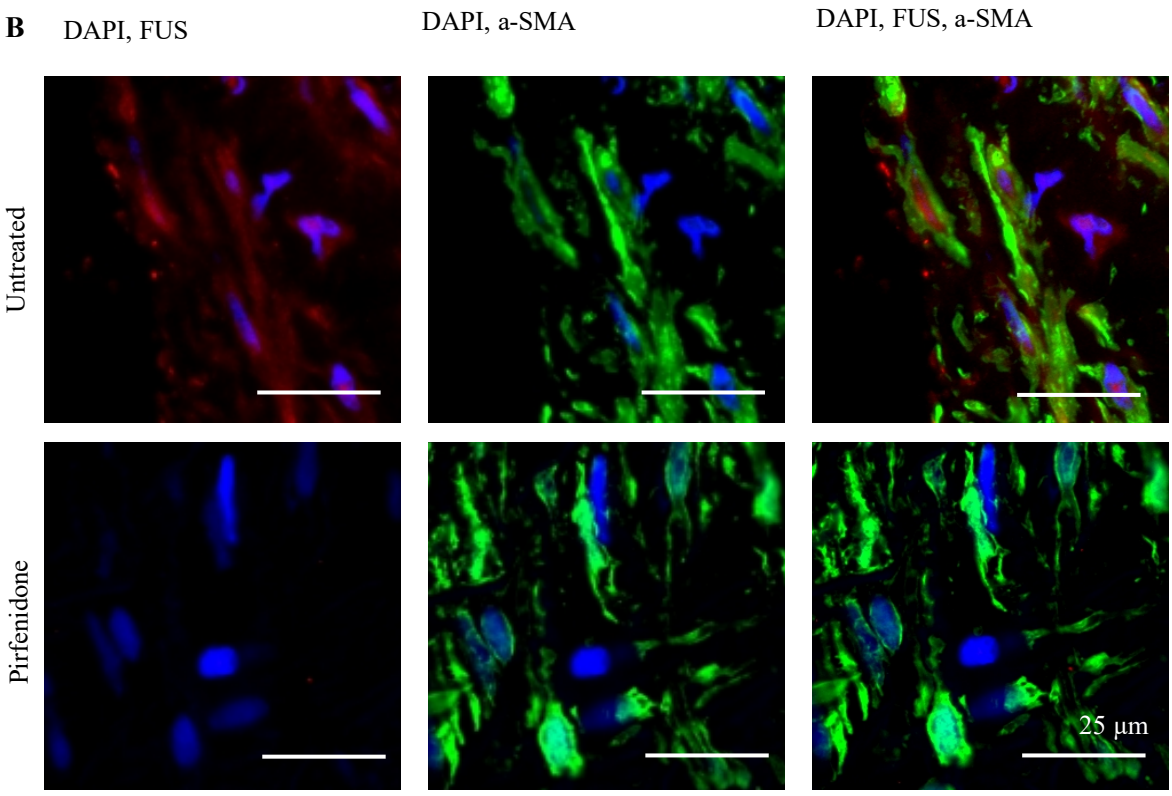

Figure 23: Pirfenidone treatment resulted in a decrease in the staining for FUS in fibroblasts in human lung PCLS slides
(A) Overview of IPF and Donor sections. Scale bar=25 µm (B) Immunofluorescence analysis of untreated (upper row) and pirfenidone treated PCLS slides on human lungs (lower row). Costaining of a-SMA (green) to indicate fibroblasts and FUS (red). Nuclei are stained with DAPI (blue). Scale bar=25 µm.

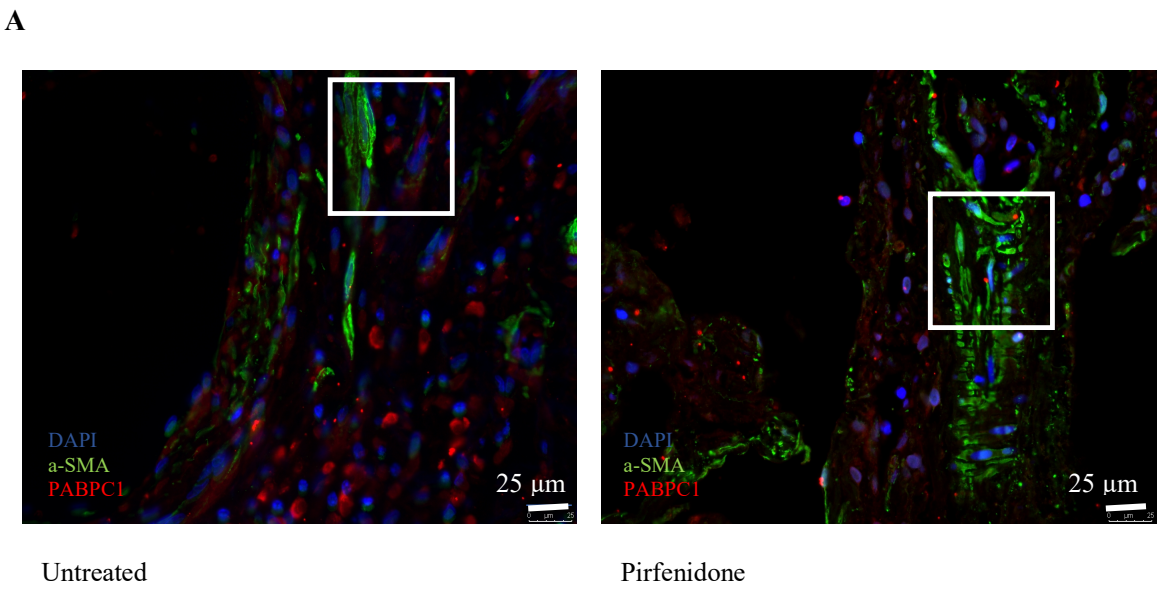

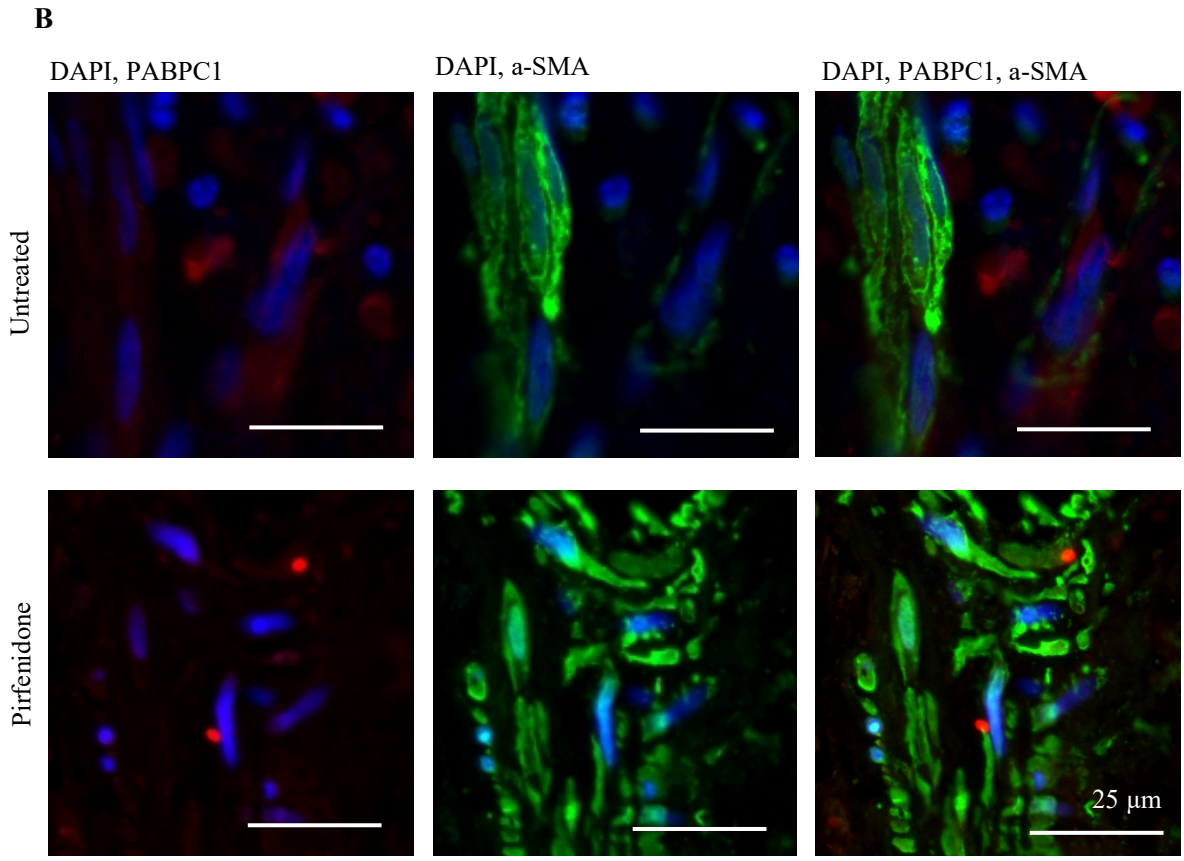

Figure 24: Pirfenidone treatment resulted in a decrease in the staining for PABPC1 in fibroblasts in human lung PCLS slides
(A) Overview of IPF and Donor sections. Scale bar=25 µm (B) Immunofluorescence analysis of untreated (upper row) and pirfenidone treated PCLS slides on human lungs (lower row). Costaining of a-SMA (green) to indicate fibroblasts and PABPC1 (red). Nuclei are stained with DAPI (blue). Scale bar=25 µm.

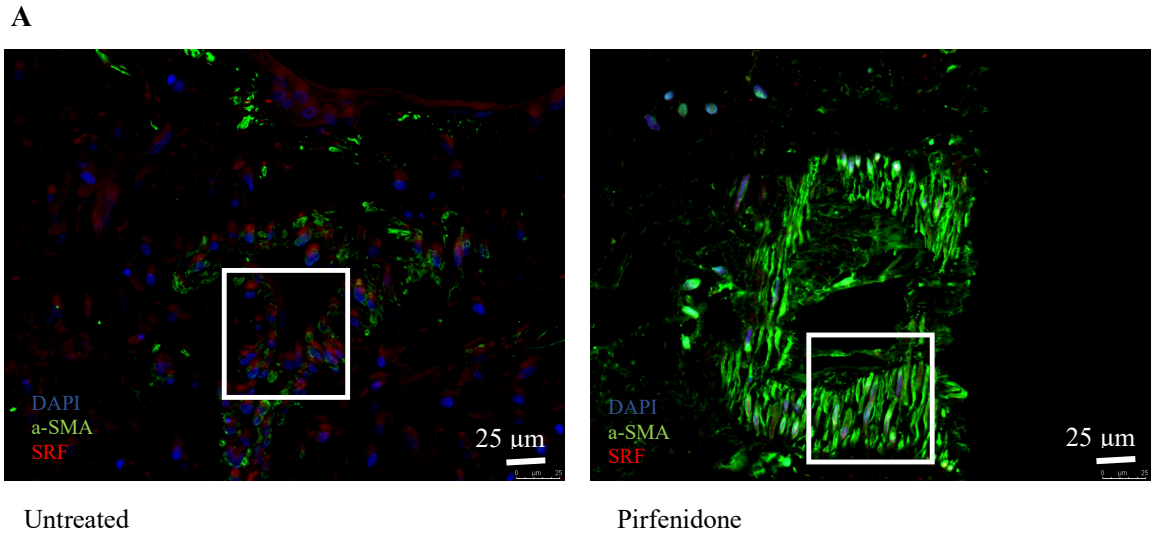

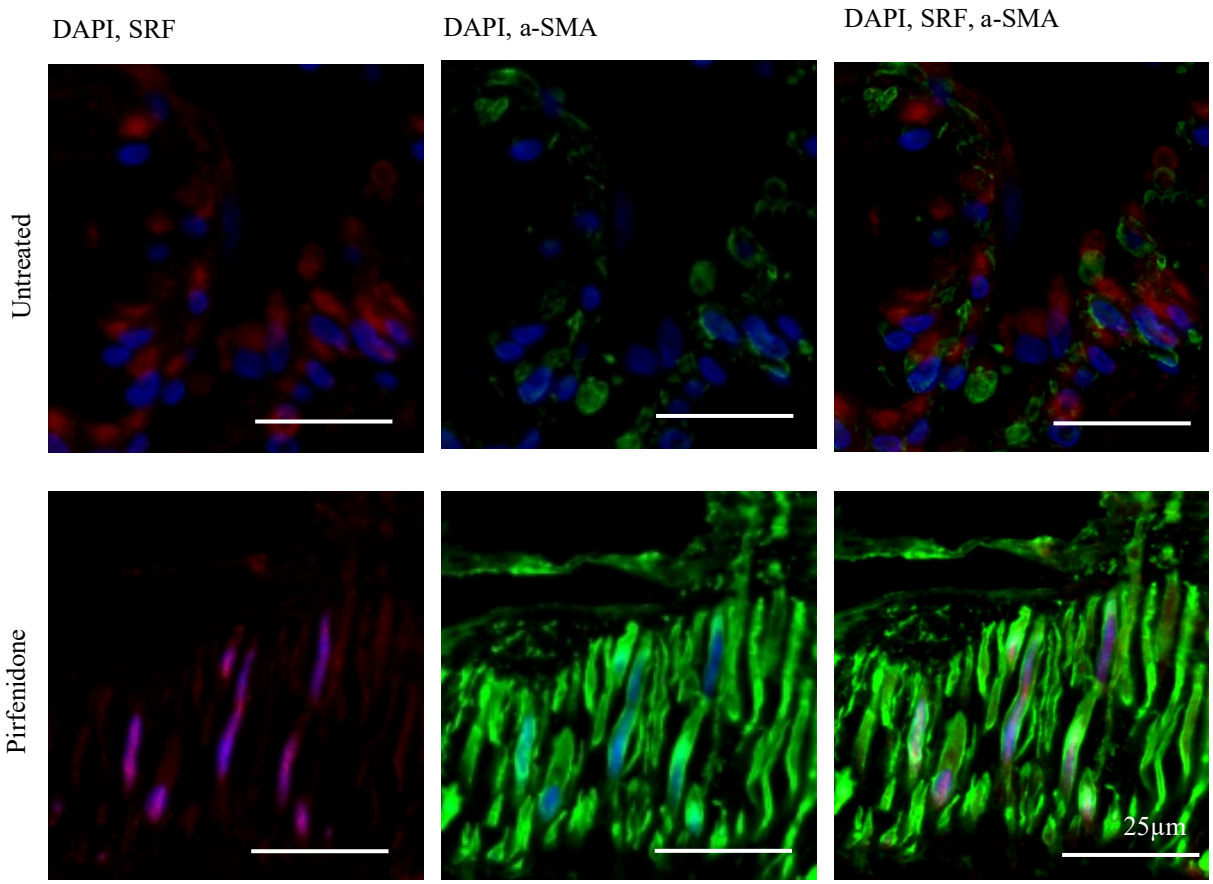

Figure 25: Pirfenidone treatment shows no decrease in the staining for SRF in fibroblasts in human lung PCLS slides
(A) Overview of IPF and Donor sections. Scale bar=25 µm (B) Immunofluorescence analysis of untreated (upper row) and pirfenidone treated PCLS slides on human lungs (lower row). Costaining of a-SMA (green) to indicate fibroblasts and SRF (red). Nuclei are stained with DAPI (blue). Scale bar=25 µm.

4. Discussion

4.1 Interpretation of our results

In the current study, we document that out of all the RNA binding proteins analyzed, FUS and PABPC1 are significantly elevated in fibroblasts and AECII of IPF patients as compared to donors. Of note, *ex vivo* treatment of IPF PCLS with the anti-fibrotic drug pirfenidone resulted in a reduced staining of both FUS and PABPC1, in the fibroblasts of IPF patients, indicating that pirfenidone directly or indirectly affects the expression of RBPs and thereby their target RNAs. The following table (Table 9) summarizes the experiments and the results of this study, and our interpretations of the observations are illustrated in the figure below (Figure 26).

	SRF	FUS	MBNL1	TDP43	PABPC1	TIA1	G3BP1
IPF tissue WB	↔	↔	↔	↔	↔	↔	↔
IPF tissue IHC	↔	↑		↑			
IPF fibroblasts WB	↔	↑	↔	↑	↑	↔	
IPF fibroblasts IF	↔	↑	↔	↑	↑		↔
AD tissue WB	↑	↔	↔	↔	↔		
AD tissue IHC			↑	↑			
AD MLE12 WB	↔	↔	↔	↔	↔	↔	
FUS over-expression		↑*					
Pirfenidon IPF PCLS IF	↔**	↓			↓		

↑ = elevated in fibrous or AD treated tissue

*overexpression drives fibroblst proliferation

↓ = Pirfenidone treatment resulted in a decrease of POI

↔ = not elevated in fibrous or AD treated tissue

** Pirfenidone treatment shows no decrease of POI

Table 9: Summary of the results of this study. Especilly FUS, TDP43 and PBPC1 are altered in fibrous or Amiodaron treated tissue.

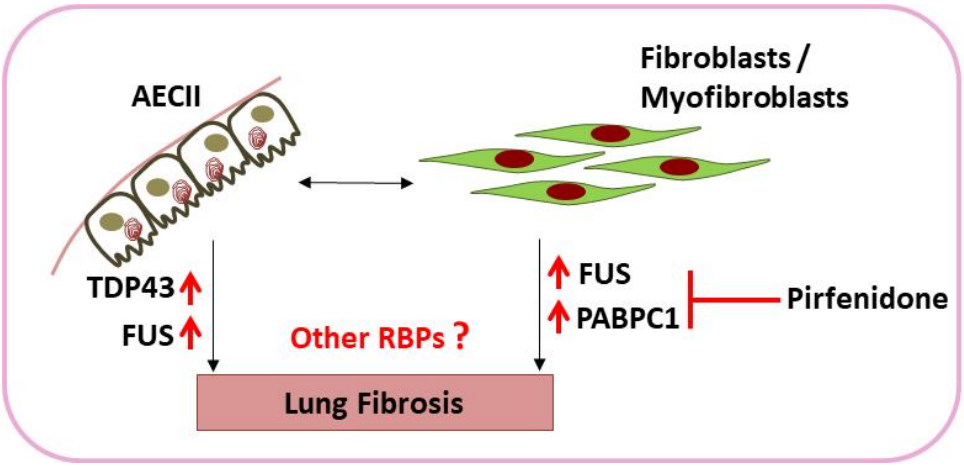

Figure 26: Cartoon summarizing the findings of this study. Depicted here is a simplified version of molecular events observed in IPF lungs in the context of RNA binding proteins. An increase in FUS protein is observed in both alveolar epithelial cells type II and fibroblasts and overexpression of full length FUS *in vitro* in healthy primary fibroblasts is sufficient to elicit fibroblast proliferation. PABPC1 is increased in IPF fibroblasts and treatment of IPF PCLS with anti-fibrotic drug pirfenidone decreases both FUS and PABPC1. AECII on the other hand show strong nuclear as well as cytosolic localization of TDP43 and FUS. Regulation of other RBPs and their role in quality control and cell fate mechanisms in IPF still remains to be elucidated.

4.2 Strengths and limitations of our study

This study provides a comprehensive overview of differentially regulated of RBPs, a very first study to report such observations in the context of lung fibrosis. Our study also hints towards the potential of RBPs as druggable candidates in IPF. However, it is apparent that this study lacks a concrete pathomechanistic understanding. Some pertinent questions could not be answered in this study, owing to the limited and stipulated time frame of this study, which is a little over six months. Such questions include: what are the target RNAs of the identified RBPs in different cell types of IPF lungs or in animal models of lung fibrosis and to what extent can the RBPs serve as new therapeutic candidates? Further long term investigations are required to answer these questions that may open up new therapeutic concepts for lung fibrosis.

4.3 Current state of research on RBPs in lung fibrosis and other diseases

4.3.1 FUS & TDP43

Nuclear exclusion of the RBPs FUS and TDP43 and subsequent cytoplasmic deposition leads to progressive disorders like Amyotrophic lateral sclerosis (ALS) and frontotemporal dementia (FTD) (Archbold *et al*, 2018) (Hanson *et al*, 2012). Both, FUS and TDP43, are ubiquitously expressed proteins. Mutations in the FUS gene cause loss of motor neurons and are associated with juvenile ALS. It was originally identified as an oncogene that is fused with the transcription factor / repressor C/EBP homologous protein 10 (CHOP), a potent ER stress molecule that is severely upregulated in the AECII of human IPF patient lungs. Its overexpression in vitro was sufficient enough to elicit apoptotic pathways, altogether indicating the key role of CHOP protein in maladaptive ER stress response and subsequent fibrosis (Klymenko *et al*, J Mol Med, 2019). Interestingly, the FUS-CHOP chimeric protein is formed by transcription of FUS gene that is then joined to CHOP exons by RNA splicing and this fused chimera was also translocated into the cytoplasm of liposarcoma cells (Rabbitts *et al,* 1993). Although FUS (in this study) and CHOP (Klymenko *et al*, 2019) proteins have been studied separately under conditions of IPF, it is still unclear if FUS-CHOP chimeric RNA or the resultant fusion protein is also differentially regulated under conditions of IPF.

Several studies report that TDP43 is cleaved, mis-localized, hyperphosphorylated or ubquitinated under different pathological conditions. Mutations in the glycine-rich C-terminal domain of TDP43 gene are associated with about 3% of familial cases of ALS (Daoud *et al*, 2009, Valdamnis *et al*, 2009). UV-cross-linking-immunoprecipitation-sequencing (CLIP-seq) analysis for TDP43 in mouse brain tissues revealed the interaction of TDP43 with more than 6,300 RNAs: its depletion resulted in alternate splicing of more than 900 mRNAs (Polymenidou *et al,* 2011). Due to its role in nonsense-mediated mRNA decay, the protein level of TDP43 is tightly maintained in healthy cells and has been suggested to be a critical RBP in cellular homeostasis. Its overexpression on the other hand may result in asymmetric interaction between TDP43 and its nascent RNA, stalling RNA polymerase II (RNA PolI) thereby leading to transcript degradation and autoregulation of TDP43 protein level. In fact, in primary neurons, overexpression of TDP35, a splice variant of TDP43, results in cytoplasmic

aggregation and neuronal cell death. Further, in response to stress, TDP43 translocates from nucleus to the cytoplasm where it binds to 14-3-3 proteins, relieving several transcription factors which then translocate into the nucleus to regulate stress response genes (Salih & Brunnet, 2008; Zhang *et al,* 2014). In addition, cytoplasmic localization of TDP43 as observed in stressed neuronal cells also plays a major role in stress granule (SG) kinetics and dynamics which are critical to cell survival (Aulas *et al*, 2012). Although such pathomechanistic relevance has been identified for these RBPS, their role in lung pathologies including IPF remains unstudied. We identified that both these RBPs are increased the lungs of IPF patients. In that, total protein levels of FUS were increased in fibroblasts of IPF patients and interestingly, its localization was also increased in both, the nucleus and the cytoplasm of these cells. On the other hand, intensive staining for TDP43 was observed in both nuclear and cytosolic compartments in the AECII of IPF patients as compared to donor lungs. This indicates strict cell specific regulation of these RBPs under conditions of IPF. Future studies will reveal if such increased FUS and / or TDP43 levels may initiate cytoplasmic inclusions and, in parallel, influence the expression and splicing of their target RNAs in the lungs of IPF patients, as previously shown in other organs and diseases.

4.3.2 SRF and MRTF

Altered RBP regulation has been documented in many neurological diseases. Some examples include Spinal Muscular Atrophy (SMA), Oculopharyngeal Muscular Dystrophy (OPMD), Myotonic Dystrophy type l (DM1) and ll and Spinocerebellar Ataxia Type ll (Hanson *et al.*, 2012). DM1, for instance, is an autosomal dominant disorder that is characterized by a highly variable phenotype and is caused by an unstable tri-CTG repeat expansion in the 3‘ untranslated region (UTR) of the dystophia myotonics protein kinase gene (DMPK) and greatly correlates with the malfunction of the RBP MBNL1 (Huin *et al*, 2013). The RBP SRF transcriptionally regulates the expression of contractile genes in smooth muscle cells (SMC) and a lack of SRF leads to hypo motility of smooth muscles, for example in the gastrointestinal tract (Lee *et al*, 2017). Reduced nuclear translocation of SRF is additionally associated with skeletal muscle atrophy in chronic obstructive pulmonary disease (COPD) (Ma *et al*, 2017). Ma et al established a cigarette-smoke induced mouse model where they investigated the role of SRF as a transcription factor which is critical in myocyte differentiation and

growth. In mice exposed to cigarette smoke, nuclear localization of SRF diminished along with its cytoplasmic accumulation and the SRF target genes involved in muscle growth and nutrition were downregulated subsequently leading to skeletal muscle atrophy (Ma *et al.*, 2017). Since COPD often coexists with IPF, and was found to be upregulated in IPF lungs, and since previous studies have implicated SRF/MRTF (Myocardin-Related Transcription Factor)-mediated signaling pathways in fibroblast differentiation and collagen production in idiopathic lung fibrosis (Sisson *et al*, 2015) (Zhou *et al*, 2013) (Sandbo *et al*, 2011) (Johnson *et al*, 2014) (Haak *et al*, 2014) (Penke *et al*, 2014), SRF was considered to be an interesting marker for RBP regulation in our study. As described in the introduction, myofibroblasts are crucial to the pathogenesis of tissue fibrosis. In the context of organ fibrosis, fibroblasts consistently differentiate into a myofibroblast phenotype, as defined by the formation of F-actin containing stress fibers, the increased expression of alpha-smooth muscle actin (SMA) and elaboration of extracellular matrix proteins, including fibronectin and collagen. Moreover, myofibroblasts exhibit an increased resistance to apoptosis (Sisson *et al.*, 2015) (Hinz *et al*, 2012). Due to their stress fiber formation, myofibroblasts exert contractile forces on their environment, thereby accentuating a typical fibrotic architectural distortion (Follonier *et al*, 2008) (Hinz *et al*, 2001) (Tomasek *et al*, 2002). The induction of fibroblast-to-myofibroblast transition depends on the activation of intracellular signaling pathways. One of these pathways is dependent on the release of MRTF from stress fibers, it functions as a transcriptional coactivator of SRF and together they regulate the expression of myofibroblast genes, including alpha-SMA and collagen (Sisson *et al.*, 2015) (Thannickal *et al*, 2014) (Tsou *et al*, 2014) (Sandbo & Dulin, 2011). SRF/MRTF signaling is intricately regulated by actin polymerization in case of a depolymerized actin MRTF is bound to the globular form and sequestered in the cytoplasm. During the polymerization from globular actin into F-actin in stress fibers MRTF is released and enabled to translocate into the nucleus (Sisson *et al.*, 2015). In fibroblasts, nuclear translocation of MRTF is induced by TGF-ß1 (Follonier *et al.*, 2008) (Scharenberg *et al*, 2014) (Small *et al*, 2010), by lysophosphatidic acid and by mechanotransduction pathways activated by stiff matrix substrates(Zhou *et al.*, 2013) (Johnson *et al*, 2013) (Sakai *et al*, 2013). Known antifibrotic mediators counter-regulate this pathway. Especially the anti-fibrotic eicosanoid prostaglandin E2 prevents TGF-ß1-mediated myofibroblast differentiation and increases myofibroblast susceptibility to Fas-mediated apoptosis by blocking nuclear localization of MRTF and preventing the

fusion with SRF (Penke *et al.*, 2014) (Ajayi *et al*, 2013) (Sisson *et al*, 2012) (Huang *et al*, 2009) (Maher *et al*, 2010) (Kolodsick *et al*, 2003). The elimination of myofibroblasts via apoptosis is crucial for the resolution of wound repair and the restoration of tissue homeostasis after injury (Tomasek *et al.*, 2002) (Thannickal & Horowitz, 2006), but these cells characteristically display a phenotype of apoptosis resistance (Sisson *et al.*, 2015) (Zhou *et al.*, 2013). Our results showing increased SRF in IPF lungs are in line with those of Sisson et al, who investigated the SRF/MRTF pathway and observed that, by blocking the nucleation of MRTF with the specific inhibitor CCG-203971, the myofibroblast differentiation is inhibited and fibrosis is reduced in two distinct murine models of lung fibrosis (Johnson *et al.*, 2013).

4.3.3 PABP and TIA1

RBPs also importantly contribute towards the assembly of stress granules (SG). Mutations that affect SG formation or persistence lead to neurodegenerative diseases including ALS, FTLD and some myopathies (Protter & Parker, 2016). Of interest is the poly(A)-binding protein (PABP), that binds to the poly(A) tail on the 3'end of mRNAs and stimulates the activity of polyadenylate polymerase by increasing its affinity towards RNA. It is also present during stages of mRNA metabolism including nonsense mediated decay and nucleocytoplasmic trafficking. PABP also protects the poly-A tail from degradation and ascertains regulated mRNA production (D.Voet & Voet, 2010). Mutations in PABP can cause Oculopharyngeal muscular dystrophy (OPMD) (Shoubridge C, 2000), but the involvement of lungs in this context remains unknown. Another important SG assembly protein that was also investigated in the current study is the T-cell intracellular antigen-1 (TIA1). In contrast to PABP, role of TIA1in lung disease has been described, and especially in the context of pulmonary sarcoidosis. Navratilova et al reported that the mRNA level of TIA1 is decreased in the bronchoalveolar lavage (BAL) fluids of patients with sarcoidosis and idiopathic interstitial pneumonias (IIPs) as compared to healthy donors and as compared to COPD and asthma (Navratilova *et al*, 2016). The pathogenic pattern of sarcoidosis includes a polarization of chronic inflammation to Th1 with elevated secretion of interleukin (IL)-2, IL-8, IL-12, Interferon (IFN) gamma and Tumor necrosis factor (TNF). A pathomechanistic relevance for Th2 cytokine profile (e.g. IL-4 and IL-6) has been

suggested for advanced sarcoidosis (Navratilova *et al.*, 2016) (1999) (Patterson *et al*, 2012). The inflammatory responses in these conditions are modulated at post-transcriptional level under the involvement of RBPs and microRNAs (Kafasla *et al*, 2014) (Gerstberger *et al*, 2014) (Ivanov & Anderson, 2013) (Gubin *et al*, 2014). We now show that TIA1 protein levels are not significantly different in IPF lung tissues or interstitial fibroblasts as compared to respective donor lungs. This could be because our study focused on the analysis of intracellular protein levels of TIA1 as compared to the study of Navaratilova et al, who reported protein levels of TIA1 in broncho alveolar fluids of IIP patients.

4.4 Conclusion

Our knowledge on the regulation of RBPs under conditions of lung fibrosis is scarce. Although preliminary, this is a first study that characterized the expression of different RBPs in the lungs of IPF patients. This study shows that RBPs are differentially regulated in a cell type specific manner in IPF patient lungs. The data obtained in this study encourages us to further study if some RBPs play a functional role in the development of lung fibrosis and identify if they may represent novel diagnostic, prognostic, and therapeutic targets for lung fibrosis.

5. References

(1999) Statement on sarcoidosis. Joint Statement of the American Thoracic Society (ATS), the European Respiratory Society (ERS) and the World Association of Sarcoidosis and Other Granulomatous Disorders (WASOG) adopted by the ATS Board of Directors and by the ERS Executive Committee, February 1999. American journal of respiratory and critical care medicine 160: 736-755

(2000) American Thoracic Society. Idiopathic pulmonary fibrosis: diagnosis and treatment. International consensus statement. American Thoracic Society (ATS), and the European Respiratory Society (ERS). *American journal of respiratory and critical care medicine* 161: 646-664

(2002) American Thoracic Society/European Respiratory Society International Multidisciplinary Consensus Classification of the Idiopathic Interstitial Pneumonias. This joint statement of the American Thoracic Society (ATS), and the European Respiratory Society (ERS) was adopted by the ATS board of directors, June 2001 and by the ERS Executive Committee, June 2001. *Am J Respir Crit Care Med* 165: 277-304

Aizer A, Brody Y, Ler LW, Sonenberg N, Singer RH, Shav-Tal Y (2008) The dynamics of mammalian P body transport, assembly, and disassembly in vivo. *Mol Biol Cell* 19: 4154-4166

Aizer A, Shav-Tal Y (2008) Intracellular trafficking and dynamics of P bodies. *Prion* 2: 131-134

Ajayi IO, Sisson TH, Higgins PD, Booth AJ, Sagana RL, Huang SK, White ES, King JE, Moore BB, Horowitz JC (2013) X-linked inhibitor of apoptosis regulates lung fibroblast resistance to Fas-mediated apoptosis. *American journal of respiratory cell and molecular biology* 49: 86-95

Alberti S, Dormann D (2019) LiquidLiquid Phase Separation in Disease. 53: 171-194

Alder JK, Chen JJ, Lancaster L, Danoff S, Su SC, Cogan JD, Vulto I, Xie M, Qi X, Tuder RM *et al* (2008) Short telomeres are a risk factor for idiopathic pulmonary fibrosis. *Proc Natl Acad Sci U S A* 105: 13051-13056

Amm I, Sommer T, Wolf DH (2014) Protein quality control and elimination of protein waste: the role of the ubiquitin-proteasome system. *Biochim Biophys Acta* 1843: 182-196

Anderson P, Kedersha N, Ivanov P (2015) Stress granules, P-bodies and cancer. *Biochim Biophys Acta* 1849: 861-870

Anstrom DM, Zhou X, Kalk CN, Song B, Lan Q (2012) Mosquitocidal properties of natural product compounds isolated from Chinese herbs and synthetic analogs of curcumin. *J Med Entomol* 49: 350-355

Archbold HC, Jackson KL, Arora A, Weskamp K, Tank EM, Li X, Miguez R, Dayton RD, Tamir S, Klein RL *et al* (2018) TDP43 nuclear export and neurodegeneration in models of amyotrophic lateral sclerosis and frontotemporal dementia. *Scientific reports* 8: 4606

Arimoto-Matsuzaki K, Saito H, Takekawa M (2016) TIA1 oxidation inhibits stress granule assembly and sensitizes cells to stress-induced apoptosis. *Nat Commun* 7: 10252

Arimoto K, Fukuda H, Imajoh-Ohmi S, Saito H, Takekawa M (2008) Formation of stress granules inhibits apoptosis by suppressing stress-responsive MAPK pathways. *Nat Cell Biol* 10: 1324-1332

Armanios MY, Chen JJ, Cogan JD, Alder JK, Ingersoll RG, Markin C, Lawson WE, Xie M, Vulto I, Phillips JA, 3rd *et al* (2007) Telomerase mutations in families with idiopathic pulmonary fibrosis. *N Engl J Med* 356: 1317-1326

Aulas A, Stabile S, Vande Velde C (2012) Endogenous TDP-43, but not FUS, contributes to stress granule assembly via G3BP. *Mol Neurodegener* 7: 54

Bajwah S, Ross JR, Peacock JL, Higginson IJ, Wells AU, Patel AS, Koffman J, Riley J (2013) Interventions to improve symptoms and quality of life of patients with fibrotic interstitial lung disease: a systematic review of the literature. *Thorax* 68: 867-879

Baraibar MA, Friguet B (2012) Changes of the proteasomal system during the aging process. *Prog Mol Biol Transl Sci* 109: 249-275

Bashkirov VI, Scherthan H, Solinger JA, Buerstedde JM, Heyer WD (1997) A mouse cytoplasmic exoribonuclease (mXRN1p) with preference for G4 tetraplex substrates. *The Journal of cell biology* 136: 761-773

Bhattacharyya SN, Habermacher R, Martine U, Closs EI, Filipowicz W (2006) Stress-induced reversal of microRNA repression and mRNA P-body localization in human cells. *Cold Spring Harbor symposia on quantitative biology* 71: 513-521

Boers JE, Ambergen AW, Thunnissen FB (1998) Number and proliferation of basal and parabasal cells in normal human airway epithelium. *Am J Respir Crit Care Med* 157: 2000-2006

Bonella F, Campo I, Zorzetto M, Boerner E, Ohshimo S, Theegraten E, Taube C, Costabel U (2021) Potential clinical utility of MUC5B und TOLLIP single nucleotid polymorphisms (SNPs) in the management of patients with IPF. *Orphanet J Rare Dis* 16:111

Boya P, Reggiori F, Codogno P (2013) Emerging regulation and functions of autophagy. *Nat Cell Biol* 15: 713-720

Boyd JD, Lee P, Feiler MS, Zauur N, Liu M, Concannon J, Ebata A, Wolozin B, Glicksman MA (2014) A high-content screen identifies novel compounds that inhibit stress-induced TDP-43 cellular aggregation and associated cytotoxicity. *J Biomol Screen* 19: 44-56

Bozyk, P. D., & Moore, B. B. (2011). Prostaglandin E2 and the pathogenesis of pulmonary fibrosis. *American journal of respiratory cell and molecular biology*, *45*(3), 445–452.

Brengues M, Parker R (2007) Accumulation of polyadenylated mRNA, Pab1p, eIF4E, and eIF4G with P-bodies in Saccharomyces cerevisiae. *Mol Biol Cell* 18: 2592-2602

Brengues M, Teixeira D, Parker R (2005) Movement of Eukaryotic mRNAs between Polysomes and Cytoplasmic Processing Bodies. *Science* 310: 486-489

Brinegar AE, Cooper TA (2016) Roles for RNA-binding proteins in development and disease. *Brain research* 1647: 1-8

Buchan JR, Kolaitis RM, Taylor JP, Parker R (2013) Eukaryotic stress granules are cleared by autophagy and Cdc48/VCP function. *Cell* 153: 1461-1474

Buchan JR, Muhlrad D, Parker R (2008) P bodies promote stress granule assembly in Saccharomyces cerevisiae. *Journal of Cell Biology* 183: 441-455

Buchan JR, Muhlrad D, Parker R (2008) P bodies promote stress granule assembly in Saccharomyces cerevisiae. *J Cell Biol* 183: 441-455

Bulteau AL, Szweda LI, Friguet B (2002) Age-dependent declines in proteasome activity in the heart. *Arch Biochem Biophys* 397: 298-304

Buzan MT, Pop CM (2015) State of the art in the diagnosis and management of interstitial lung disease. *Clujul Med* 88: 116-123

Cao X, Jin X, Liu B (2020) The involvement of stress granules in aging and aging-associated diseases. *Aging cell* 19: 1

Castello A, Horos R, Strein C, Fischer B, Eichelbaum K, Steinmetz LM, Krijgsveld J, Hentze MW (2013) System-wide identification of RNA-binding proteins by interactome capture. *Nature protocols* 8: 491-500

Chapman HA (2004) Disorders of lung matrix remodeling. *J Clin Invest* 113: 148-157

Chaudhary A, Fresquez TM, Naranjo MJ (2007) Tyrosine kinase Syk associates with toll-like receptor 4 and regulates signaling in human monocytic cells. *Immunol Cell Biol* 85: 249-256

Chen L, Liu B (2017) Relationships between Stress Granules, Oxidative Stress, and Neurodegenerative Diseases. *Oxid Med Cell Longev* 2017: 1809592

Cherkasov V, Hofmann S, Druffel-Augustin S, Mogk A, Tyedmers J, Stoecklin G, Bukau B (2013) Coordination of translational control and protein homeostasis during severe heat stress. *Curr Biol* 23: 2452-2462

Chernov KG, Barbet A, Hamon L, Ovchinnikov LP, Curmi PA, Pastre D (2009) Role of microtubules in stress granule assembly: microtubule dynamical instability favors the formation of micrometric stress granules in cells. *J Biol Chem* 284: 36569-36580

Cherry AA, Ananvoranich S (2014) Characterization of a homolog of DEAD-box RNA helicases in Toxoplasma gondii as a marker of cytoplasmic mRNP stress granules. *Gene* 543: 34-44

Chilosi M, Poletti V, Murer B, Lestani M, Cancellieri A, Montagna L, Piccoli P, Cangi G, Semenzato G, Doglioni C (2002) Abnormal re-epithelialization and lung remodeling in idiopathic pulmonary fibrosis: the role of deltaN-p63. *Lab Invest* 82: 1335-1345

Chilosi M, Poletti V, Zamo A, Lestani M, Montagna L, Piccoli P, Pedron S, Bertaso M, Scarpa A, Murer B *et al* (2003) Aberrant Wnt/beta-catenin pathway activation in idiopathic pulmonary fibrosis. *Am J Pathol* 162: 1495-1502

Cogan JD, Kropski JA, Zhao M, Mitchell DB, Rives L, Markin C, Garnett ET, Montgomery KH, Mason WR, McKean DF *et al* (2015) Rare variants in RTEL1 are associated with familial interstitial pneumonia. *Am J Respir Crit Care Med* 191: 646-655

Collard HR, Moore BB, Flaherty KR, Brown KK, Kaner RJ, King TE, Jr., Lasky JA, Loyd JE, Noth I, Olman MA *et al* (2007) Acute exacerbations of idiopathic pulmonary fibrosis. *Am J Respir Crit Care Med* 176: 636-643

Conte E, Gili E, Fruciano M, Korfei M, Fagone E, Iemmolo M, Lo Furno D, Giuffrida R, Crimi N, Guenther A *et al* (2013) PI3K p110γ overexpression in idiopathic pulmonary fibrosis lung tissue and fibroblast cells: in vitro effects of its inhibition. *Lab Invest* 93: 566-576

Cottin V, Hirani NA, Hotchkin DL, Nambiar AM, Ogura T, Otaola M, Skowasch D, Park JS, Poonyagariyagorn HK, Wuyts W *et al* (2018) Presentation, diagnosis and clinical course of the spectrum of progressive-fibrosing interstitial lung diseases. *Eur Respir Rev* 27

D.Voet, Voet JG (2010) *Biochemistry, 4th Edition*. Wiley

Dang Y, Kedersha N, Low WK, Romo D, Gorospe M, Kaufman R, Anderson P, Liu JO (2006) Eukaryotic initiation factor 2alpha-independent pathway of stress granule induction by the natural product pateamine A. *J Biol Chem* 281: 32870-32878

Daoud H, Valdmanis PN, Kabashi E, Dion P, Dupré N, Camu W, Meininger V, Rouleau GA (2009) Contribution of TARDBP mutations to sporadic amyotrophic lateral sclerosis. *J Med Genet* 46: 112-114

Davidson JN (1945) Cytoplasmic ribonucleoproteins. *The Biochemical journal* 39: lix-lxi

De Conti L, Baralle M, Buratti E (2017) Neurodegeneration and RNA-binding proteins. *Wiley interdisciplinary reviews RNA* 8

De Sadeleer LJ, Meert C, Yserbyt J, Slabbynck H, Verschakelen JA, Verbeken EK, Weynand B, De Langhe E, Lenaerts JL, Nemery B *et al* (2018) Diagnostic Ability of a Dynamic Multidisciplinary Discussion in Interstitial Lung Diseases: A Retrospective Observational Study of 938 Cases. *Chest* 153: 1416-1423

Decker CJ, Teixeira D, Parker R (2007) Edc3p and a glutamine/asparagine-rich domain of Lsm4p function in processing body assembly in Saccharomyces cerevisiae. *J Cell Biol* 179: 437-449

Denoth Lippuner A, Julou T, Barral Y (2014) Budding yeast as a model organism to study the effects of age. *FEMS Microbiol Rev* 38: 300-325

Desai TJ, Brownfield DG, Krasnow MA (2014) Alveolar progenitor and stem cells in lung development, renewal and cancer. *Nature* 507: 190-194

Dewey CM, Cenik B, Sephton CF, Johnson BA, Herz J, Yu G (2012) TDP-43 aggregation in neurodegeneration: Are stress granules the key? *Brain Research* 1462: 16

du Bois RM, Weycker D, Albera C, Bradford WZ, Costabel U, Kartashov A, King TE, Jr., Lancaster L, Noble PW, Sahn SA *et al* (2011) Forced vital capacity in patients with idiopathic pulmonary fibrosis: test properties and minimal clinically important difference. *Am J Respir Crit Care Med* 184: 1382-1389

Falahati H, Haji-Akbari A (2019) Thermodynamically driven assemblies and liquidliquid phase separations in biology. *Soft Matter* 15: 1135-1154

Federico A, Cardaioli E, Da Pozzo P, Formichi P, Gallus GN, Radi E (2012) Mitochondria, oxidative stress and neurodegeneration. *J Neurol Sci* 322: 254-262

Flaherty KR, Brown KK, Wells AU, Clerisme-Beaty E, Collard HR, Cottin V, Devaraj A, Inoue Y, Le Maulf F, Richeldi L *et al* (2017) Design of the PF-ILD trial: a double-blind, randomised, placebo-controlled phase III trial of nintedanib in patients with progressive fibrosing interstitial lung disease. *BMJ Open Respir Res* 4: e000212

Flaherty KR, Mumford JA, Murray S, Kazerooni EA, Gross BH, Colby TV, Travis WD, Flint A, Toews GB, Lynch JP, 3rd *et al* (2003) Prognostic implications of physiologic and radiographic changes in idiopathic interstitial pneumonia. *Am J Respir Crit Care Med* 168: 543-548

Follonier L, Schaub S, Meister JJ, Hinz B (2008) Myofibroblast communication is controlled by intercellular mechanical coupling. *Journal of cell science* 121: 3305-3316

Fournier MJ, Gareau C, Mazroui R (2010) The chemotherapeutic agent bortezomib induces the formation of stress granules. *Cancer Cell Int* 10: 12

Freibaum BD, Lu Y, Lopez-Gonzalez R, Kim NC, Almeida S, Lee KH, Badders N, Valentine M, Miller BL, Wong PC *et al* (2015) GGGGCC repeat expansion in C9orf72 compromises nucleocytoplasmic transport. *Nature* 525: 129-133

Fujimura K, Sasaki AT, Anderson P (2012) Selenite targets eIF4E-binding protein-1 to inhibit translation initiation and induce the assembly of non-canonical stress granules. *Nucleic Acids Res* 40: 8099-8110

Fujita K, Yamafuji M, Nakabeppu Y, Noda M (2012) Therapeutic approach to neurodegenerative diseases by medical gases: focusing on redox signaling and related antioxidant enzymes. *Oxid Med Cell Longev* 2012: 324256

Gandhi S, Abramov AY (2012) Mechanism of oxidative stress in neurodegeneration. *Oxid Med Cell Longev* 2012: 428010

Gasset-Rosa F, Chillon-Marinas C, Goginashvili A, Atwal RS, Artates JW, Tabet R, Wheeler VC, Bang AG, Cleveland DW, Lagier-Tourenne C (2017) Polyglutamine-Expanded Huntingtin Exacerbates Age-Related Disruption of Nuclear Integrity and Nucleocytoplasmic Transport. *Neuron* 94: 48-57.e44

Gebauer F, Hentze MW (2004) Molecular mechanisms of translational control. *Nat Rev Mol Cell Biol* 5: 827-835

Gerstberger S, Hafner M, Tuschl T (2014) A census of human RNA-binding proteins. *Nature reviews Genetics* 15: 829-845

Gilks N, Kedersha N, Ayodele M, Shen L, Stoecklin G, Dember LM, Anderson P (2004) Stress granule assembly is mediated by prion-like aggregation of TIA-1. *Mol Biol Cell* 15: 5383-5398

Gimenez A, Storrer K, Kuranishi L, Soares MR, Ferreira RG, Pereira CAC (2018) Change in FVC and survival in chronic fibrotic hypersensitivity pneumonitis. *Thorax* 73: 391-392

Gribbin J, Hubbard RB, Le Jeune I, Smith CJ, West J, Tata LJ (2006) Incidence and mortality of idiopathic pulmonary fibrosis and sarcoidosis in the UK. *Thorax* 61: 980-985

Gubin MM, Techasintana P, Magee JD, Dahm GM, Calaluce R, Martindale JL, Whitney MS, Franklin CL, Besch-Williford C, Hollingsworth JW *et al* (2014) Conditional knockout of the RNA-binding protein HuR in CD4(+) T cells reveals a gene dosage effect on cytokine production. *Mol Med* 20: 93-108

Guzikowski AR, Chen YS, Zid BM (2019) Stress-induced mRNP granules: Form and function of processing bodies and stress granules. *Wiley Interdisciplinary Reviews: RNA* 10: n/a-n/a

Haak AJ, Tsou PS, Amin MA, Ruth JH, Campbell P, Fox DA, Khanna D, Larsen SD, Neubig RR (2014) Targeting the myofibroblast genetic switch: inhibitors of myocardin-related transcription factor/serum response factor-regulated gene transcription prevent fibrosis in a murine model of skin injury. *The Journal of pharmacology and experimental therapeutics* 349: 480-486

Hanazawa M, Yonetani M, Sugimoto A (2011) PGL proteins self associate and bind RNPs to mediate germ granule assembly in C. elegans. *J Cell Biol* 192: 929-937

Hansell DM, Bankier AA, MacMahon H, McLoud TC, Muller NL, Remy J (2008) Fleischner Society: glossary of terms for thoracic imaging. *Radiology* 246: 697-722

Hanson KA, Kim SH, Tibbetts RS (2012) RNA-binding proteins in neurodegenerative disease: TDP-43 and beyond. *Wiley interdisciplinary reviews RNA* 3: 265-285

Helder S, Blythe AJ, Bond CS, Mackay JP (2016) Determinants of affinity and specificity in RNA-binding proteins. *Current opinion in structural biology* 38: 83-91

Hellmich B (2017) *Fallbuch Innere Medizin*. Georg Thieme Verlag

Heyd F, Lynch KW (2011) Degrade, move, regroup: signaling control of splicing proteins. *Trends in biochemical sciences* 36: 397-404

Hilberg F, Roth GJ, Krssak M, Kautschitsch S, Sommergruber W, Tontsch-Grunt U, Garin-Chesa P, Bader G, Zoephel A, Quant J *et al* (2008) BIBF 1120: triple angiokinase inhibitor with sustained receptor blockade and good antitumor efficacy. *Cancer Res* 68: 4774-4782

Hilliker A, Gao Z, Jankowsky E, Parker R (2011) The DEAD-box protein Ded1 modulates translation by the formation and resolution of an eIF4F-mRNA complex. *Mol Cell* 43: 962-972

Hinz B, Celetta G, Tomasek JJ, Gabbiani G, Chaponnier C (2001) Alpha-smooth muscle actin expression upregulates fibroblast contractile activity. *Molecular biology of the cell* 12: 2730-2741

Hinz B, Phan SH, Thannickal VJ, Prunotto M, Desmouliere A, Varga J, De Wever O, Mareel M, Gabbiani G (2012) Recent developments in myofibroblast biology: paradigms for connective tissue remodeling. *The American journal of pathology* 180: 1340-1355

Hong KU, Reynolds SD, Watkins S, Fuchs E, Stripp BR (2004) Basal cells are a multipotent progenitor capable of renewing the bronchial epithelium. *Am J Pathol* 164: 577-588

Horowitz JC, Thannickal VJ (2006) Epithelial-mesenchymal interactions in pulmonary fibrosis. *Semin Respir Crit Care Med* 27: 600-612

Huang SK, White ES, Wettlaufer SH, Grifka H, Hogaboam CM, Thannickal VJ, Horowitz JC, Peters-Golden M (2009) Prostaglandin E(2) induces fibroblast apoptosis by modulating multiple survival pathways. *FASEB journal : official publication of the Federation of American Societies for Experimental Biology* 23: 4317-4326

Hubbard R (2001) Occupational dust exposure and the aetiology of cryptogenic fibrosing alveolitis. *Eur Respir J Suppl* 32: 119s-121s

Hughes AL, Gottschling DE (2012) An early age increase in vacuolar pH limits mitochondrial function and lifespan in yeast. *Nature* 492: 261-265

Huin V, Vasseur F, Schraen-Maschke S, Dhaenens CM, Devos P, Dupont K, Sergeant N, Buee L, Lacour A, Hofmann-Radvanyi H *et al* (2013) MBNL1 gene variants as modifiers of disease severity in myotonic dystrophy type 1. *Journal of neurology* 260: 998-1003

Hunninghake GW, Lynch DA, Galvin JR, Gross BH, Muller N, Schwartz DA, King TE, Jr., Lynch JP, 3rd, Hegele R, Waldron J *et al* (2003) Radiologic findings are strongly associated with a pathologic diagnosis of usual interstitial pneumonia. *Chest* 124: 1215-1223

Hutchinson J, Fogarty A, Hubbard R, McKeever T (2015) Global incidence and mortality of idiopathic pulmonary fibrosis: a systematic review. *Eur Respir J* 46: 795-806

Ito D, Suzuki N (2011) Conjoint pathologic cascades mediated by ALS/FTLD-U linked RNA-binding proteins TDP-43 and FUS. *Neurology* 77: 1636-1643

Ivanov P, Anderson P (2013) Post-transcriptional regulatory networks in immunity. *Immunological reviews* 253: 253-272

Jain S, Wheeler JR, Walters RW, Agrawal A, Barsic A, Parker R (2016) ATPase-Modulated Stress Granules Contain a Diverse Proteome and Substructure. *Cell* 164: 487-498

Jay RS, Gregory JR, Andrew GH, Richard ER, Valerie LS, Stanley FH, Byron C (2005) The most infectious prion protein particles. *Nature* 437: 257

Jegal Y, Kim DS, Shim TS, Lim CM, Do Lee S, Koh Y, Kim WS, Kim WD, Lee JS, Travis WD *et al* (2005) Physiology is a stronger predictor of survival than pathology in fibrotic interstitial pneumonia. *Am J Respir Crit Care Med* 171: 639-644

Johnson LA, Rodansky ES, Haak AJ, Larsen SD, Neubig RR, Higgins PD (2014) Novel Rho/MRTF/SRF inhibitors block matrix-stiffness and TGF-beta-induced fibrogenesis in human colonic myofibroblasts. *Inflammatory bowel diseases* 20: 154-165

Johnson LA, Rodansky ES, Sauder KL, Horowitz JC, Mih JD, Tschumperlin DJ, Higgins PD (2013) Matrix stiffness corresponding to strictured bowel induces a fibrogenic response in human colonic fibroblasts. *Inflammatory bowel diseases* 19: 891-903

Jonas S, Izaurralde E (2013) The role of disordered protein regions in the assembly of decapping complexes and RNP granules. *Genes Dev* 27: 2628-2641

Josefson R, Andersson R, Nyström T (2017) How and why do toxic conformers of aberrant proteins accumulate during ageing? *Essays Biochem* 61: 317-324

Kaehler C, Isensee J, Hucho T, Lehrach H, Krobitsch S (2014) 5-Fluorouracil affects assembly of stress granules based on RNA incorporation. *Nucleic Acids Res* 42: 6436-6447

Kafasla P, Skliris A, Kontoyiannis DL (2014) Post-transcriptional coordination of immunological responses by RNA-binding proteins. *Nature immunology* 15: 492-502

Kastle M, Grune T (2011) Protein oxidative modification in the aging organism and the role of the ubiquitin proteasomal system. *Curr Pharm Des* 17: 4007-4022

Kato M, Han TW, Xie S, Shi K, Du X, Wu LC, Mirzaei H, Goldsmith EJ, Longgood J, Pei J *et al* (2012) Cell-free formation of RNA granules: low complexity sequence domains form dynamic fibers within hydrogels. *Cell* 149: 753-767

Kedersha N, Anderson P (2009) Regulation of translation by stress granules and processing bodies. *Prog Mol Biol Transl Sci* 90: 155-185

Kedersha N, Cho MR, Li W, Yacono PW, Chen S, Gilks N, Golan DE, Anderson P (2000) Dynamic shuttling of TIA-1 accompanies the recruitment of mRNA to mammalian stress granules. *J Cell Biol* 151: 1257-1268

Kedersha N, Ivanov P, Anderson P (2013) Stress granules and cell signaling: more than just a passing phase? *Trends in Biochemical Sciences* 38: 494-506

Kedersha N, Stoecklin G, Ayodele M, Yacono P, Lykke-Andersen J, Fritzler MJ, Scheuner D, Kaufman RJ, Golan DE, Anderson P (2005) Stress granules and processing bodies are dynamically linked sites of mRNP remodeling. *J Cell Biol* 169: 871-884

Kedersha NL, Gupta M, Li W, Miller I, Anderson P (1999) RNA-binding proteins TIA-1 and TIAR link the phosphorylation of eIF-2 alpha to the assembly of mammalian stress granules. *J Cell Biol* 147: 1431-1442

Kim Nam c, Tresse E, Kolaitis R-M, Molliex A, Thomas Ruth e, Alami Nael h, Wang B, Joshi A, Smith Rebecca b, Ritson Gillian p *et al* (2013) VCP Is Essential for Mitochondrial Quality Control by PINK1/Parkin and this Function Is Impaired by VCP Mutations. *Neuron* 78: 65-80

King TE, Jr., Bradford WZ, Castro-Bernardini S, Fagan EA, Glaspole I, Glassberg MK, Gorina E, Hopkins PM, Kardatzke D, Lancaster L *et al* (2014) A phase 3 trial of pirfenidone in patients with idiopathic pulmonary fibrosis. *N Engl J Med* 370: 2083-2092

King TE, Jr., Pardo A, Selman M (2011) Idiopathic pulmonary fibrosis. *Lancet* 378: 1949-1961

King TE, Jr., Tooze JA, Schwarz MI, Brown KR, Cherniack RM (2001) Predicting survival in idiopathic pulmonary fibrosis: scoring system and survival model. *Am J Respir Crit Care Med* 164: 1171-1181

Kistler KD, Nalysnyk L, Rotella P, Esser D (2014) Lung transplantation in idiopathic pulmonary fibrosis: a systematic review of the literature. *BMC Pulm Med* 14: 139

Klar J, Sobol M, Melberg A, Mabert K, Ameur A, Johansson AC, Feuk L, Entesarian M, Orlen H, Casar-Borota O *et al* (2013) Welander distal myopathy caused by an ancient founder mutation in TIA1 associated with perturbed splicing. *Hum Mutat* 34: 572-577

Klymenko O, Huehn M, Wilhelm J, Wasnick R, Shalashova I, Ruppert C, Henneke I, Hezel S, Guenther K, Mahavadi P *et al* (2019) Regulation and role of the ER stress transcription factor CHOP in alveolar epithelial type-II cells. *J Mol Med (Berl)* 97: 973-990

Kolodsick JE, Peters-Golden M, Larios J, Toews GB, Thannickal VJ, Moore BB (2003) Prostaglandin E2 inhibits fibroblast to myofibroblast transition via E. prostanoid receptor 2 signaling and cyclic adenosine monophosphate elevation. *American journal of respiratory cell and molecular biology* 29: 537-544

Korfei M, Skwarna S, Henneke I, MacKenzie B, Klymenko O, Saito S, Ruppert C, von der Beck D, Mahavadi P, Klepetko W *et al* (2015) Aberrant expression and activity of histone deacetylases in sporadic idiopathic pulmonary fibrosis. *Thorax* 70: 1022-1032

Kramer B (2017) Collagen vascular diseases associated with interstitial lung diseases - Analysis of alveolar epithelial cellular stress mechanisms. *VVB Laufersweiler Vertrag Dissertation*

Kreuter M, Wälscher J, Behr J (2017) Antifibrotic drugs as treatment of nonidiopathic pulmonary fibrosis interstitial pneumonias: the time is now (?). *Curr Opin Pulm Med* 23: 418-425

Kropski JA, Lawson WE, Blackwell TS (2012) Right place, right time: the evolving role of herpesvirus infection as a "second hit" in idiopathic pulmonary fibrosis. *Am J Physiol Lung Cell Mol Physiol* 302: L441-444

Kropski JA, Lawson WE, Blackwell TS (2015) Personalizing Therapy in Idiopathic Pulmonary Fibrosis: A Glimpse of the Future? *Am J Respir Crit Care Med* 192: 1409-1411

Kroschwald S, Maharana S, Mateju D, Malinovska L, Nuske E, Poser I, Richter D, Alberti S (2015) Promiscuous interactions and protein disaggregases determine the material state of stress-inducible RNP granules. *Elife* 4: e06807

Kumar-Singh S (2011) Progranulin and TDP-43: mechanistic links and future directions. *J Mol Neurosci* 45: 561-573

Lam YT, Aung-Htut MT, Lim YL, Yang H, Dawes IW (2011) Changes in reactive oxygen species begin early during replicative aging of Saccharomyces cerevisiae cells. *Free Radic Biol Med* 50: 963-970

Langer F, Eisele YS, Fritschi SK, Staufenbiel M, Walker LC, Jucker M (2011) Soluble Aβ seeds are potent inducers of cerebral β-amyloid deposition. *The Journal of neuroscience : the official journal of the Society for Neuroscience* 31: 14488

Lechler MC, David DC (2017) More stressed out with age? Check your RNA granule aggregation. *Prion* 11: 313-322

Lee MY, Park C, Ha SE, Park PJ, Berent RM, Jorgensen BG, Corrigan RD, Grainger N, Blair PJ, Slivano OJ *et al* (2017) Serum response factor regulates smooth muscle contractility via myotonic dystrophy protein kinases and L-type calcium channels. *PloS one* 12: e0171262

Li YR, King OD, Shorter J, Gitler AD (2013) Stress granules as crucibles of ALS pathogenesis. *J Cell Biol* 201: 361-372

Lin Y, Protter DS, Rosen MK, Parker R (2015) Formation and Maturation of Phase-Separated Liquid Droplets by RNA-Binding Proteins. *Mol Cell* 60: 208-219

Ling SC, Polymenidou M, Cleveland DW (2013) Converging mechanisms in ALS and FTD: disrupted RNA and protein homeostasis. *Neuron* 79: 416-438

Liu-Yesucevitz L, Bilgutay A, Zhang YJ, Vanderweyde T, Citro A, Mehta T, Zaarur N, McKee A, Bowser R, Sherman M *et al* (2010) Tar DNA binding protein-43 (TDP-43) associates with stress granules: analysis of cultured cells and pathological brain tissue. *PLoS One* 5: e13250

López-Otín C, Blasco MA, Partridge L, Serrano M, Kroemer G (2013) The Hallmarks of Aging. *Cell* 153: 1194-1217

Loschi M, Leishman CC, Berardone N, Boccaccio GL (2009) Dynein and kinesin regulate stress-granule and P-body dynamics. *J Cell Sci* 122: 3973-3982

Ma R, Gong X, Jiang H, Lin C, Chen Y, Xu X, Zhang C, Wang J, Lu W, Zhong N (2017) Reduced nuclear translocation of serum response factor is associated with skeletal muscle atrophy in a cigarette smoke-induced mouse model of COPD. *International journal of chronic obstructive pulmonary disease* 12: 581-587

Mahavadi P, Henneke I, Ruppert C, Knudsen L, Venkatesan S, Liebisch G, Chambers RC, Ochs M, Schmitz G, Vancheri C *et al* (2014) Altered surfactant homeostasis and alveolar epithelial cell stress in amiodarone-induced lung fibrosis. *Toxicological sciences : an official journal of the Society of Toxicology* 142: 285-297

Mahavadi P, Knudsen L, Venkatesan S, Henneke I, Hegermann J, Wrede C, Ochs M, Ahuja S, Chillappagari S, Ruppert C *et al* (2015) Regulation of macroautophagy in amiodarone-induced pulmonary fibrosis. *J Pathol Clin Res* 1: 252-263

Mahavadi P, Korfei M, Henneke I, Liebisch G, Schmitz G, Gochuico BR, Markart P, Bellusci S, Seeger W, Ruppert C *et al* (2010) Epithelial stress and apoptosis underlie Hermansky-Pudlak syndrome-associated interstitial pneumonia. *Am J Respir Crit Care Med* 182: 207-219

Maher TM (2012) Diffuse parenchymal lung disease. *Medicine* 40: 314-321

Maher TM, Evans IC, Bottoms SE, Mercer PF, Thorley AJ, Nicholson AG, Laurent GJ, Tetley TD, Chambers RC, McAnulty RJ (2010) Diminished prostaglandin E2 contributes to the apoptosis paradox in idiopathic pulmonary fibrosis. *American journal of respiratory and critical care medicine* 182: 73-82

Martinez FJ, Collard HR, Pardo A, Raghu G, Richeldi L, Selman M, Swigris JJ, Taniguchi H, Wells AU (2017) Idiopathic pulmonary fibrosis. *Nat Rev Dis Primers* 3: 17074

Mason TA, Kolobova E, Liu J, Roland JT, Chiang C, Goldenring JR (2011) Darinaparsin is a multivalent chemotherapeutic which induces incomplete stress response with disruption of microtubules and Shh signaling. *PLoS One* 6: e27699

Mazroui R, Di Marco S, Kaufman RJ, Gallouzi IE (2007) Inhibition of the ubiquitin-proteasome system induces stress granule formation. *Mol Biol Cell* 18: 2603-2618

McFaline-Figueroa JR, Vevea J, Swayne TC, Zhou C, Liu C, Leung G, Boldogh IR, Pon LA (2011) Mitochondrial quality control during inheritance is associated with lifespan and mother-daughter age asymmetry in budding yeast. *Aging Cell* 10: 885-895

Mikolasch TA, Porter JC (2014) Transbronchial cryobiopsy in the diagnosis of interstitial lung disease: a cool new approach. *Respirology* 19: 623-624

Mirzaei H, Regnier F (2008) Protein:protein aggregation induced by protein oxidation. *J Chromatogr B Analyt Technol Biomed Life Sci* 873: 8-14

Moeller BJ, Cao Y, Li CY, Dewhirst MW (2004) Radiation activates HIF-1 to regulate vascular radiosensitivity in tumors: role of reoxygenation, free radicals, and stress granules. *Cancer Cell* 5: 429-441

Mokas S, Mills JR, Garreau C, Fournier MJ, Robert F, Arya P, Kaufman RJ, Pelletier J, Mazroui R (2009) Uncoupling stress granule assembly and translation initiation inhibition. *Mol Biol Cell* 20: 2673-2683

Molliex A, Temirov J, Lee J, Coughlin M, Kanagaraj AP, Kim HJ, Mittag T, Taylor JP (2015a) Phase separation by low complexity domains promotes stress granule assembly and drives pathological fibrillization. *Cell* 163: 123-133

Molliex A, Temirov J, Lee J, Coughlin M, Kanagaraj Anderson p, Kim Hong j, Mittag T, Taylor Jp (2015b) Phase Separation by Low Complexity Domains Promotes Stress Granule Assembly and Drives Pathological Fibrillization. *Cell* 163: 123-133

Moreno JA, Radford H, Peretti D, Steinert JR, Verity N, Martin MG, Halliday M, Morgan J, Dinsdale D, Ortori CA *et al* (2012) Sustained translational repression by eIF2alpha-P mediates prion neurodegeneration. *Nature* 485: 507-511

Moujaber O, Mahboubi H, Kodiha M, Bouttier M, Bednarz K, Bakshi R, White J, Larose L, Colmegna I, Stochaj U (2017) Dissecting the molecular mechanisms that impair stress granule formation in aging cells. *BBA - Molecular Cell Research* 1864: 475-486

Nadezhdina ES, Lomakin AJ, Shpilman AA, Chudinova EM, Ivanov PA (2010) Microtubules govern stress granule mobility and dynamics. *Biochim Biophys Acta* 1803: 361-371

Naikawadi RP, Disayabutr S, Mallavia B, Donne ML, Green G, La JL, Rock JR, Looney MR, Wolters PJ (2016) Telomere dysfunction in alveolar epithelial cells causes lung remodeling and fibrosis. *JCI Insight* 1: e86704

Navratilova Z, Novosadova E, Hagemann-Jensen M, Kullberg S, Kolek V, Grunewald J, Petrek M (2016) Expression Profile of Six RNA-Binding Proteins in Pulmonary Sarcoidosis. *PloS one* 11: e0161669

Noble PW, Albera C, Bradford WZ, Costabel U, Glassberg MK, Kardatzke D, King TE, Jr., Lancaster L, Sahn SA, Szwarcberg J *et al* (2011) Pirfenidone in patients with idiopathic pulmonary fibrosis (CAPACITY): two randomised trials. *Lancet* 377: 1760-1769

Nogee LM, Dunbar AE, 3rd, Wert SE, Askin F, Hamvas A, Whitsett JA (2001) A mutation in the surfactant protein C gene associated with familial interstitial lung disease. *N Engl J Med* 344: 573-579

Noth I, Anstrom KJ, Calvert SB, de Andrade J, Flaherty KR, Glazer C, Kaner RJ, Olman MA (2012) A placebo-controlled randomized trial of warfarin in idiopathic pulmonary fibrosis. *Am J Respir Crit Care Med* 186: 88-95

Onomoto K, Yoneyama M, Fung G, Kato H, Fujita T (2014) Antiviral innate immunity and stress granule responses. *Trends Immunol* 35: 420-428

Panas MD, Ivanov P, Anderson P (2016) Mechanistic insights into mammalian stress granule dynamics. *J Cell Biol* 215: 313-323

Park IN, Jegal Y, Kim DS, Do KH, Yoo B, Shim TS, Lim CM, Lee SD, Koh Y, Kim WS *et al* (2009) Clinical course and lung function change of idiopathic nonspecific interstitial pneumonia. *Eur Respir J* 33: 68-76

Pataer A, Swisher SG, Roth JA, Logothetis CJ, Corn PG (2009) Inhibition of RNA-dependent protein kinase (PKR) leads to cancer cell death and increases chemosensitivity. *Cancer Biol Ther* 8: 245-252

Patel A, Lee Hyun o, Jawerth L, Maharana S, Jahnel M, Hein Marco y, Stoynov S, Mahamid J, Saha S, Franzmann Titus m *et al* (2015a) A Liquid-to-Solid Phase Transition of the ALS Protein FUS Accelerated by Disease Mutation. *Cell* 162: 1066-1077

Patel A, Lee HO, Jawerth L, Maharana S, Jahnel M, Hein MY, Stoynov S, Mahamid J, Saha S, Franzmann TM *et al* (2015b) A Liquid-to-Solid Phase Transition of the ALS Protein FUS Accelerated by Disease Mutation. *Cell* 162: 1066-1077

Patten DA, Germain M, Kelly MA, Slack RS (2010) Reactive oxygen species: stuck in the middle of neurodegeneration. *J Alzheimers Dis* 20 Suppl 2: S357-367

Patterson KC, Hogarth K, Husain AN, Sperling AI, Niewold TB (2012) The clinical and immunologic features of pulmonary fibrosis in sarcoidosis. *Translational research : the journal of laboratory and clinical medicine* 160: 321-331

Penke LR, Huang SK, White ES, Peters-Golden M (2014) Prostaglandin E2 inhibits alpha-smooth muscle actin transcription during myofibroblast differentiation via distinct mechanisms of modulation of serum response factor and myocardin-related transcription factor-A. *The Journal of biological chemistry* 289: 17151-17162

Polymenidou M, Lagier-Tourenne C, Hutt KR, Huelga SC, Moran J, Liang TY, Ling SC, Sun E, Wancewicz E, Mazur C *et al* (2011) Long pre-mRNA depletion and RNA missplicing contribute to neuronal vulnerability from loss of TDP-43. *Nat Neurosci* 14: 459-468

Protter DSW, Parker R (2016) Principles and Properties of Stress Granules. *Trends Cell Biol* 26: 668-679

Rabbitts TH, Forster A, Larson R, Nathan P (1993) Fusion of the dominant negative transcription regulator CHOP with a novel gene FUS by translocation t(12;16) in malignant liposarcoma. *Nat Genet* 4: 175-180

Raghu G (2011) Idiopathic pulmonary fibrosis: increased survival with "gastroesophageal reflux therapy": fact or fallacy? *Am J Respir Crit Care Med* 184: 1330-1332

Raghu G, Collard HR, Egan JJ, Martinez FJ, Behr J, Brown KK, Colby TV, Cordier JF, Flaherty KR, Lasky JA *et al* (2011a) An official ATS/ERS/JRS/ALAT statement: idiopathic pulmonary fibrosis: evidence-based guidelines for diagnosis and management. *American journal of respiratory and critical care medicine* 183: 788-824

Raghu G, Collard HR, Egan JJ, Martinez FJ, Behr J, Brown KK, Colby TV, Cordier JF, Flaherty KR, Lasky JA *et al* (2011b) An official ATS/ERS/JRS/ALAT statement: idiopathic pulmonary fibrosis: evidence-based guidelines for diagnosis and management. *Am J Respir Crit Care Med* 183: 788-824

Raghu G, Rochwerg B, Zhang Y, Garcia CA, Azuma A, Behr J, Brozek JL, Collard HR, Cunningham W, Homma S *et al* (2015) An Official ATS/ERS/JRS/ALAT Clinical Practice Guideline: Treatment of Idiopathic Pulmonary Fibrosis. An Update of the 2011 Clinical Practice Guideline. *Am J Respir Crit Care Med* 192: e3-19

Raghu G, Weycker D, Edelsberg J, Bradford WZ, Oster G (2006) Incidence and prevalence of idiopathic pulmonary fibrosis. *Am J Respir Crit Care Med* 174: 810-816

Ramaswami M, Taylor JP, Parker R (2013) Altered ribostasis: RNA-protein granules in degenerative disorders. *Cell* 154: 727-736

Richeldi L, Collard HR, Jones MG (2017) Idiopathic pulmonary fibrosis. *Lancet* 389: 1941-1952

Richeldi L, du Bois RM, Raghu G, Azuma A, Brown KK, Costabel U, Cottin V, Flaherty KR, Hansell DM, Inoue Y *et al* (2014) Efficacy and safety of nintedanib in idiopathic pulmonary fibrosis. *N Engl J Med* 370: 2071-2082

Rock JR, Barkauskas CE, Cronce MJ, Xue Y, Harris JR, Liang J, Noble PW, Hogan BL (2011) Multiple stromal populations contribute to pulmonary fibrosis without evidence for epithelial to mesenchymal transition. *Proc Natl Acad Sci U S A* 108: E1475-1483

Ryerson CJ, Cayou C, Topp F, Hilling L, Camp PG, Wilcox PG, Khalil N, Collard HR, Garvey C (2014) Pulmonary rehabilitation improves long-term outcomes in interstitial lung disease: a prospective cohort study. *Respir Med* 108: 203-210

Saez I, Vilchez D (2014) The Mechanistic Links Between Proteasome Activity, Aging and Age-related Diseases. *Curr Genomics* 15: 38-51

Sakai N, Chun J, Duffield JS, Wada T, Luster AD, Tager AM (2013) LPA1-induced cytoskeleton reorganization drives fibrosis through CTGF-dependent fibroblast proliferation. *FASEB journal : official publication of the Federation of American Societies for Experimental Biology* 27: 1830-1846

Salih DA, Brunet A (2008) FoxO transcription factors in the maintenance of cellular homeostasis during aging. *Curr Opin Cell Biol* 20: 126-136

Sandbo N, Dulin N (2011) Actin cytoskeleton in myofibroblast differentiation: ultrastructure defining form and driving function. *Translational research : the journal of laboratory and clinical medicine* 158: 181-196

Sandbo N, Lau A, Kach J, Ngam C, Yau D, Dulin NO (2011) Delayed stress fiber formation mediates pulmonary myofibroblast differentiation in response to TGF-beta. *American journal of physiology Lung cellular and molecular physiology* 301: L656-666

Santangelo PJ, Lifland AW, Curt P, Sasaki Y, Bassell GJ, Lindquist ME, Crowe JE, Jr. (2009) Single molecule-sensitive probes for imaging RNA in live cells. *Nat Methods* 6: 347-349

Schaefer JA, Cronkite RC, Hu KU (2011) Differential relationships between continuity of care practices, engagement in continuing care, and abstinence among subgroups of patients with substance use and psychiatric disorders. *J Stud Alcohol Drugs* 72: 611-621

Scharenberg MA, Pippenger BE, Sack R, Zingg D, Ferralli J, Schenk S, Martin I, Chiquet-Ehrismann R (2014) TGF-beta-induced differentiation into myofibroblasts involves specific regulation of two MKL1 isoforms. *Journal of cell science* 127: 1079-1091

Scheckhuber CQ, Erjavec N, Tinazli A, Hamann A, Nyström T, Osiewacz HD (2007) Reducing mitochondrial fission results in increased life span and fitness of two fungal ageing models. *Nat Cell Biol* 9: 99-105

Scotton CJ, Chambers RC (2007) Molecular targets in pulmonary fibrosis: the myofibroblast in focus. *Chest* 132: 1311-1321

Seibold M, Wise A, Speer M, Steele M, Brown K, Loyd J, Fingerlin T, Zhang W, Gudmundsson G, Groshong S (2011) A common MUC5B Promotor Polymorphism and Pulmoary fibrosis. *N Engl J Med* 364(16):1503-1512

Selman M, King TE, Pardo A (2001) Idiopathic pulmonary fibrosis: prevailing and evolving hypotheses about its pathogenesis and implications for therapy. *Ann Intern Med* 134: 136-151

Sheinberger J, Shav-Tal Y (2017) mRNPs meet stress granules. *FEBS Lett* 591: 2534-2542

Sheth U, Parker R (2003a) Decapping and decay of messenger RNA occur in cytoplasmic processing bodies. *Science (New York, NY)* 300: 805-808

Sheth U, Parker R (2003b) Decapping and decay of messenger RNA occur in cytoplasmic processing bodies. *Science* 300: 805-808

Shoubridge C GJ, 2000. POLYALANINE TRACT DISORDERS AND NEUROCOGNITIVE PHENOTYPES, In: Madame Curie Bioscience Database. Austin (TX): Landes Bioscience.

Sisson TH, Ajayi IO, Subbotina N, Dodi AE, Rodansky ES, Chibucos LN, Kim KK, Keshamouni VG, White ES, Zhou Y *et al* (2015) Inhibition of myocardin-related transcription factor/serum response factor signaling decreases lung fibrosis and promotes mesenchymal cell apoptosis. *The American journal of pathology* 185: 969-986

Sisson TH, Maher TM, Ajayi IO, King JE, Higgins PD, Booth AJ, Sagana RL, Huang SK, White ES, Moore BB *et al* (2012) Increased survivin expression contributes to apoptosis-resistance in IPF fibroblasts. *Adv Biosci Biotechnol* 3: 657-664

Small EM, Thatcher JE, Sutherland LB, Kinoshita H, Gerard RD, Richardson JA, Dimaio JM, Sadek H, Kuwahara K, Olson EN (2010) Myocardin-related transcription factor-a controls myofibroblast activation and fibrosis in response to myocardial infarction. *Circulation research* 107: 294-304

Solomon JJ, Olson AL, Fischer A, Bull T, Brown KK, Raghu G (2013) Scleroderma lung disease. *Eur Respir Rev* 22: 6-19

Somasekharan SP, El-Naggar A, Leprivier G, Cheng H, Hajee S, Grunewald TG, Zhang F, Ng T, Delattre O, Evdokimova V *et al* (2015) YB-1 regulates stress granule formation and tumor progression by translationally activating G3BP1. *J Cell Biol* 208: 913-929

Soto-Rifo R, Valiente-Echeverria F, Rubilar PS, Garcia-de-Gracia F, Ricci EP, Limousin T, Decimo D, Mouland AJ, Ohlmann T (2014) HIV-2 genomic RNA accumulates in stress granules in the absence of active translation. *Nucleic Acids Res* 42: 12861-12875

Sowa ME, Bennett EJ, Gygi SP, Harper JW (2009) Defining the human deubiquitinating enzyme interaction landscape. *Cell* 138: 389-403

Squier TC (2001) Oxidative stress and protein aggregation during biological aging. *Exp Gerontol* 36: 1539-1550

Stuart BD, Choi J, Zaidi S, Xing C, Holohan B, Chen R, Choi M, Dharwadkar P, Torres F, Girod CE *et al* (2015) Exome sequencing links mutations in PARN and RTEL1 with familial pulmonary fibrosis and telomere shortening. *Nat Genet* 47: 512-517

Tabner BJ, El-Agnaf OM, German MJ, Fullwood NJ, Allsop D (2005) Protein aggregation, metals and oxidative stress in neurodegenerative diseases. *Biochem Soc Trans* 33: 1082-1086

Taskar VS, Coultas DB (2006) Is idiopathic pulmonary fibrosis an environmental disease? *Proc Am Thorac Soc* 3: 293-298

Teter SA, Eggerton KP, Scott SV, Kim J, Fischer AM, Klionsky DJ (2001) Degradation of lipid vesicles in the yeast vacuole requires function of Cvt17, a putative lipase. *J Biol Chem* 276: 2083-2087

Thannickal VJ, Henke CA, Horowitz JC, Noble PW, Roman J, Sime PJ, Zhou Y, Wells RG, White ES, Tschumperlin DJ (2014) Matrix biology of idiopathic pulmonary fibrosis: a workshop report of the national heart, lung, and blood institute. *The American journal of pathology* 184: 1643-1651

Thannickal VJ, Horowitz JC (2006) Evolving concepts of apoptosis in idiopathic pulmonary fibrosis. *Proceedings of the American Thoracic Society* 3: 350-356

Thomas MG, Martinez Tosar LJ, Loschi M, Pasquini JM, Correale J, Kindler S, Boccaccio GL (2005) Staufen recruitment into stress granules does not affect early mRNA transport in oligodendrocytes. *Molecular biology of the cell* 16: 405-420

Tomasek JJ, Gabbiani G, Hinz B, Chaponnier C, Brown RA (2002) Myofibroblasts and mechano-regulation of connective tissue remodelling. *Nature reviews Molecular cell biology* 3: 349-363

Tourriere H, Chebli K, Zekri L, Courselaud B, Blanchard JM, Bertrand E, Tazi J (2003) The RasGAP-associated endoribonuclease G3BP assembles stress granules. *J Cell Biol* 160: 823-831

Travis WD, Costabel U, Hansell DM, King TE, Jr., Lynch DA, Nicholson AG, Ryerson CJ, Ryu JH, Selman M, Wells AU *et al* (2013) An official American Thoracic Society/European Respiratory Society statement: Update of the international multidisciplinary classification of the idiopathic interstitial pneumonias. *Am J Respir Crit Care Med* 188: 733-748

Tsakiri KD, Cronkhite JT, Kuan PJ, Xing C, Raghu G, Weissler JC, Rosenblatt RL, Shay JW, Garcia CK (2007) Adult-onset pulmonary fibrosis caused by mutations in telomerase. *Proc Natl Acad Sci U S A* 104: 7552-7557

Tsou PS, Haak AJ, Khanna D, Neubig RR (2014) Cellular mechanisms of tissue fibrosis. 8. Current and future drug targets in fibrosis: focus on Rho GTPase-regulated gene transcription. *American journal of physiology Cell physiology* 307: C2-13

Valdmanis PN, Daoud H, Dion PA, Rouleau GA (2009) Recent advances in the genetics of amyotrophic lateral sclerosis. *Curr Neurol Neurosci Rep* 9: 198-205

van Dijk E, Cougot N, Meyer S, Babajko S, Wahle E, Seraphin B (2002) Human Dcp2: a catalytically active mRNA decapping enzyme located in specific cytoplasmic structures. *The EMBO journal* 21: 6915-6924

Vanderweyde T, Yu H, Varnum M, Liu-Yesucevitz L, Citro A, Ikezu T, Duff K, Wolozin B (2012) Contrasting pathology of the stress granule proteins TIA-1 and G3BP in tauopathies. *J Neurosci* 32: 8270-8283

Veatch JR, McMurray MA, Nelson ZW, Gottschling DE (2009) Mitochondrial dysfunction leads to nuclear genome instability via an iron-sulfur cluster defect. *Cell* 137: 1247-1258

Wallace EW, Kear-Scott JL, Pilipenko EV, Schwartz MH, Laskowski PR, Rojek AE, Katanski CD, Riback JA, Dion MF, Franks AM *et al* (2015) Reversible, Specific, Active Aggregates of Endogenous Proteins Assemble upon Heat Stress. *Cell* 162: 1286-1298

Walther Dirk m, Kasturi P, Zheng M, Pinkert S, Vecchi G, Ciryam P, Morimoto Richard i, Dobson Christopher m, Vendruscolo M, Mann M *et al* (2015) Widespread Proteome Remodeling and Aggregation in Aging C. elegans. *Cell* 161: 919-932

Wang IF, Guo B-S, Liu Y-C, Wu C-C, Yang C-H, Tsai K-J, Shen C-KJ (2012) Autophagy activators rescue and alleviate pathogenesis of a mouse model with proteinopathies of the TAR DNA-binding protein 43. *Proceedings of the National Academy of Sciences of the United States of America* 109: 15024

Wang X, Fan H, Ying Z, Li B, Wang H, Wang G (2010) Degradation of TDP-43 and its pathogenic form by autophagy and the ubiquitin-proteasome system. *Neuroscience Letters* 469: 112-116

Wang Y, Kuan PJ, Xing C, Cronkhite JT, Torres F, Rosenblatt RL, DiMaio JM, Kinch LN, Grishin NV, Garcia CK (2009) Genetic defects in surfactant protein A2 are associated with pulmonary fibrosis and lung cancer. *Am J Hum Genet* 84: 52-59

Wells AU, Brown KK, Flaherty KR, Kolb M, Thannickal VJ (2018) What's in a name? That which we call IPF, by any other name would act the same. *Eur Respir J* 51

Wikenheiser, K. A., Vorbroker, D. K., Rice, W. R., Clark, J. C., Bachurski, C. J., Oie, H. K., & Whitsett, J. A. (1993). Production of immortalized distal respiratory epithelial cell lines from surfactant protein C/simian virus 40 large tumor antigen transgenic mice. *Proceedings of the National Academy of Sciences of the United States of America*, *90*(23), 11029–11033.

Wilson MS, Wynn TA (2009) Pulmonary fibrosis: pathogenesis, etiology and regulation. *Mucosal Immunol* 2: 103-121

Woerner AC, Frottin F, Hornburg D, Feng LR, Meissner F, Patra M, Tatzelt J, Mann M, Winklhofer KF, Hartl FU *et al* (2016) Cytoplasmic protein aggregates interfere with nucleocytoplasmic transport of protein and RNA. *Science (New York, NY)* 351: 173

Woldemichael GM, Turbyville TJ, Vasselli JR, Linehan WM, McMahon JB (2012) Lack of a functional VHL gene product sensitizes renal cell carcinoma cells to the apoptotic effects of the protein synthesis inhibitor verrucarin A. *Neoplasia* 14: 771-777

Wolozin B (2012) Regulated protein aggregation: stress granules and neurodegeneration. *Mol Neurodegener* 7: 56

Wolozin B, Apicco D (2015) RNA binding proteins and the genesis of neurodegenerative diseases. *Advances in experimental medicine and biology* 822: 11-15

Xaubet A, Ancochea J, Molina-Molina M (2017) Idiopathic pulmonary fibrosis. *Med Clin (Barc)* 148: 170-175

Xiang S, Kato M, Wu LC, Lin Y, Ding M, Zhang Y, Yu Y, McKnight SL (2015) The LC Domain of hnRNPA2 Adopts Similar Conformations in Hydrogel Polymers, Liquid-like Droplets, and Nuclei. *Cell* 163: 829-839

Zhang H, Elbaum-Garfinkle S, Langdon EM, Taylor N, Occhipinti P, Bridges AA, Brangwynne CP, Gladfelter AS (2015a) RNA Controls PolyQ Protein Phase Transitions. *Mol Cell* 60: 220-230

Zhang K, Donnelly CJ, Haeusler AR, Grima JC, Machamer JB, Steinwald P, Daley EL, Miller SJ, Cunningham KM, Vidensky S *et al* (2015b) The C9orf72 repeat expansion disrupts nucleocytoplasmic transport. *Nature* 525: 56-61

Zhang T, Baldie G, Periz G, Wang J (2014) RNA-processing protein TDP-43 regulates FOXO-dependent protein quality control in stress response. *PLoS Genet* 10: e1004693

Zheng D, Ezzeddine N, Chen CY, Zhu W, He X, Shyu AB (2008) Deadenylation is prerequisite for P-body formation and mRNA decay in mammalian cells. *J Cell Biol* 182: 89-101

Zhou Y, Huang X, Hecker L, Kurundkar D, Kurundkar A, Liu H, Jin TH, Desai L, Bernard K, Thannickal VJ (2013) Inhibition of mechanosensitive signaling in myofibroblasts ameliorates experimental pulmonary fibrosis. *The Journal of clinical investigation* 123: 1096-1108

6. Erklärung

Hiermit erkläre ich, dass ich die vorliegende Arbeit selbständig und ohne unzulässige Hilfe oder Benutzung anderer als der angegebenen Hilfsmittel angefertigt habe. Alle Textstellen, die wörtlich oder sinngemäß aus veröffentlichten oder nichtveröffentlichten Schriften entnommen sind, und alle Angaben, die auf mündlichen Auskünften beruhen, sind als solche kenntlich gemacht. Bei den von mir durchgeführten und in der Dissertation erwähnten Untersuchungen habe ich die Grundsätze guter wissenschaftlicher Praxis, wie sie in der „Satzung der Justus-Liebig-Universität Gießen zur Sicherung guter wissenschaftlicher Praxis“ niedergelegt sind, eingehalten sowie ethische, datenschutzrechtliche und tierschutzrechtliche Grundsätze befolgt. Ich versichere, dass Dritte von mir weder unmittelbar noch mittelbar geldwerte Leistungen für Arbeiten erhalten haben, die im Zusammenhang mit dem Inhalt der vorgelegten Dissertation stehen, oder habe diese nachstehend spezifiziert. Die vorgelegte Arbeit wurde weder im Inland noch im Ausland in gleicher oder ähnlicher Form einer anderen Prüfungsbehörde zum Zweck einer Promotion oder eines anderen Prüfungsverfahrens vorgelegt. Alles aus anderen Quellen und von anderen Personen übernommene Material, das in der Arbeit verwendet wurde oder auf das direkt Bezug genommen wird, wurde als solches kenntlich gemacht. Insbesondere wurden alle Personen genannt, die direkt und indirekt an der Entstehung der vorliegenden Arbeit beteiligt waren. Mit der Überprüfung meiner Arbeit durch eine Plagiatserkennungssoftware bzw. ein internetbasiertes Softwareprogramm erkläre ich mich einverstanden.

_____ _____

Ort, Datum Unterschrift

7. Danksagung

Ich bedanke mich bei Professor Dr. med. Werner Seeger für die Möglichkeit der Durchführung dieser Arbeit.

Prof. Dr. med. Andreas Günther danke ich für die Aufnahme in seine Arbeitsgruppe und für das Einbinden in die täglichen Abläufe der Labortätigkeiten sowie in die organisatorischen und informellen Labor-Meetings. Die Gelegenheit der Teilnahme an wissenschaftlichen Kongressen hat mir die Möglichkeit eröffnet, mich mit anderen Wissenschaftlern auszutauschen, das eigene Projekt vorzustellen sowie hilfreiche Rückmeldungen zu erhalten. Prof. Günthers wissenschaftliche Kompetenz und Leidenschaft für die Forschung waren eine große Motivation für mich bei der Erstellung dieser Arbeit.

Einen ganz besondereren Dank möchte ich an meine Beteuerin Frau PD Dr. Poornima Mahavadi richten. Frau PD Dr. Mahavadi hat mich mit ihrem großartigen Sachverstand in das wissenschaftliche Arbeiten eingeführt und stand mir jederzeit bei Fragen mit Rat und Tat zur Seite. Dank ihrer Unterstützung, Anleitung und Förderung war es mir möglich, diese Dissertation zu verfassen.

Darüber hinaus danke ich den Mitarbeiterinnen und Mitarbeitern sowie allen anderen Doktorandinnen und Doktoranden der Arbeitsgruppe für ihre Geduld und ihre Hilfsbereitschaft. Es war mir eine Freude, für die Zeit meiner Doktorarbeit ein Teil des Teams gewesen sein zu dürfen.

Abschließend möchte ich mich auch bei meiner Familie und meinem Partner für den stetigen Rückhalt und die bedingungslose Unterstützung bedanken.